Exploring the Regulation and Molecular Mechanism of Autophagy Using *Saccharomyces cerevisiae* as the Model System

by

Xin Wen

A dissertation submitted in partial fulfillment
of the requirements for the degree of
Doctor of Philosophy
(Molecular, Cellular and Developmental Biology)
in the University of Michigan
2022

Doctoral Committee:
Professor Daniel J. Klionsky, Chair
Professor Mara Duncan
Professor Anuj Kumar
Professor Ming Li

Xin Wen

xinwen@umich.edu

ORCID iD: 0000-0001-6513-8623

DEDICATION

To my parents and grandparents

ACKNOWLEDGMENTS

First and foremost, I would like to show my greatest gratitude to my advisor Dr. Daniel J. Klionsky not only for his professional guidance during my Ph.D. journey, but also for his wholehearted support to all my decisions. In the early years of my graduate school, Dan's passion and expertise about sciences always inspired me to move forward. In the past recent two years, I felt even more supported by Dan, both in my research and in my future career choice. The COVID-19 pandemic has transformed many people's ideas about their future, including myself. When I decided that I would like to try some untraditional career paths, instead of rejecting all my wild thoughts, Dan helped me secure a new fellowship allowing me to explore more career options. Looking back, I am proud to say that joining Klionsky Lab is the best decision I have ever made. Words really cannot express all my appreciation of having Dan as my mentor, and I will carry what I have learned from Dan for my whole life. Moreover, I would like to thank my thesis committee, Dr. Mara Duncan, Dr. Anuj Kumar, Dr. Ming Li, for their continuous guidance and support since 2016. Their challenging questions and insightful suggestions are indispensable for my projects. More importantly, their support for my career exploration helped me build the confidence to try something outside my comfort zone. I am also grateful to have strong administrative support from Mary Carr and other MCDB staff ever since my admittance to the Ph.D. program.

I sincerely thank all past and current Klionsky Lab members for their help and encouragement during my time in the lab. I would like to thank Dr. Xu Liu for his patience and guidance during my first few years of graduate school, and for his kindness to allow me to step in one of his projects as shown in this thesis. I am beyond excitement when I know that he found a great position that matched his interest and expertise. Along with that, I would also like to thank all other lab members, who

together made my lab life meaningful and enjoyable. Finally, a special thank is here to Dr. Damián Gatica, who is my best friend, my Chilean brother, and my always sports companion. I cannot imagine how I could get through those dark days without him being my support, and my life in Klionsky Lab has changed a lot because of him. I am also glad to witness his important moments, including engagement, graduation and move to an exciting new position. Cheers to friendship!

I also have a quite amazing journey after I was awarded the CHEAR-LSI Child Health Policy Scholars fellowship since 2020, which enhanced my biology training by providing new skills and more exposure to public health and policy. I want to thank Dr. Susan B. Meister, Dr. Roger Cone and Dr. Lisa Prosser to make this fellowship into reality, and recommendations from Dan and Dr. Ming Li to help me get it. I would like to say thank you to Dr. Susan Woolford, who guided me to conduct research in a field I have never touched base on before, and I appreciated all the help from Woolford's team members. I am honored to be the inaugural recipient of this prestigious fellowship, which has paved a different career path for me.

Last, I want to thank my whole family for their unconditional love. My graduate school life tends to be longer than expected, for several internal and external reasons, but my family is always behind me, showing their strongest support to all my decisions. Finally, I would like to reserve this special thank to my partner Dr. J. Frank Li, who has been with me all the time. I cannot ask for a better partner than him, and hopefully, I will be a Wolverine Ph.D. as he is, in a short time.

Wherever We Go, Forever Go Blue!

PREFACE

This thesis summarizes the research projects I have participated in while working in Dr. Daniel J. Klionsky's laboratory since joining in May 2015. Through these projects we have gained a better understanding of the transcriptional regulation of different autophagy-related (*ATG*) gene mRNA transcripts and also new insights into the molecular mechanisms of non-selective and selective autophagy.

CHAPTER I contains parts of three review papers published in *Journal of Molecular Biology* (doi: 10.1016/j.jmb.2016.02.021), *Seminar in Cancer Biology* (doi: 10.1016/j.semcancer.2019.11.005) and *Molecular Aspects of Medicine* (doi: 10.1016/j.mam.2021.100966), with a few modifications.

CHAPTER II demonstrates that the transcriptional factor Spt4-Spt5 protein complex can regulate autophagy by modulating the transcription of *ATG8* and *ATG41* in *Saccharomyces cerevisiae*. This research was published in *Autophagy* (doi: 10.1080/15548627.2019.1659573). I initiated the whole project and generated most of the data. Dr. Damián Gatica helped in generating Spt5 mutation strains for experiments to confirm that dephosphorylation of Spt5 could negatively modulate autophagy by downregulating *ATG41* mRNA and protein levels. Zhangyuan Yin from the Klionsky lab and Zehan Hu from Dr. Jörn Dengjel's laboratory at the University of Fribourg provided large-scale SILAC data for identifying possible kinases of the Spt4-Spt5 protein complex.

CHAPTER III summarizes two projects that I worked on with Dr. Damián Gatica and Dr. Xu Liu in revealing the molecular mechanism of autophagy. The first paper was published in *Autophagy* (doi: 10.1080/15548627.2020.1776474) showing the important role of Vac8 in autophagy, and the

second paper was published in *Contact (Thousand Oaks)* (doi: 10.1177/2515256418821584) suggesting that ER-mitochondria contact sites are crucial for pexophagy. The ideas were initiated by Dr. Damián Gatica and Dr. Xu Liu, respectively. I co-designed the project and conducted experiments with Dr. Damián Gatica and Dr. Xu Liu, respectively. I played a major part in generating data for figures listed in CHAPTER III.

CHAPTER VI summarizes the major implications of my thesis research and future directions.

TABLE OF CONTENTS

LIST OF TABLES

LIST OF FIGURES

ABSTRACT

Macroautophagy/autophagy is a highly regulated cellular primarily catabolic process, conserved from yeast to more complex eukaryotes. During autophagy, cytoplasmic materials are delivered into the lysosome (or the analogous organelle, the vacuole, in yeast) for degradation by resident hydrolases; the resulting breakdown products are recycled back to the cytoplasm to maintain cellular homeostasis. Under normal nutrient conditions, autophagy occurs at a basal level, which can play a critical role in cell homeostasis. When cells face stimuli or stress, autophagy can be massively upregulated to handle the increased demand. The malfunction of autophagy is associated with various diseases, including cancer, aging, metabolic and neurodegenerative diseases. There has been substantial progress in understanding the regulation and molecular mechanisms of autophagy in different organisms; however, many questions about the most fundamental aspects of autophagy remain unresolved. For example, little is known about the complicated modulation of gene expression and specific transcriptional regulators of autophagy. Meanwhile, we currently have a limited understanding of most steps in the autophagic process.

In Chapter II, I examine the question of whether yeast might employ a mechanism of promoter-proximal pausing, similar to that in higher eukaryotes. The promoter-proximal pausing is defined by a temporal halt of transcription within ~100 nucleotides downstream of the transcription start site (TSS). The DRB sensitivity-inducible factor (DSIF, composed of SUPT4H1 and SUPT5H) works with negative elongation factor (NELF) to impart the pausing. Upon specific stimulation, the temporal state of pausing will be reversed, and the status of DSIF can be changed to promote transcription elongation.

The budding yeast expresses homologs of SUPT4H1 and SUPT5H, named Spt4 and Spt5, but there is no clear evidence of the presence of NELF. Therefore, most studies have focused on the positive role of the Spt4-Spt5 complex in transcription. Interestingly, our data show that the Spt4-Spt5 complex may act in a gene-specific manner in yeast, with Spt4 having an additional and clear negative role for certain *ATG* genes under growing conditions.

Chapter III further investigates the mechanism of both nonselective and selective autophagy. In budding yeast, autophagosome formation occurs at the phagophore assembly site (PAS), a specific perivacuolar location that works as an organizing center for the recruitment of different autophagy-related (Atg) proteins. However, the PAS is a poorly defined structure, and one unanswered question is what determines the localization of the PAS. The first part in Chapter III reveals that the vacuolar membrane protein Vac8 is required for the correct vacuolar localization of the PAS. We also provide evidence that Vac8 anchors the PAS to the vacuolar membrane by recruiting the Atg1-Atg13 initiation complex. In the second part of Chapter III, we examine another aspect of the dynamic role of intracellular membranes and autophagy machinery, in this case focusing on a type of selective autophagy, pexophagy (specifically degrade surplus or damaged peroxisomes). Recently, studies have implicated the role of membrane contact sites in nonselective autophagy, but no papers had been published on the topic of pexophagy. We found that endoplasmic reticulum (ER)-mitochondria contact sites are necessary for efficient pexophagy, and disruption of the ER-mitochondria encounter structure (ERMES) results in a severe defect in pexophagy.

Together the research presented in this dissertation expands our understanding of regulation and molecular mechanism of autophagy using *Saccharomyces cerevisiae* as the model system.

CHAPTER I Introduction[1]

1.1 Overview of Autophagy

Macroautophagy/Autophagy, a term from the Greek words “auto” (self) and “phagine” (to eat), is a highly regulated cellular degradation and recycling process. It is conserved in all eukaryotes [1]. Initially in yeast, a limited number of genes that have products primarily involved in autophagy was unified under the name autophagy-related (*ATG*) [2]. Whereas the proteasome is responsible for the degradation of most short-lived proteins, long-lived proteins, large protein complexes and organelles are degraded by autophagy. One key definition of autophagy is that it involves the delivery and typically the degradation of cytoplasmic cargo within the lysosome/vacuole [3]; during autophagy the cargo is initially sequestered in a compartment that is separate from the lysosome/ vacuole and the initial sequestration process involves a transient membrane structure, the phagophore [4]. Although precise details regarding phagophore nucleation and formation are not known, this compartment likely expands sequentially around cargo, providing tremendous flexibility regarding capacity. Upon completion, the phagophore membranes scission to generate the double-membrane autophagosome; this double-membrane vesicle subsequently fuses with the lysosome/vacuole [5]. The morphological hallmark of autophagy is the formation of the phagophore and its subsequent expansion and maturation into an autophagosome, which is a large cytoplasmic double-membrane vesicle [6]. Once completed, the outer membrane of the autophagosome fuses with the lysosome/vacuole; the inner membrane and

[1] This chapter is reprinted partly from Xin Wen, Daniel J. Klionsky (2016) *Journal of Molecular Biology* (doi: 10.1016/j.jmb.2016.02.021), partly from Xin Wen, Daniel J. Klionsky (2020) *Seminar in Cancer Biology* (doi: 10.1016/j.semcancer.2019.11.005), and partly from Xin Wen, Ying Yang, Daniel J. Klionsky (2021) *Molecular Aspects of Medicine* (doi: 10.1016/j.mam.2021.100966), with minor modifications.

the cargo are thereby exposed to the lumenal contents of this organelle and subsequently degraded by resident hydrolases.

1.2 Process of Autophagy

The process of autophagy can be divided into the following stages: induction, nucleation of the phagophore, expansion of the phagophore, completion of the autophagosome, docking and fusion with the vacuole, and the final steps of degradation and efflux of the breakdown products (Figure 1.1). In yeast, the induction of autophagy begins at a single perivacuolar site that is proximal to the vacuole, called the phagophore assembly site (PAS), a step regulated by the Atg1 complex (including at least Atg1, Atg13 and the Atg17–Atg31–Atg29 ternary subcomplex; details shown in Figure 1.2) [7, 8]. Then the Atg14-containing class III phosphatidylinositol 3-kinase (PtdIns3K) complex I (which consists of Vps34, Vps30, Vps15, Atg14 and Atg38) is recruited to the PAS in the nucleation stage [9]. From induction to nucleation, the current model is that the PAS gradually generates a primary double membrane sequestering compartment, the phagophore [10].

Next, in the expansion and completion stage, the phagophore first begins to expand. There may be different mechanisms that operate in the expansion phase depending on whether the process is selective or nonselective. Key components that participate at this include two conjugation systems involving ubiquitin-like (Ubl) proteins [11]. These two systems use the Ubl proteins Atg12 (along with the components Atg5, Atg7, Atg10 and Atg16) and Atg8 (and Atg3, Atg4 and Atg7) [12, 13] (Figure 1.3). One model for the expansion stage also involves cycling of Atg9; this transmembrane protein may cycle between the PAS and peripheral structures, carrying or directing the delivery of membrane, although there are currently no direct data supporting this hypothesis [14] (Figure 1.4). Following the expansion of the phagophore, the double-membrane autophagosome fully surrounds the cargo. Although the mechanism and regulation of the final closure step have not been well characterized,

completion of the autophagosome is likely to involve membrane scission [15]. Based on other processes requiring vesicular membrane sealing, such as the multi-vesicular body pathway, it is likely that the endosomal sorting complex required for transport (ESCRT) components play a role [16, 17]. Along these lines, the Arabidopsis chmp1 mutant, defective for a component of ESCRT-III, displays a phenotype that is consistent with a partial block in phagophore closure [18]. Once the autophagosome is complete, it will deliver its cargo to the vacuole in yeast by fusing with the vacuolar membrane, and the timing of this docking and fusion process is key to ensure degradation and has therefore to be finely regulated [19].

Finally, the autophagic body (the inner autophagosome vesicle) is degraded with the help of the lipase Atg15, and the cargo is typically degraded by various hydrolases present in the vacuole [20]. The final step of the process consists of the release of the breakdown products into the cytoplasm, which is not well characterized, although the vacuole contains hydrolases for all the major macromolecules, essentially nothing is known about the recycling of nucleic acid, carbohydrate, or lipid breakdown products.

1.3 Regulation of Autophagy

Autophagy works primarily as a cytoprotective mechanism. Under normal conditions, autophagy occurs constitutively at a basal state. When the cell is exposed to stress stimuli (e.g., nutrient or energy starvation in yeast), autophagy is massively induced. This promotes the turnover of cytoplasmic materials required for cell survival or removes superfluous or damaged organelles. Too little or too much degradation from uncontrolled autophagy is harmful, and autophagy dysfunction is associated with various diseases, such as cancer, aging and neurodegeneration; thereby, the process must be tightly regulated [21]. Accordingly, considerable research has focused on understanding the complex

network of regulatory pathways that control autophagy. Here, we discuss aspects of autophagy regulation from the epigenetic to the post-translational level.

1.3.1 Epigenetic regulation

Several epigenetic modifications including methylation and acetylation/deacetylation of histone H3 and H4 participate in the control of autophagy [22]. For example, spermidine, a natural polyamine that induces autophagy, can cause histone H3 deacetylation by repressing histone acetyltransferases, resulting in a global hypoacetylation in yeast [23]. Based on a genomic study, target of rapamycin (TOR; a component of a protein complex that acts as a master nutrient sensor in regulating protein synthesis, thereby acting as a primary negative regulator of autophagy) signaling was found to positively modulate the acetylation on histone H3 Lys56 (H3K56ac). Accordingly, the level of H3K56ac is lower following the addition of rapamycin, a TOR inhibitor and an alanine substitution at this position makes yeast cells more sensitive to rapamycin [24]. The knockout of the sirtuin deacetylases Hst3 and Hst4 can restore the reduced level of H3K56ac caused by TOR inhibition, but the precise role of H3K56 deacetylation in autophagy is still under further investigation [24]. Upon autophagy induction, a decrease of H4K16ac is also observed, which occurs through downregulation of the histone acetyltransferase Sas2 (mammalian KAT8/hMOF) [25]. The joint reduction in the levels of both H4K16ac and trimethylated H3K4 (H3K4me3) is extended when autophagy is stimulated [25]. Collectively, different histone modifications likely play a role in controlling *ATG* gene expression, but current epigenetic studies in this field have been relatively limited.

1.3.2 Transcriptional regulation

Upregulation of Atg protein synthesis is not absolutely required for autophagosome formation but is important to generate normal-sized autophagosomes [26]. For example, the dramatic increase in *ATG8* mRNA transcripts under starvation conditions corresponds to a significant rise of the Atg8 protein

level, suggesting that transcriptional control-and in particular that of *ATG8*-is important in modulating autophagy [26-28]. Accordingly, yeast *atg8*Δ strains form abnormally small autophagosomes. To date, there are several transcriptional regulators that have been identified that can regulate different *ATG* genes, as discussed below.

Ume6 and ATG8: Ume6, a yeast DNA-binding protein, is involved in transcriptional repression dependent on Sin3 (a co-repressor) and Rpd3 (a histone deacetylase), both of which can negatively regulate a variety of yeast genes [29-31]. The deletion of UME6, SIN3 and/or RPD3 results in a substantial increase in *ATG8* mRNA (and subsequently Atg8 protein) under growing conditions (when *ATG8* transcription is otherwise repressed) and leads to a more rapid autophagic response when cells are shifted to autophagy-inducing conditions [32]. In addition, Ume6-deficient cells form larger autophagosomes than wild-type cells. The URS1 sequence, which corresponds to a consensus binding site for Ume6, is present within the *ATG8* promoter. It is thought that this negative regulator binds the promoter under growing conditions, negatively regulating autophagy at the transcriptional level, while under autophagy-inducing conditions, phosphorylation of Ume6 releases its repression of *ATG8* transcription [32]. The *ATG8* transcription is also regulated by the kinase Rim15, a positive regulator of autophagy that can integrate signals from TOR, and cAMP-activated protein kinase A (PKA), a second messenger-dependent enzyme that regulates various signaling pathways [33, 34].

Rph1 and ATG7: Similar to Ume6, Rph1 is also a DNA-binding protein that regulates autophagy through the control of *ATG* gene expression [35, 36]. Under nutrient-replete conditions, Rph1 inhibits the transcription of several *ATG* genes by binding to, at least, the *ATG7* promoter, and the Rph1-dependent regulation of *ATG7* expression plays a role in modulating autophagy activity [37]. Thus, Rph1 represents another example of how yeast cells maintain autophagy at a low basal level, and the inhibitory phosphorylation of Rph1 is also dependent on Rim15 upon starvation. Moreover, the

regulation of autophagy by Rph1 is conserved; a similar pathway has been confirmed in mammals involving KDM4A, a homolog of Rph1 [37].

Pho23 and ATG9: Pho23 modulates gene expression in yeast by working with the Rpd3 histone deacetylase [38]. Pho23 also negatively regulates mRNA and protein levels of several *ATG*/Atg genes/proteins, including Atg1, Atg7, Atg8, Atg9 and Atg14. Pho23 has a major impact on *ATG9* expression. Notably, the level of Atg9 correlates with the number of autophagosomes, suggesting Pho23 likely regulates autophagosome number via its effects on Atg9. Indeed, *pho23Δ* cells generate more autophagosomes than to the wild type, and these autophagosomes are normal sized [39]. Therefore, Pho23 could be an important transcriptional repressor of autophagy that targets the frequency of autophagosome formation by negatively regulating the level of *ATG9* expression.

Other transcriptional regulators: In addition to Ume6, Rph1 and Pho23, a recent large-scale analysis of *ATG* gene expression has identified several new positive and negative transcription regulators [40]. Gln3 and Gat1 are nitrogen catabolite repression-sensitive GATA-type transcription factors, which can upregulate gene expression upon nutrient starvation conditions [41, 42]. After starvation, the expression of *ATG7*, *ATG8*, *ATG9*, *ATG29* and *ATG32* decreases in cells lacking Gln3 or Gat1, but double deletion of these two factors does not exert an additive effect on *ATG* expression, suggesting they may function in a single pathway for *ATG* gene expression [40]. Moreover, TOR can phosphorylate Gln3 and Ure2, resulting in retention of Gln3 in the cytosol, thereby negatively regulating autophagy [43]. Spt10 represses *ATG8* and *ATG9* expression, and Fyv5 has a negative effect on the expression of *ATG1*, *ATG8*, *ATG9* and *ATG14* [40]. Other DNA-binding proteins have also been identified as positive regulators of *ATG* gene expression. For example, Gcn4, which directly binds to the *ATG1* promoter, is required for its upregulation after nitrogen starvation, while the over-expression of Sfl1 may increase the transcription of several *ATG* genes, especially *ATG8* [40, 44].

1.3.3 Post-transcriptional regulation

Autophagy may also be subject to post-transcriptional regulation. This has been observed in *ATG* transcripts in two fungal species and in human cells. Dhh1/Vad1/DDX6, homologous members of the RNA helicase RCK family in budding yeast, Cryptococcus neoformans and mammals, respectively, can negatively regulate autophagy, along with the decapping enzyme Dcp2/DCP2 [45]. Dhh1/Vad1/DDX6 binds the 5′ untranslated region of certain transcripts and recruits Dcp2, and the latter enzyme is phosphorylated and activated by TOR, resulting in the decapping, and degradation of specific transcripts, which maintains autophagy at a basal level [46]. Another study from our lab indicated that the RNA-binding complex Pat1-Lsm can prevent the 3' to 5' exosome-mediated degradation of a specific subset of *ATG* mRNAs during nitrogen starvation. The dephosphorylation of Pat1 at residues S456 and S457 further result in *ATG* mRNA accumulation, Atg protein synthesis and robust autophagy induction [47].

1.3.4 Post-translational regulation

Finally, autophagy is subject to post-translational regulation. There are three major types of post-translational modifications (PTMs), namely, phosphorylation, ubiquitination and acetylation [48-50]. These modifications may act to modulate the function of Atg proteins or other regulatory factors. One or more types of PTMs may occur on a single protein at one or more sites and/or in a temporally dependent manner in response to different types of stress [51]. Here, we briefly discuss these three types of PTMs as they concern the autophagy core machinery.

Phosphorylation is the best-characterized PTM on Atg proteins, and many studies have identified kinases involved in autophagy regulation. In contrast, the complementary phosphatases have been less well characterized. In yeast, one example of the role of phosphorylation-dependent regulation in autophagy is seen with the Atg1 kinase complex [52, 53]. The Atg1 kinase complex (Atg1, Atg13,

Atg17–Atg31–Atg29) acts early in the induction step of autophagy and is negatively regulated by the TOR kinase [54]. Under nutrient-rich conditions, TOR-dependent phosphorylation of Atg1 and Atg13 results in reduced Atg1 kinase activity [55, 56]. Upon nitrogen starvation or treatment with rapamycin, TOR is suppressed, leading to dephosphorylation of Atg13 and Atg1 as well as autophagy induction [57]. PKA also directly phosphorylates these two proteins, which, in particular, affects the localization of Atg13 to the PAS [58]. Either the inactivation of PKA alone or the mutation to alanine of the residues on Atg13 can lead to autophagy induction. Furthermore, Atg13 dephosphorylation facilitates its interaction with Atg1 or Atg17, and alters its conformation to activate the Atg1 kinase complex [52, 54, 59]. However, autophosphorylation in the Atg1 kinase-activation loop is required for maintaining Atg1 activity after TOR inhibition [60]. To date, there is still some controversy regarding whether the kinase activity of Atg1 has a more significant role during growing conditions (e.g., for the Cvt pathway) or under starvation conditions [61, 62]. Further phosphorylation events include modifications of Atg29 and Atg31, which are necessary to generate an active Atg17–Atg31–Atg29 complex upon starvation [63, 64]. Some studies in yeast suggest that Atg9 phosphorylation directly by the Atg1 kinase is required in early steps of autophagy/phagophore elongation, and phosphorylated Atg9 then recruits Atg8 and Atg18 to the PAS [65, 66]. Furthermore, phosphorylation of Atg19 and Atg36 by Hrr25, and phosphorylation of Atg32 on Ser114 by casein kinase 2 are involved in selective types of autophagy [67, 68]. For example, Atg32 phosphorylation mediates the interaction of Atg32–Atg11 during mitophagy [67].

As mentioned above, class III PtdIns3K complex I (Vps34, Vps30, Vps15, Atg14 and Atg38) plays a role in the nucleation stage of autophagy. The Ser/Thr protein kinase Vps15 modulates Vps34 phosphorylation, which is important for forming the lipid kinase complex [69]. Additionally, Vps34 can phosphorylate phosphatidylinositol to generate PtdIns3P, which plays a crucial role in

autophagosome formation [70]. Indeed, many Atg proteins, including Atg18, Atg20, Atg21 and Atg24, bind to PtdIns3P and are thus recruited to the PAS [71-73]. In yeast, the PtdIns3P phosphatase Ymr1 is localized at the PAS during an early stage of autophagy, and the Ymr1-dependent dephosphorylation of PtdIns3P is essential for Atg protein disassembly during autophagosome maturation, thus revealing the positive role of Ymr1 in autophagy [74]. In contrast, other PtdIns3P phosphatases may negatively control autophagy by lowering the level of this phosphoinositide, as seen in Caenorhabditis elegans or mammalian cells [75, 76]. These data imply that phosphorylation/dephosphorylation of PtdIns/PtdIns3P can either positively or negatively regulate autophagy, depending on the organism and stage of the process.

Ubiquitination can serve multiple functions in the cell including protein targeting and degradation. For example, after proteins are tagged by the small regulatory protein ubiquitin (Ub), in particular on Lys 48 and 63, they can be recognized by the 26S proteasome for degradation. The complete process of ubiquitination has three steps including activation, conjugation and ligation, performed by E1 (a Ub activating enzyme), E2 (a Ub conjugating enzyme) and E3 (a Ub ligase) enzymes, respectively [77]. Under some conditions, an E4 (a Ub chain elongation factor) enzyme is also required. The two Ubl systems (Atg8-related and Atg12-related) are the best examples of ubiquitination-like conjugation in yeast. In mammalian cells, an E3 ubiquitin protein ligase TRAF6 can modify both BECN1 (the Vps30/Atg6 ortholog in mammals) and ULK1 (the Atg1 ortholog) [78, 79]. The ubiquitination of BECN1 is required for autophagy induction, while ubiquinated ULK1 is stabilized and can auto-activate. Another E3 ligase, RNF5, promotes the degradation of Atg4 by ubiquitination, leading to suppression of autophagy [80].

Acetylation can participate in controlling autophagy. In yeast, Esa1, the catalytic subunit of NuA4, is a histone acetyltransferase participating in autophagy regulation [81]. Upon starvation,

acetylation of Atg3 increases in an Esa1-dependent manner. Lys19, Lys48 and Lys183 of Atg3 are acetylated, among which Lys19 and Lys48 modifications are critical for autophagy. The repression of this acetylation blocks Atg8–Atg3 interaction and Atg8 lipidation. The function the Rpd3 deacetylase counters the effect of Esa1: the deletion of *RPD3* results in increased acetylation of Atg3 and upregulation of autophagy. The mammalian ortholog of Esa1, KAT5, can also directly acetylate ULK1, suggesting that acetylation of Atg proteins may be important in regulating autophagy in all eukaryotes [81, 82].

1.4 Core Recognition in Selective Autophagy

Autophagy can either be non-selective or selective: the non-selective mode is thought to involve degradation of random portions of cytoplasm, whereas the selective mode is highly specific for certain components. In non-selective autophagy, the degradation of random portions of cytoplasm is critical for cell survival upon nutrient and energy deprivation. However, autophagy can also be highly specific, and selective autophagy, along with basal constitutive autophagy, functions more in cell maintenance and homeostasis, as well as in the cellular remodeling that accompanies the shift to a preferred carbon source [10]. During selective autophagy (Figure 1.5), the phagophore membrane is closely opposed to the cargo, preventing the sequestration of bulk cytoplasm, and finally transports the sequestered contents to the vacuole [83]. Due to the *de novo* mechanism of phagophore formation, a wide range of cargo, including entire organelles, can be selectively degraded through autophagy. These include mitochondria (mitophagy), peroxisomes (pexophagy), protein aggregates (aggrephagy), lipid droplets (lipophagy) and intracellular pathogens (xenophagy); accordingly, each process involves specific components (such as receptors) and the core machinery [84]. Moreover, in contrast to the normal pattern of autophagy, selective autophagy can also work as a biosynthetic mechanism. In the Cvt pathway, precursor aminopeptidase I (prApe1) is the primary cargo protein. This precursor is

synthesized in the cytosol, and assembles into dodecamers, which subsequently form a larger oligomer (termed the Ape1 complex). It is this complex that binds the Cvt pathway receptor Atg19 [85], and the scaffold Atg11, allowing selective sequestration by the phagophore. The binding of Atg11 to Atg19 occurs after Atg19 interacts with prApe1, and the WXXL motif on the C terminus of Atg19 allows for its binding to Atg8 [86]. Upon completion, the double-membrane Cvt vesicle (analogous to an autophagosome in nonselective autophagy) fuses with the vacuole; as with non-selective autophagy, this results in the release of the inner vesicle into the vacuole lumen generating the Cvt body (equivalent to the autophagic body). After the single-membrane vesicle is broken down, the cargo is exposed to the resident vacuolar hydrolases, but in this case, the contents of the Cvt body are not degraded; prApe1 is proteolytically matured by removal of a propeptide, and it now functions as another vacuolar protease [87]. Atg19 also binds to Ape4 and Ams1, two additional resident hydrolases that are delivered to the vacuole via the Cvt pathway, whereas Atg34 can replace Atg19 in binding to Ams1 under starvation conditions [88-90]. The Cvt pathway provides a general model for selective autophagy, involving interactions among the cargo (prApe1), a ligand (the prApe1 propeptide), a receptor (Atg19) and a scaffold (Atg11), which link the cargo with the autophagy machinery via binding to Atg8. Similarly, during mitophagy, the Atg32 receptor initially binds to Atg11 and subsequently to Atg8, although in this case there is not a clear ligand [91, 92]. Atg33, a transmembrane protein on the mitochondrial outer membrane, is also required by mitophagy that is induced in the post-log phase [93]. In pexophagy, Atg36 functions as the receptor, also interacting with Atg11 and Atg8 [94].

1.5 Pathology of Autophagy in Human Diseases

Using mice as the model system, researchers have found that failure of autophagy can promote cellular degeneration, age-related changes, tumor formation and influence the progression or persistence of infections [95]. Human genetic studies have shown the involvement of autophagy, or autophagic

dysfunction, in many diseases [96, 97]. The relation between autophagy and cancer or autophagy and neurodegenerative diseases has been the major focus of many reviews [98-101], and the role of autophagy in some less-documented diseases, such as metabolic disorders and rare diseases, has gradually attracted more attention, which further underscores the importance of autophagy.

1.5.1 Autophagy and metabolic disorders

The most important and evolutionarily conserved role of autophagy is to maintain metabolic homeostasis, primarily by releasing amino acids, lipids, and other metabolic precursors [102]. Conversely, the metabolic status can control the nature and extent of autophagic induction. Autophagy may be a key part in the MTORC1- or AMPK-hub against various metabolic diseases, such as obesity, diabetes, and non-alcoholic fatty liver disease (NAFLD). The complex interplay between genetic and environmental factors is responsible for these metabolic disorders, among which excess caloric intake and unbalanced energy expenditure are the major contributors that have been well-documented to inhibit autophagy activities [103]. However, both increased and decreased levels of autophagy have been observed in these disorders, while most mouse genetic studies have shown that the block of autophagy could facilitate the transition from obesity to diabetes, as well as enhancing the risk of atherosclerosis and NAFLD [97, 104]. Therefore, the precise mechanism of autophagy in these metabolic disorders is complicated, and we need further investigation on the controversial research results to fill in the knowledge gap.

1.5.2 Autophagy and rare diseases

The importance of autophagy in human health has been further underscored by its emerging role in rare diseases. A rare disease is defined differently depending on geographical region; for example, this is a condition that affects fewer than 200,000 or 2000 people in the United States and the European Union, respectively [105]. While individual diseases are rare, the total population that is suffering from

rare diseases is large. There is an estimation of over 7000 rare diseases existing, and exact causes of many of them are still unknown. Fortunately, accumulating studies have revealed the relation between autophagy and rare disease, which can help open new directions for future treatment.

An important group of rare diseases is the lysosomal storage diseases (LSDs), which are a group of inherited metabolic disorders characterized by enzyme deficiencies; the role of autophagy has also been recognized in many of them ([106]. One of the most extensively studied LSDs is Niemann-Pick type C disease, which is characterized by accumulation of lipids in various tissues [107]. The disease is caused by mutations in the NPC1 or NPC2 gene, which are inherited in an autosomal recessive manner. The NPC1 protein is a late-endosomal protein, whereas NPC2 is a ubiquitous soluble glycoprotein [108, 109]. The accumulation of autophagosomes and lysosomes have been observed in this disease, and the resulting defects of autophagy are regarded as a major cause of the disease phenotype [107, 110, 111]. A failure in the STX17 (syntaxin 17)-VAMP8 SNARE machinery, and reduced levels of VEGF (vascular endothelial growth factor) are responsible for the impaired autophagy activity [112, 113]. The loss of GBA/glucocerebrosidase activity in Gaucher disease leads to accumulation of glucocerebroside and widespread pathology [114, 115]. A mutation in GBA1 may be the cause of the block in autophagy; concomitant downregulation of TFEB and the associated impairment in autophagosome maturation is seen in neurons differentiated from patient-specific induced pluripotent stem cells [116]. The disease mouse model shows accumulation of secondary autophagy substrates including SQSTM1, dysfunctional mitochondria and ubiquitinated protein aggregates, accompanied by impaired autophagic influx [117-120].

1.5.3 Conclusions

Although many preclinical and clinical trials for diseases such as cancer show that autophagy can be a promising therapeutic target, we should be aware that the complexity of autophagy might create

substantial problems regarding disease treatment. For example, the role of autophagy is tissue-specific in metabolic disorders, suggesting that the global pharmacological modulation of autophagy may lead to worsened conditions. Considering the double-edged sword role of autophagy in many diseases, whether it is ultimately better to induce or to inhibit autophagy is still a prominent question. In addition, the measurement of autophagy activity is not consistent in many studies, leaving some results controversial and unreliable. It is critical to have more solid answers to these questions to move forward. We still have a long way to go in treating diseases by specifically targeting autophagy, but we are optimistic that an increasing number of studies are establishing the bridge between autophagy and human health.

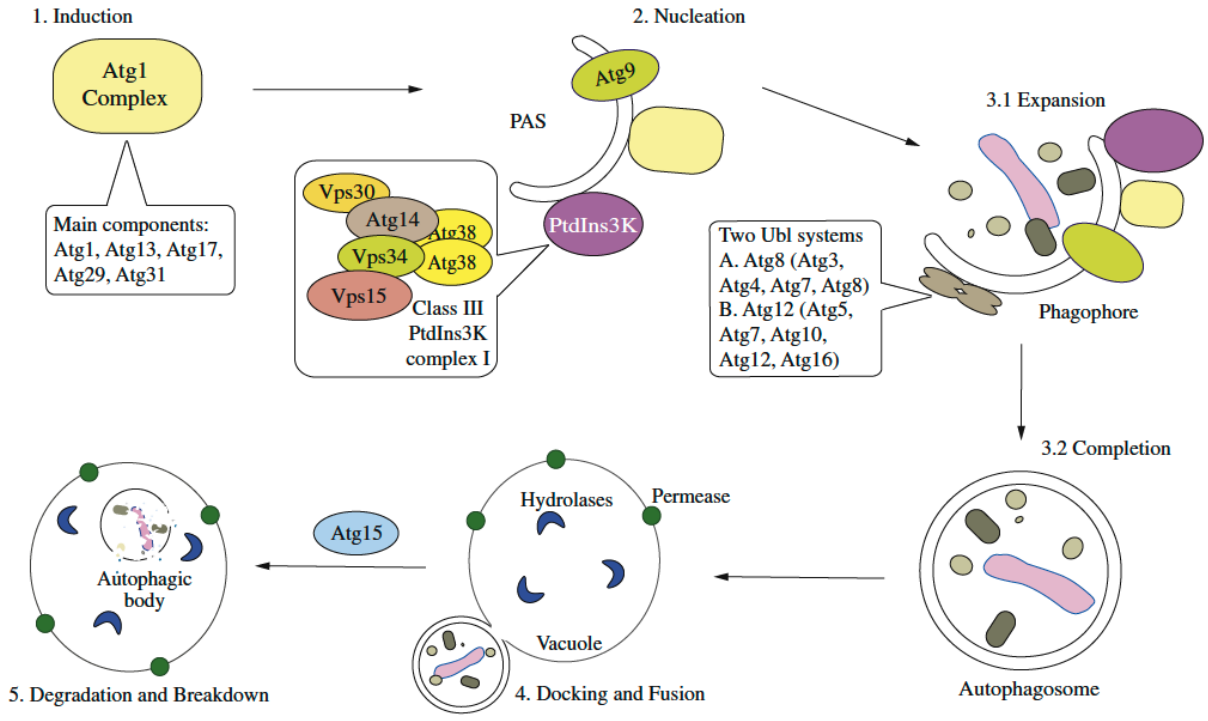

Figure 1.1 A model of different stages of autophagy in yeast
In yeast, autophagy can be generally divided into the following stages: induction, nucleation, expansion and completion, docking and fusion, and finally degradation and efflux. The Atg proteins form most of the primary machinery that function in each of these stages.

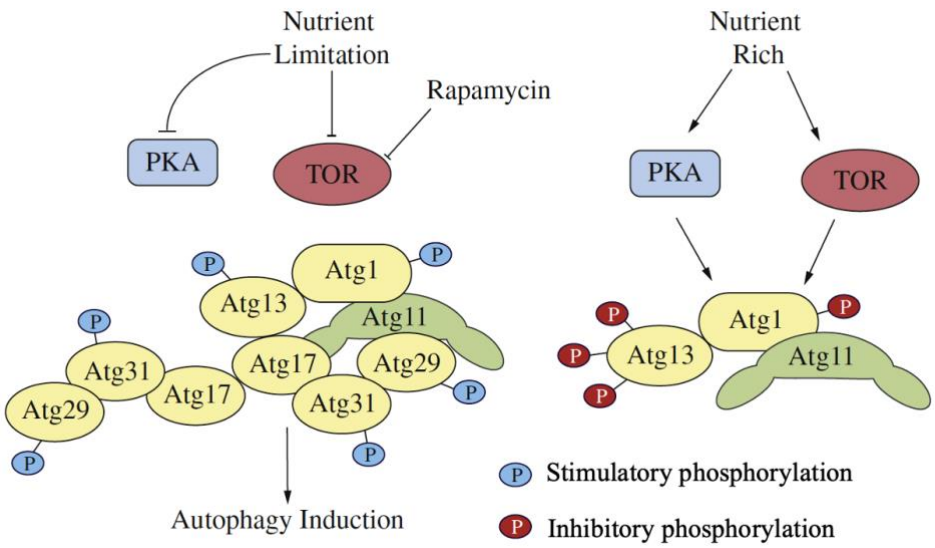

Figure 1.2 The interactome of the Atg1 kinase complex
Upon autophagy induction, the Atg1 complex is mainly composed of three components: Atg1, Atg13 and the Atg17–Atg31–Atg29 subcomplex. Atg13 can bind to Atg1 and the Atg17–Atg31–Atg29 subcomplex directly, whereas there is no known binding site on Atg1 for the subcomplex. The scaffold protein Atg11, which plays a critical role under growing conditions, and for selective autophagy, interacts the with Atg1 kinase complex by binding to Atg1, Atg17 and Atg29.

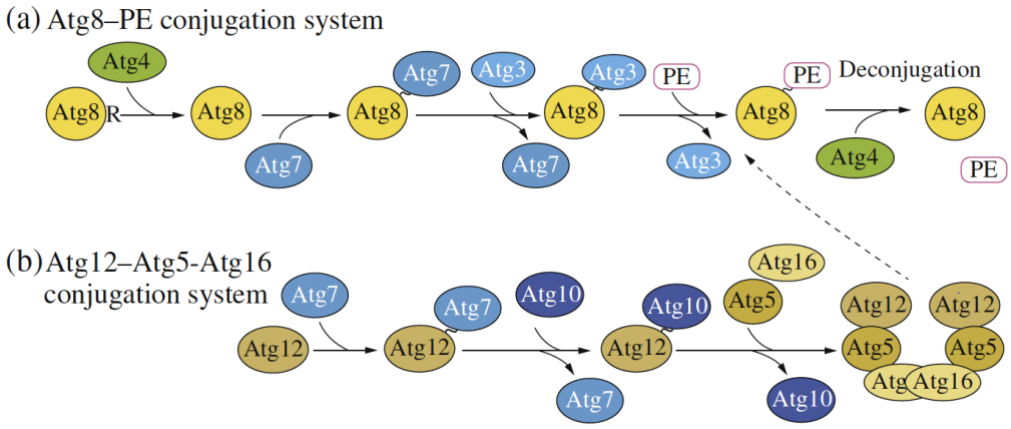

Figure 1.3 Two ubiquitin-like conjugation systems
The two ubiquitin-like proteins Atg8 and Atg12 are used to generate the conjugation products Atg8–PE and Atg12–Atg5-Atg16, respectively. These two Ubl conjugation systems use the same E1-like enzyme Atg7, but different E2-like enzymes, Atg3 for Atg8 and Atg10 for Atg12. Furthermore, the Atg12–Atg5-Atg16 complex can work as an E3-like enzyme for Atg8–PE formation.

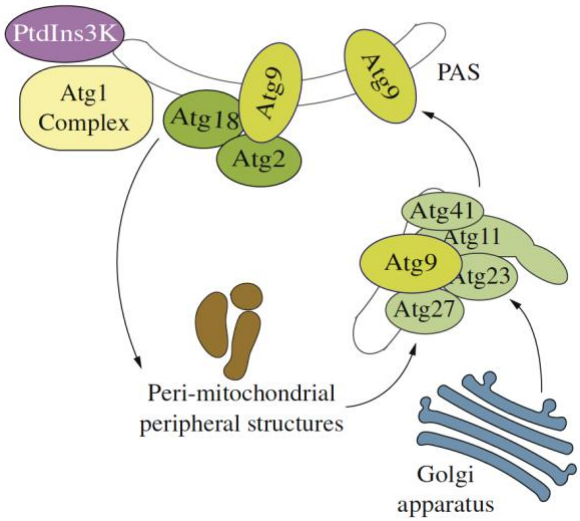

Figure 1.4 The Atg9 complex

The transmembrane protein Atg9 can reside at the PAS and peripheral structures proximal to mitochondria. With the help of Atg11, Atg23, Atg27 and Atg41, Atg9 can travel from the peripheral structures to the PAS, playing a role in orchestrating membrane delivery. Retrograde movement relies on the Atg2-Atg18, Atg1-Atg13 and Atg14-containing PtdIns3K complexes.

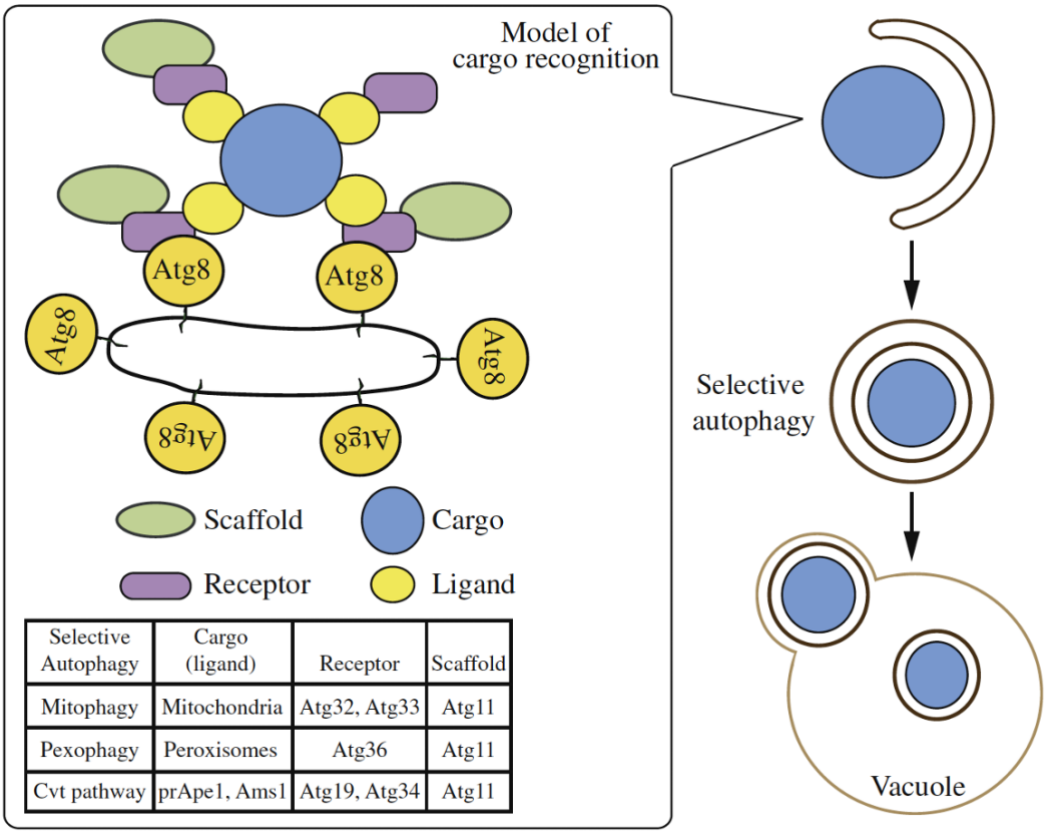

Selective Autophagy	Cargo (ligand)	Receptor	Scaffold
Mitophagy	Mitochondria	Atg32, Atg33	Atg11
Pexophagy	Peroxisomes	Atg36	Atg11
Cvt pathway	prApe1, Ams1	Atg19, Atg34	Atg11

Figure 1.5 A general model of selective autophagy in yeast
For different kinds of selective autophagy in yeast, there is a commonly used mechanism to allow for cargo recognition. This schematic depicts three kinds of selective autophagy: Cvt pathway, mitophagy and pexophagy. Detailed information is provided in the corresponding table.

CHAPTER II The Transcription Factor Spt4-Spt5 Complex Regulates the Expression of *ATG8* and *ATG41*[2]

2.1 Abstract

Macroautophagy/autophagy, a highly conserved dynamic process, is one of the major degradative pathways in cells. Over 40 autophagy-related (*ATG*) genes have been identified in *Saccharomyces cerevisiae* (*S. cerevisiae*), most of which have homologs in more complex eukaryotes. Autophagy plays a crucial role in cell survival and maintenance, and its dysfunction is observed in many diseases, indicating that the proper regulation of autophagy is important. Although the overall process of autophagy has been extensively studied, and the function of the Atg proteins are generally known, relatively little is known about the regulatory mechanisms that control autophagy activity. Here we reveal regulation of autophagy by Spt4-Spt5 protein complex. Spt5, a highly conserved transcriptional factor, is found in all domains of life. Spt5 can form a complex with Spt4, together playing a central role in transcription. In higher eukaryotic cells, the Spt4-Spt5 complex plays a dual role in gene regulation. It can delay transcription through promoter-proximal pausing, while it can also facilitate transcriptional elongation. In contrast, in *S. cerevisiae*, only the positive function of the Spt4-Spt5 complex has been identified. Here, we show for the first time that the Spt4-Spt5 transcription factor complex negatively regulates *ATG* genes in *S. cerevisiae*, inhibiting autophagy activity during active

[2] This chapter is reprinted from Xin Wen, Damián Gatica, Zhangyuan Yin, Zehan Hu, Jörn Dengjel, and Daniel J. Klionsky (2020) The transcription factor Spt4-Spt5 complex regulates the expression of *ATG8* and *ATG41*. *Autophagy*; 16(7):1172-1185. doi: https://doi.org/10.1080/15548627.2019.1659573

growth. Under autophagy-inducing conditions, the repression is released by Spt5 phosphorylation, allowing an upregulation of autophagy activity.

2.2 Introduction

Autophagy is a highly regulated degradative process that allows cells to break down their own components within the vacuole in yeast and plants, or the lysosome in more complex eukaryotes [1, 2]. A basal level of autophagy is usually maintained in physiological conditions, while in response to different stimuli (e.g., nutrient limitation, hypoxia and other stress conditions), autophagy is induced. Depending on how substrates are transported, autophagy is divided into 2 main types (macroautophagy and microautophagy) in yeast, whereas additional types of autophagic pathways including chaperone-mediated autophagy, chaperone-assisted selective autophagy and endosomal microautophagy exist in mammals [3]. Both macroautophagy and microautophagy have nonselective and selective modes: the nonselective process refers to the turnover of bulk cytoplasm, whereas the selective pathway can specifically target damaged or superfluous organelles, protein aggregates, invasive pathogens and other intracellular components [121]. In this paper, we mainly focus on yeast nonselective macroautophagy (hereafter autophagy), in which random cytoplasm is first sequestered within the phagophore, a transient double-membrane structure. The phagophore then expands and matures into a large cytoplasmic double-membrane vesicle termed the autophagosome [122]. Once completed, the outer membrane of the autophagosome fuses with the vacuole, allowing the inner membrane and cargo to become exposed to the lumenal contents of this organelle and degraded by resident hydrolases [123]. The breakdown products are finally released back into the cytosol to recycle the macromolecular constituents, and to generate energy to maintain cell viability under unfavorable conditions [124].

Our understanding of the molecular mechanism of autophagy has greatly been advanced by yeast genetic studies in the past 2 decades. So far, more than 40 autophagy-related (*ATG*) genes have

been identified in yeast, and most of the corresponding protein products are important factors that function to initiate, complete and regulate autophagy [125, 126]. Because most work has focused on the basic mechanism, how autophagy is regulated still remains largely unexplored. In particular, little is known about the complicated modulation of gene expression and specific transcriptional regulators of autophagy. The dysfunction of autophagy resulting from altered *ATG* gene expression is related to various human diseases, indicating the importance of proper regulation of autophagy at the transcription level [127]. In *S. cerevisiae*, a dramatic increase in *ATG8* and *ATG41* mRNA transcripts occurs when autophagy is induced, leading to a significant rise in the corresponding protein levels. Moreover, the expression level of Atg8 correlates with autophagosome size, whereas that of Atg41 is related to the frequency of autophagosome formation [128, 129]. These results suggest that transcriptional control—and especially that of *ATG8* and *ATG41*—is important in modulating autophagy [32, 128]. Our lab previously showed that the transcriptional regulator Ume6 can negatively modulate autophagy, by binding to the promoter region of *ATG8* in growing conditions [32]. Another recently published study showed that the positive transcriptional regulator Gcn4 regulates *ATG41* during starvation-induced autophagy [128]. Here, we decided to further investigate autophagy regulation through transcriptional modulation.

Transcription, accomplished by RNA polymerase II (RNAP II), is a dynamic and highly regulated process. The success of transcription requires contributions from different transcription accessory factors, one of which is the heterodimeric Spt4-Spt5 complex [130]. This complex can tightly associate with RNAP II in a transcription-dependent manner, and many studies have identified its essential role in promoting transcription elongation [130]. The homolog of the Spt4-Spt5 complex in complex eukaryotes, DRB sensitivity-inducible factor (DSIF, composed of SUPT4H1 and SUPT5H), also shows inhibitory activities in the early stage of transcription [131]. DSIF works with another multi-

subunit complex, the negative elongation factor (NELF) to impart a promoter-proximal pausing mechanism to regulate RNAP II activity [132]. This repressive state can be overcome by the positive transcription elongation factor b (P-TEFb) complex, phosphorylating POLR2A/RPB1 (the largest subunit of RNAP II) and the DSIF-NELF complex, which not only causes dissociation of NELF from RNAP II but also changes the DSIF status to promote transcription elongation [133-135]. Because there is no clear evidence showing the presence of NELF in yeast, most studies have only focused on the positive role of the Spt4-Spt5 complex in this organism. A recently published study does point out that there is a pause in early elongation specific to *S. pombe*, which resembles promoter-proximal pausing in metazoans [136], but it still remains an open question as to whether the Spt4-Spt5 complex can play a dual role in transcription in *S. cerevisiae*.

Here, we show that Spt4 may work as a negative transcriptional regulator of autophagy in *S. cerevisiae*. The deletion of *SPT4* leads to an increase in both mRNA and protein levels of *ATG8*/Atg8 and *ATG41*/Atg41 in growing conditions, and these changes correlate with an upregulated level of autophagy. During starvation, we observe a higher level of Spt5 phosphorylation, and the Sgv1/Bur1-Bur2 kinase complex, a homolog of P-TEFb, is responsible for this modification. The dephosphorylation of Spt5 or a transient loss of this protein results in autophagy deficiency and a clear reduction in *ATG41*/Atg41 expression, suggesting that Spt4 and Spt5 may play a distinct role in regulating autophagy. Chromatin immunoprecipitation (ChIP) analysis indicates that the Spt4-Spt5 complex can interact with DNA regions downstream of the transcription start site (TSS) on *ATG41* in an Spt4-dependent manner in growing conditions. Together this reveals the first time a negative function of Spt4 in budding yeast and provide the first identification of a negative regulator of *ATG41* expression. In addition, these studies also advance our understanding of the fine-tuned regulation of autophagy at the transcriptional level.

2.3 Result

2.3.1 Spt4 negatively regulates the transcription of *ATG8* and *ATG41* in growing conditions

The Spt4-Spt5 complex functions as a transcriptional factor, acting to promote transcription elongation in yeast. However, many regulatory factors have opposite effects on *ATG* genes compared to genes encoding proteins that function primarily during vegetative growth. Accordingly, we decided to examine the effect of mutations in Spt4 and Spt5 on *ATG* gene expression. *SPT5* is an essential gene; we therefore started our analysis with an *spt4*Δ strain. Initially, we focused on *ATG8* and *ATG41*, because these genes show the greatest increase in synthesis following autophagy induction. Furthermore, the Atg8 and Atg41 protein levels provide rapid indirect indicators for transcriptional induction of autophagy.

Protein extracts were prepared from cells in growing conditions and analyzed by western blot. When testing the protein level of Atg8, in both wild-type (WT) and mutant strains, we deleted the *PEP4* gene. Pep4 is a key hydrolase needed to activate many vacuolar enzymes; *pep4*Δ cells are largely protease defective [137]. It is important to use this background to monitor Atg8 protein levels. This is due to the fact that Atg8 (in the form conjugated to phosphatidylethanolamine [PE]) lines both sides of the phagophore and remains attached to the inner surface of the completed autophagosome; this portion of Atg8 is delivered to the vacuole and degraded, but this degradation is blocked in the absence of Pep4 [129]. Thus, the WT strain we refer to in this experiment actually corresponds to *pep4*Δ.

We observed a consistent increase in the Atg8 protein level (which was detected primarily as Atg8–PE) in growing conditions (SD-N, t = 0 h) in an *spt4*Δ strain relative to the WT control (Figure 2.1A,B). To determine the protein level of Atg41, we integrated a protein A (PA) epitope tag at the C terminus of *ATG41* at the chromosomal locus. Moreover, we used a *PEP4* WT strain to examine the Atg41 protein level because Atg41 is not degraded within the vacuole. As with Atg8, we observed a

massive upregulation of Atg41 in growing conditions when *SPT4* was deleted (Figure 2.1C,D). In contrast, upon starvation (SD-N, t = 2 h), the difference in Atg8 and Atg41 protein levels between WT and *spt4*Δ cells was not significant (Figure 2.1B,D), suggesting that the predominant negative effect of Spt4 on autophagy may take place in growing conditions; the protein level of Spt4 was similar under both growing and starvation conditions (Figure 2.S1A), indicating that the increase in Atg8–PE and Atg41 in the WT strain relative to the *spt4*Δ mutant during starvation was not due to the loss of Spt4 in the former.

Next, we examined the mRNA levels of *ATG8*, *ATG41* and other *ATG* genes in both WT and *spt4*Δ cells, by real-time quantitative PCR (RT-qPCR; Figure 1E). There was a relative increase of *ATG8* and an especially significant *ATG41* increase during the vegetative stage in *spt4*Δ cells, whereas no obvious change was observed for the other *ATG* genes that we examined. We used *YAT1* as a control in this analysis (Figure 2.1E). *YAT1* expression is downregulated in *spt4*Δ cells, presumably due to the loss of Spt4-dependent transcription elongation [138]. As expected, we found a decrease in *YAT1* expression in the absence of Spt4. We also examined the protein levels of some Atg proteins for which there was no obvious difference in gene expression in the *spt4*Δ cells, and observed no significant change in protein amount relative to the WT (Figure 2.S1B–D). Therefore, in growing conditions, Spt4 acts as a negative regulator in modulating the expression of at least *ATG8* and *ATG41* at the transcriptional level, a phenotype that is opposite to the known positive transcriptional role of Spt4.

2.3.2 Cells lacking Spt4 display increased autophagy activity

To test whether Spt4 can regulate autophagy activity, we applied 3 different well-established assays to measure autophagy activity in WT and *spt4*Δ cells. First, we measured autophagy activity using the quantitative Pho8Δ60 assay. In *S. cerevisiae*, *PHO8* encodes a vacuolar phosphatase that is delivered to the vacuole through the secretory pathway, leading to the activation of phosphatase activity [139].

We generated a truncated form of Pho8, Pho8Δ60, which lacks the N-terminal transmembrane domain and can only transit to the vacuole through nonselective autophagy [140]. Thus, by measuring the phosphatase activity in cells expressing only Pho8Δ60, we can measure autophagy flux. A significant increase in autophagy activity was observed in *spt4*Δ cells in 2 h nitrogen-starvation conditions compared to the WT cells (Figure 2.2A). This upregulated autophagy activity could also be seen in the mutant cells after a longer period of starvation, although the difference relative to the WT was reduced; this change likely reflects the fact that the negative effect of Spt4 is blocked in WT cells under starvation conditions so that the greatest difference is seen shortly after shifting out of growing conditions.

We then used the GFP-Atg8 processing assay. The principle behind this assay relies on the delivery of the population of GFP-Atg8 that is attached on the inner membrane of the autophagosome and exposed to the vacuolar hydrolases following autophagosome-vacuole fusion. Compared to Atg8, GFP is more resistant to degradation; thereby, free GFP is generated in the vacuole lumen, and the conversion of GFP-Atg8 into GFP can be a readout for nonselective autophagic degradation [141]. Because we determined that Spt4 can influence *ATG8*/Atg8 expression, we used the exogenous CUP1 promoter to drive GFP-Atg8 expression, thus eliminating Spt4-dependent effects. We observed an increasing amount of GFP-Atg8 processing in both WT and *spt4*Δ cells after starvation (SD-N), with more free GFP detected in *spt4*Δ cells compared to the WT (Figure 2.2B,C), indicating an elevated level of autophagy activity in the mutant cells.

To further support the results from the previous 2 assays, we used another method to monitor autophagy, which relies on the processing of precursor aminopeptidase I (prApe1). Ape1 is a resident vacuolar hydrolase that is initially synthesized as a cytosolic precursor with an N-terminal propeptide. The prApe1 can be delivered to the vacuole through either nonselective autophagy or the cytoplasm-

to-vacuole targeting (Cvt) pathway. Furthermore, this analysis can be conducted similar to a pulse-chase assay by taking advantage of the *vac8*Δ phenotype. In the absence of *VAC8*, prApe1 processing is blocked under vegetative conditions; upon starvation (that is, following autophagy induction), prApe1 is delivered to the vacuole through a process that still requires a receptor and scaffold protein for maximal efficiency [142]. Following delivery, prApe1 is processed to a mature, lower molecular mass species; thereby, we can monitor vacuolar delivery by western blot. As expected, in WT (*vac8Δ*) cells there was essentially no mature Ape1 in growing conditions (SD-N, t = 0), and a clear increase in this species with increasing time in starvation conditions (Figure 2.2D,E). We detected a higher level of prApe1 processing in *spt4*Δ *vac8*Δ cells with a faint band corresponding to mature Ape1 visible even at the 0 h time point, again suggesting an increase in autophagy activity.

Taken together, these results indicate that there is an elevated level of autophagy in *spt4*Δ cells, suggesting that Spt4 negatively regulates this process, and that the deletion of *SPT4* releases this repressive effect.

2.3.3. Spt5 phosphorylation correlates with the upregulation of *ATG41* expression and increased autophagy activity during starvation

After starvation, the protein levels of Atg8 and Atg41 in the WT strain are almost equivalent to those in the *spt4*Δ mutant (Figure 2.1B,D); this is not due to changes in the Spt4 protein level (Figure 2.S1A). In addition, there was no further increase in the protein amounts in *spt4*Δ cells, indicating that there is probably a mechanism for the release of Spt4-dependent negative regulation when autophagy is induced. Spt4 is a small protein with limited known functions, but its partner, Spt5, is required for transcription; previous reports have shown that the phosphorylation of SUPT5H/Spt5 is especially critical for processive transcription elongation [134]. Therefore, we decided to examine the

phosphorylation status of yeast Spt5 under starvation conditions and determine whether this modification can reverse the negative effect of Spt4.

We first used an Spt5-PA strain to monitor the expression and mobility of Spt5 in both nutrient-rich and nutrient-deprived conditions. In +N conditions we detected a single band of the expected molecular mass (150 kDa) for Spt5-PA (Figure 2.3A). When we starved cells, we again saw a band of 150 kDa, and a second band displaying reduced mobility. The same experiment was repeated using strains in which Spt5 was tagged with GFP and MYC, and we observed the same result-a single band in +N conditions, and a second band of higher molecular mass under starvation conditions (Figure 2.3A). Liu et al. (2009) generated antisera specific for the phosphorylated form of a 6-amino-acid consensus sequence derived from 15 repeats in the C terminus of Spt5 (anti-p-Spt5) [143]. Using this anti-p-Spt5 antibody, we detected a faint band in growing conditions, which became more intense after starvation, whereas the total protein amount of Spt5 remained at a similar level in both growing and starvation conditions (Figure 2.3B). To further examine the effect of Spt4 on regulation, we examined potential Spt5 phosphorylation in the *spt4*Δ strain. The phosphorylation of Spt5 was more obvious in *spt4*Δ cells than WT cells under growing conditions, and it was massively increased after starvation (Figure 2.3C). Using Spt5-PA and *spt4*Δ Spt5-PA strains, we detected a band shift of Spt5 in *spt4*Δ cells in growing conditions, similar to the level seen in WT cells following autophagy induction (Figure 2.3D). The above results suggest that Spt5 can be further phosphorylated under autophagy-inducing conditions, and there is an increased level of Spt5 phosphorylation in the absence of Spt4.

We next examined whether interfering with Spt5 phosphorylation would influence *ATG* expression and autophagy activity. Based on information from several previous studies [143-145], we decided to carry out site-directed mutagenesis on the last 7 serine residues (S1009, S1015, S1025, S1032, S1043, S1052, S1058) in the C terminus of Spt5. Conversion of these residues to alanine

resulted in the generation of a nonphosphorylable mutant, Spt5[S7A]. A clear mobility difference was observed between WT and Spt5[S7A] cells after starvation, indicating the relative absence of phosphorylation of Spt5 in Spt5[S7A]-expressing cells (Figure 2.4A). We further applied the GFP-Atg8 assay to test autophagy activity, which showed a significantly decreased GFP-Atg8 processing in mutant cells after starvation (Figure 2.4B,C); therefore autophagy activity was reduced when Spt5 phosphorylation was blocked. As predicted based on these results, Spt5[S7A] cells exhibited decreased mRNA and protein levels of *ATG41*/Atg41 in the nutrient-deficient condition, whereas there was no difference under growing conditions (Figure 2.4D,E). However, the influence of Spt5 dephosphorylation on *ATG8* mRNA level was not obvious, indicating that Spt5 may play a role primarily in regulating *ATG41* (Figure 2.S2A).

We also established a phosphomimetic form of the protein Spt5[S7E] by mutating the Spt5 serine residues in the C terminus to glutamate. We first measured autophagic activity in both Spt5[S7A] and Spt5[S7E] cells using the quantitative Pho8Δ60 assay. Compared to WT cells, Spt5[S7A] showed a decrease of autophagy activity, whereas the Spt5[S7E] mutant exhibited upregulated autophagy activity after 4 h of starvation (Figure 2.S2B). The GFP-Atg8 processing assay also indicated that autophagy activity was enhanced in Spt5[S7E] cells (Figure 2.S2C,D). Because Spt5 phosphorylation is maintained at a basal level in growing conditions and is further upregulated after starvation, the most obvious phenotype of the phosphomimetic mutant should be observed in nutrient-rich conditions. In agreement with our hypothesis, the mRNA level of *ATG41* showed a slight increase in the Spt5[S7E]-expressing cells in growing conditions, while the Atg41 protein level did not change compared to the WT in both growing and starvation conditions, suggesting that the slight increase in *ATG41* mRNA level was not sufficient to drive a detectable upregulation of the protein level (Figure 2.S2E,F). Thus,

with the Spt5[S7E] mutant, a positive role in transcription elongation of other factors may account for the observed increase in autophagy activity.

Because *SPT5* is an essential gene, we took advantage of an auxin-inducible degron (AID) system to generate an Spt5-inducible degradation strain [146]. After 30 min of auxin treatment, Spt5 protein levels were undetectable in the Spt5-inducible degradation strain (Spt5-AID-MYC), which provided us with a method to conditionally control the expression of this protein (Figure 2.S3A). With this strain, we used the GFP-Atg8 processing assay to test autophagy activity. The autophagy activity decreased when Spt5 was temporally depleted (Figure 2.S3B,C). Correspondingly, the expression of *ATG41*/Atg41 decreased when applying auxin treatment to the Spt5-AID strain (Figure 2.S3D,E). Therefore, in contrast to Spt4, Spt5 appears to always play a positive role in regulating autophagy, which agrees with its essential role in transcription elongation.

We extended this analysis by examining an additional Spt5 mutant. In this case, we transformed centromeric plasmids expressing *SPT5* WT and mutant (MUT; which contains an Spt5 derivative with 15 potentially phosphorylated C-terminal domain serine residues changed to alanine) into the Spt5-inducible degradation strain. These strains thus contain 2 copies of SPT5 after transformation; the application of auxin resulted in the degradation of the WT Spt5-AID-MYC. After starvation, WT cells treated with the chemical carrier DMSO and probed with the anti-p-Spt5 phospho-specific antiserum displayed 2 bands (Figure 2.S4A). The upper band corresponded to the phosphorylated Spt5 from the WT chromosomally integrated Spt5-AID-MYC, whereas the lower band marked the position of phosphorylated Spt5 expressed from the plasmid; only the WT form of the latter protein, not the [S15A] version, was detected with the anti-p-Spt5 serum. After auxin treatment, Spt5-AID-MYC was completely degraded so that the only species of Spt5 that remained was derived from the plasmid. In the nutrient-depleted condition, we observed a decreased *ATG41* mRNA level in mutant cells with

auxin treatment whereas the *ATG8* mRNA level showed no change (Figure 2.S4B); this was similar to results from Spt5[S7A] cells (Figure 2.4D and Figure 2.S2A). Therefore, we conclude that Spt4 plays a negative role in regulating *ATG41* in growing conditions, and that this inhibitory role is reversed by Spt5 phosphorylation when autophagy is induced.

2.3.4 The Sgv1/Bur1-Bur2 complex phosphorylates Spt5 after starvation

Yeast Sgv1/Bur1, which is similar in sequence to mammalian P-TEFb, can phosphorylate the C terminal domain of both Spt5 and RNAP II under normal growth conditions [143]. Sgv1 forms a complex with the regulatory protein Bur2, a divergent cyclin; the Sgv1-Bur2 complex together plays a role in regulating transcription [147]. Although *SGV1* is essential, *BUR2* is not an essential gene. Therefore, we analyzed Spt5-PA phosphorylation in WT and *bur2Δ* cells. The band shift of Spt5 that was observed in the WT strain following autophagy induction disappeared in *bur2Δ* mutant cells (Figure 2.5A). The phosphorylated band was also absent in the mutant cells probed with the anti-p-Spt5 antibody (Figure 2.5B). Therefore, the Sgv1-Bur2 complex is responsible for the observed phosphorylation of Spt5 in starvation conditions. Because the deletion of *BUR2* was sufficient to block the phosphorylation of Spt5, we further used the *bur2Δ* strain to examine its influence on *ATG41*. In the nutrient-deficient condition, both mRNA and protein levels of *ATG41*/ Atg41 decreased when *BUR2* was deleted (Figure 2.5C,D), which corresponded to our observations with the nonphosphorylable Spt5[S7A] mutant (Figure 2.4D,E).

In addition, we extended our analysis on the regulation of Spt5 by examining potential connections with other kinases in regulating autophagy. Rim15 plays a crucial role in integrating many nutrient-regulatory signals, and previous work from our lab has found that Rim15 positively regulates autophagy activity [148]. In *rim15*Δ cells, phosphorylation of the Sgv1 kinase was suppressed, and the phosphorylation of Spt5 was largely, but not completely, blocked under starvation conditions (Figure

2.5E), suggesting that Rim15 may function upstream of the Sgv1-Bur2 complex to control Spt5. However, mRNA and protein levels of *ATG41*/Atg41 showed no clear difference in the *rim15*Δ mutant, indicating that the partial block of Spt5 phosphorylation was not enough to affect *ATG41* expression (Figure 2.5F,G). Atg1 is the only protein kinase in the core autophagy machinery [54], and we further tested its potential effect on Spt5 phosphorylation. In *atg1*Δ cells, we could detect a partial decrease of the Spt5 phosphorylated band after starvation, but there was no significant change in *ATG41* mRNA level (Figure 2.S5A,B), which was similar to the phenotype of *rim15*Δ cells (Figure 2.5F,G). These results suggest that, after starvation, a small population of phosphorylated Spt5 may be sufficient to induce *ATG41* expression.

2.3.5 Spt5 binds to *ATG41* DNA in an Spt4-dependent manner

Based on the above experiments, the Spt4-Spt5 complex plays a major role in regulating *ATG41*/Atg41 expression. Thus, we decided to investigate the mechanism through which the Spt4-Spt5 complex regulates the transcription of *ATG41*. Because this complex is a transcription factor, we used a chromatin immunoprecipitation (ChIP) approach in both Spt5-PA and Spt4-PA strains to test whether this complex can directly bind to DNA. We designed several pairs of primers, each spanning approximately 130 to 170 nucleotides of different regions from the promoter to the open reading frame (ORF) of *ATG41*. The results showed that the +20 base pair (bp) and +110 bp regions in the ORF of *ATG41* were highly enriched in the DNA fragments precipitated with Spt5-PA, suggesting that Spt5 might bind tightly to these regions when autophagy is not induced (Figure 2.6A). A similar enrichment was also observed in the Spt4-PA strain in growing conditions (Figure 2.6B). The relative accumulation of the Spt4-Spt5 complex at these 2 regions near the TSS presumably reflects the normal situation, and thus maintains low expression of *ATG41* in growing conditions. In contrast, we did not observe an enrichment of *ATG1* DNA bound to Spt5-PA and Spt4-PA (Figure 2.S6A,B), in agreement with the

lack of an effect of Spt4 on *ATG1* expression (Figure 2.1E and Figure 2.S1D). In *spt4*Δ cells, the mRNA level of *ATG41* increased dramatically (Figure 2.1E), indicating active transcription of *ATG41* when Spt4 was absent. Accordingly, the increase in the enrichment of the *ATG41* +20 bp and +110 bp regions with Spt5-PA ChIP went down in *spt4*Δ cells compared to WT cells, suggesting a release from the temporary "halting" at the early stage of *ATG41* transcription (Figure 2.6C). Taken together, we propose that in nutrient-rich conditions, Spt4 acts negatively on Spt5, interfering with phosphorylation of the latter, and causing the complex to accumulate at regions near the *ATG41* TSS; this regulation is part of the mechanism that functions to maintain a low, basal level of gene expression.

2.4 Discussion

When facing different environmental stress conditions, it is important to finely tune the magnitude of autophagy in order to maintain cell homeostasis and prevent diseases. The efficient response of autophagy requires the upregulation of many *ATG* genes, among which *ATG8* and *ATG41* display the most dramatic changes. Previous studies from our lab have identified 2 transcription factors in autophagy: Ume6 as a repressor of *ATG8*, and Gcn4 as an activator of *ATG41* [32, 128]. We found that the absence of Ume6 did not affect the level of Atg41 (Figure 2.S7A). However, our understanding about the transcriptional regulation of even these genes is still limited. Here, we present data supporting a previously unknown negative role of Spt4 in regulating the expression of *ATG8* and *ATG41* in budding yeast. Furthermore, Spt4 is the first identified negative transcriptional regulator of *ATG41*, and this negative function was not due to a change of Gcn4 expression (Figure 2.S7B).

The heterodimeric Spt4-Spt5 complex is a highly conserved transcription regulator, and it can tightly bind to the coiled domain of RNAP II in a transcription-dependent manner [149]. Many studies have revealed the essential role of the Spt4-Spt5 complex in promoting transcription elongation, and, in more complex eukaryotes, further work on DSIF (the Spt4-Spt5 homolog), in conjunction with the

NELF complex, has indicated the existence of a mechanism that pauses transcription at the early stage. Genome-wide studies have revealed that pausing is widespread in mammalian cells, defined by a temporary halt of transcription within ~100 nucleotides downstream of the TSS [150]. The release from pausing relies on phosphorylation of the SUPT5H C terminus by the P-TEFb kinase, thereby changing the status of DSIF to positively regulate transcription elongation [133]. Follow-up precision run-on sequencing (PRO-seq) studies have also identified a promoter-proximal pause-like phenomenon in fission yeast [136].

However, in other organisms that lack NELF such as *S. cerevisiae*, currently there are no reports showing a role of the Spt4-Spt5 complex in transcriptional pausing; although PRO-Seq data provide an indication that Spt4 may have some negative role in transcription [136]. Compared to the published large-scale genome studies, our data show that the Spt4-Spt5 complex may act in a gene-specific manner in budding yeast, with Spt4 having an additional and clear negative role for certain *ATG* genes under growing conditions. This type of regulation fits with the observation that stress-response genes, such as *ATG* genes are regulated in a manner that is opposite to most genes encoding proteins that function during vegetative growth [47, 151]. The deletion of *SPT4* leads to an increase of *ATG8*/Atg8 and *ATG41*/Atg41, and the change in *ATG41* expression in particular facilitates an increase in autophagy activity. After starvation, we observed an enhanced phosphorylation of Spt5. Of note, Spt5 phosphorylation also increases when *SPT4* is absent. Accordingly, the dephosphorylation of Spt5 results in a clear autophagy deficiency and a significant decrease in *ATG41* expression, which demonstrates that Spt5 phosphorylation is important for regulating autophagy after starvation, with Spt4 having a largely negative role in regulation for *ATG41*. The deletion of *BUR2*, the regulatory partner of the Sgv1 kinase complex, blocks Spt5 phosphorylation and leads to a lower expression of *ATG41*/Atg41, further suggesting the importance of Spt5 phosphorylation in *ATG41* transcription. In

addition, both Spt4 and Spt5 can bind to the DNA region in the ORF of *ATG41*, whereas the absence of Spt4 prevents the accumulation of Spt5 at the *ATG41* TSS, suggesting that Spt4 might influence the function of Spt5 by controlling its access to the Sgv1 kinase, and its subsequent interaction with DNA.

2.5 Materials and methods

2.5.1 Yeast strains, media and culture conditions

Yeast strains used are listed in Table 2.1. We applied standard methods to generate gene deletions and/or for C-terminal tagging [152, 153]. Yeast cells were grown in rich medium at 30°C (YPD: 1% [w:v] yeast extract, 2% [w:v] peptone, and 2% [w:v] glucose). Autophagy was induced upon nitrogen starvation by shifting mid-log phase cells from YPD to SD-N (0.17% yeast nitrogen base without ammonium sulfate or amino acids, and 2% [w:v] glucose) for the indicated times.

2.5.2 Antibodies and antisera

Anti-YFP antibody, which detects GFP, was from Clontech (JL-8; 63281), anti-PA antibody was from Jackson Immuno Research (323-005-024), anti-MYC was from Sigma (M4439), and anti-Pgk1 is a generous gift from Dr. Jeremy Thorner (University of California, Berkeley). Anti-p-Spt5 antibody was generously provided by Dr. Steven Hahn [143]. Antibodies to Ape1, Atg1 and Atg8 were described previously [154-156].

2.5.3 Plasmids

GFP-Atg8(405) contains the GFP-Atg8 open reading frame with the endogenous *ATG8* promoter. pCu-GFP-ATG8(405) was constructed by replacing the endogenous *ATG8* promoter with the *CUP1* promoter, containing the GFP-Atg8 open reading frame [157]. These plasmids were linearized and integrated into the corresponding strains listed in Table 2.1. Plasmids expressing Flag-tagged WT Spt5 and Spt5[S15A] were provided by Dr. Steven Hahn [143].

2.5.4 Real-time quantitative PCR

Yeast cells were cultured in YPD to mid-log phase and shifted to SD-N for autophagy induction. Total RNA was extracted with an RNA extraction kit (NucleoSpin RNA II; Clontech, 740955.50), and reverse transcription was undertaken using the High-Capacity cDNA Reverse Transcription Kit (ThermoFisher Scientific, 4368814). RT-qPCR was performed using the Power SYBR Green PCR Mix (ThermoFisher Scientific, 4367659) or Radiant Green Lo-ROX qPCR kit (Alkali Scientific, QS1020). All primer information can be found in Table 2.2.

2.5.5 Auxin-inducible degron (AID) system and transcriptional inhibition

WLY176 cells were first transformed with the plasmid pNHK53 (*ADH1p-OsTIR1-9MYC*; National BioResource Project–Yeast [Japan]), and Spt5 was then tagged with AID-9MYC (Addgene, 99522; deposited by Dr. Helle Ulrich) by homologous recombination. The auxin-inducible degron (AID) refers to the 71–116 amino acids of the AT1G04250/ATIAA17 protein in plants. To control Spt5 protein levels, the cells were treated with 300 μM 3-indoleacetic acid (auxin; Sigma, I2886) or DMSO (vehicle) in the vegetative condition for 30 min to induce degradation of Spt5. Then the cells were shifted to SD-N for nitrogen starvation with application of auxin or DMSO. After 1 h of starvation and treatment, samples were collected for western blot and RNA extraction.

2.5.6 Chromatin immunoprecipitation (ChIP)

ChIP was performed with some modifications from a method described previously [158]. The strains that are used in the study are Spt5-PA (WXY102), Spt4-PA (WLY106) and *spt4Δ* Spt5-PA (WXY103). After yeast cells grew to OD600 ~ 0.8 in YPD medium, a final concentration of 1% formaldehyde was added to perform cross-linking and the cultures were shaken for 20 min at room temperature. Glycine was added to 0.2 M to stop cross-linking. Samples were then harvested, washed in PBS and resuspended in FA lysis buffer (50 mM HEPES, pH 7.5, 150 mM NaCl, 1 mM EDTA, 1% Triton X-100 [Sigma, T8787], 0.1% sodium deoxycholate [Sigma, D6750], 0.1% SDS). The cells were lysed

with glass beads by being vortexed at 4°C, and then were centrifuged at 1000 x g for 1 min. The supernatant was collected for sonication (4 cycles of 25 s on, 59 s off, pulse at a power output of 20%) at 4°C. Sonicated samples were collected by centrifugation, and the supernatant was collected and then divided into input and IP fractions. Half of the IP fractions were incubated with IgG Sepharose 6 Fast Flow beads (Fisher Scientific, 45-000-173) while the other half were incubated with PA beads ("non-antibody" mock control) for 4 h at 4°C. After immunoprecipitation, the beads were washed with FA lysis buffer and wash buffer (10 mM Tris-HCl, pH 8.0, 0.25 M LiCl, 1 mM EDTA, 0.5% Nonidet P-40 [IGEPAL; Fisher Scientific, NC9983875], 0.5% sodium deoxycholate), resuspended in elution buffer (50 mM Tris-HCl, pH 7.5, 10 mM EDTA, 1% SDS) and incubated at 70°C for 12 min (with mixing by vortex every 3 min). With the addition of proteinase K (Fisher Scientific, NC9404543), reverse cross-linking was performed by incubation for 2 h at 42°C followed by 6 h at 65°C. The reverse cross-linked samples were then incubated with RNase A (Qiagen, 19,101) at 37°C for 30 min. The purified DNA was examined by RT-qPCR analysis, which was performed using the Power SYBR Green PCR Mix (ThermoFisher Scientific, 4367659). The information for all primers is listed in Table 2.2.

2.5.7 Other methods

Western blot, GFP-Atg8 processing, and prApe1 processing were described previously [3].

2.5.8 Statistical analysis

Two-tailed Student's t test and two-tailed paired Student's t test were used to determine statistical significance.

Table 2.1 List of strains used in this study

Name	Genotype	Reference
BY4741	MATa *his3Δ1 leu2Δ0 met15Δ0 ura3Δ0*	[159]
BY4742	MATα *his3Δ1 leu2Δ0 lys2Δ0 ura3Δ0*	[159]
DGY047	WLY176 *SPT5-MYC::TRP1*	This study
DGY048	WLY176 *SPT5-MYC* S1009A S1015A S1025A S1032A S1043A S1052A S1058A*::TRP1*	This study
DGY049	WLY176 *SPT5-MYC* S1009E S1015E S1025E S1032E S1043E S1052E S1058E*::TRP1*	This study
DGY050	WLY176 *GFP-ATG8(405)::LEU2 SPT5-MYC::TRP1*	This study
DGY051	WLY176 *GFP-ATG8(405)::LEU2 SPT5-MYC* S1009A S1015A S1025A S1032A S1043A S1052A S1058A*::TRP1*	This study
DGY052	WLY176 *GFP-ATG8(405)::LEU2 SPT5-MYC* S1009E S1015E S1025E S1032E S1043E S1052E S1058E*::TRP1*	This study
JMY97	WLY176, *ume6Δ::HIS3*	[32]
JMY347	SEY6210, *ZEO1p-pho13Δ pho8Δ60, CUP1p-GFP-ATG8(405)::LEU2*	This study
SEY6210	MATα *leu2-3,112 ura3-52 his3-Δ200 trp1-Δ901 suc2-Δ9 lys2-801; GAL*	[159]
TVY1	MAT*α leu2–3,112 ura3–52 his3-Δ200 trp1-Δ901 lys2–801 suc2-Δ9 GAL pep4Δ::LEU2*	[160]
WLY176	SEY6210 *pho13Δ pho8Δ60*	[93]
WXY100	TVY1 *spt4Δ::HIS3*	This study
WXY101	TVY1 *bur2Δ::URA3*	This study
WXY102	WLY176 *SPT5-PA::TRP1*	This study
WXY103	WLY176 *spt4Δ::KAN SPT5-PA::TRP1*	This study
WXY104	WLY176 *bur2Δ::URA3 SPT5-PA::TRP1*	This study
WXY105	WLY176 *spt4Δ::HIS3*	This study
WXY106	WLY176 *SPT4-PA::TRP1*	This study
WXY107	WLY176 *SPT5-GFP::KAN*	This study
WXY108	WLY176 *ATG5-PA::TRP1*	This study
WXY109	WLY176 *spt4Δ::KAN ATG5-PA::TRP1*	This study
WXY110	WLY176 *ATG20-PA::TRP1*	This study
WXY111	WLY176 *spt4Δ::URA3 ATG20-PA::TRP1*	This study
WXY112	WLY176 *CUP1p-GFP-ATG8(405)::LEU2*	This study
WXY113	WLY176 *spt4Δ::URA3 CUP1p-GFP-ATG8(405)::LEU2*	This study
WXY114	ZYY108 *spt4Δ::URA3*	This study
WXY115	WLY176 *bur2Δ::KAN*	This study
WXY116	WLY176 *bur2Δ::KAN ATG41-PA::TRP1*	This study
WXY117	WLY176 *SPT5-PA::TRP1 SGV1-MYC::KAN*	This study
WXY120	WLY176 *rim15Δ::URA3 SPT5-PA::TRP1 SGV1-MYC::KAN*	This study
WXY121	BY4741 *vac8Δ::HIS3*	This study
WXY122	BY4741 *spt4Δ::URA3 vac8Δ::HIS3*	This study

WXY123	WLY176 *rim15Δ::URA3*	This study
WXY124	ZYY108 *rim15Δ::URA3*	This study
WXY125	WLY176, *pNHK53::URA3 SPT5-AID-MYC::KAN*	This study
WXY126	SEY6210, *atg1Δ::HIS3*	This study
WXY127	ZYY108 *SPT5-MYC::TRP1*	This study
WXY128	ZYY108 *SPT5-MYC* S1009A S1015A S1025A S1032A S1043A S1052A S1058A*::TRP1*	This study
WXY129	ZYY108 *ume6Δ::URA3*	This study
WXY130	ZYY124 *spt4Δ::URA3*	This study
WXY131	JMY347, *spt4Δ::URA3*	This study
WXY132	ZYY108 *SPT5-MYC* S1009E S1015E S1025E S1032E S1043E S1052E S1058E*::TRP1*	This study
WXY133	WXY125, *CUP1p-GFP-ATG8(405)::LEU2*	This study
WXY134	WXY125, *ATG41-PA:: TRP1*	This study
YZY007	BY4742 *arg4Δ::URA3*	This study
YZY076	BY4742 *arg4Δ::URA3 rim15Δ::KAN*	This study
ZYY108	WLY176 *ATG41-PA::HIS3*	[128]
ZYY124	WLY176 *GCN4-PA::LEU2*	[128]

Table 2.2 Oligonucleotide primers used in this study

Name	Sequence	Use
ATG1_F	ATCTAAGATGGCCGCACATATG	*ATG1* mRNA level check
ATG1_R	AGGGTAGTCACCATAGGCATTC	*ATG1* mRNA level check
ATG5_F	TCGGTCAACGAAGCTCGAAA	*ATG5* mRNA level check
ATG5_R	GATGAGCGGTATATGTCGCG	*ATG5* mRNA level check
ATG7_F	ATGAGCATTGTCCAGCATGTAG	*ATG7* mRNA level check
ATG7_R	GACCTCCTGCTTTATGACTGAC	*ATG7* mRNA level check
ATG8_F	GAAGGCCATCTTCATTTTTGTC	*ATG8* mRNA level check
ATG8_R	TTCTCCTGAGTAAGTGACATAC	*ATG8* mRNA level check
ATG9_F	CGTACTAACAGAGTCTTTCCTTG	*ATG9* mRNA level check
ATG9_R	CTAAGACACCACCCTTATTGAG	*ATG9* mRNA level check
ATG20_F	CAGGTAGCGGTGGGAAATCA	*ATG20* mRNA level check
ATG20_R	TGCGGTATGCGGATCTGTTT	*ATG20* mRNA level check
ATG41_F	CGAGTACTGAAGACGATTGCAT	*ATG41* mRNA level check *ATG41* ChIP-qPCR check
ATG41_R	TGCGACATTGGCAAAGGCAT	*ATG41* mRNA level check *ATG41* ChIP-qPCR check
YAT1_F	CTCGGTTTGCGTCGCTCATG	*YAT1* mRNA level check
YAT1_R	GTAGCCGGACAACAGGTATT	*YAT1* mRNA level check
ALG9_F	CACGGATAGTGGCTTTGGTGAACAATTAC	RT-qPCR check
ALG9_R	TATGATTATCTGGCAGCAGGAAAGAACTTGGG	RT-qPCR check
TFC1_F	GCTGGCACTCATATCTTATCGTTTCACAATGG	ChIP-qPCR check
TFC1_R	GAACCTGCTGTCAATACCGCCTGGAG	ChIP-qPCR check

ATG1-500_F	TCCTTGTTCGTTTCGTGTATCTG	*ATG1* ChIP-qPCR check
ATG1-500_R	GGTTTAAGAAATCAGAGCCGAGC	*ATG1* ChIP-qPCR check
ATG1+80_F	TAAAGATCACACAACCTCTGTGAACC	*ATG1* ChIP-qPCR check
ATG1+80_R	GATACTTCCTTTATGGCTACATGCTG	*ATG1* ChIP-qPCR check
ATG1+330_R	ATTGACTGTGAACGAACATCAACAG	*ATG1* ChIP-qPCR check
ATG1+330_F	GGTTCTCACTCGGTGGAGGGTATTT	*ATG1* ChIP-qPCR check
ATG41-100_F	GCGGCTCTGCGTAAAAAGGT	*ATG41* ChIP-qPCR check
ATG41-100_R	TTGGTTGGTTTGGTGTAGCC	*ATG41* ChIP-qPCR check
ATG41+20_F	GGCTACACCAAACCAACCAA	*ATG41* ChIP-qPCR check
ATG41+20_R	GGCTCGAAAGCAACGTTTGA	*ATG41* ChIP-qPCR check
ATG41+110_F	TCAAACGTTGCTTTCGAGCC	*ATG41* ChIP-qPCR check
ATG41+110_R	GTGCATTCTGACTCATCGAC	*ATG41* ChIP-qPCR check
ATG41+200_F	TTTTCCGCTATCGTACCCGA	*ATG41* ChIP-qPCR check
ATG41+200_R	TCCTTACTAGCAGCAGCAAC	*ATG41* ChIP-qPCR check
ATG8-20_F	GGGAACCATTAAAGGTTGAGGAG	*ATG8* ChIP-qPCR check
ATG8-20_R	AATCCTCTCCGACTCCGCCTTC	*ATG8* ChIP-qPCR check
ATG8+50_F	ACTAGAGACATGAAGTCTACATTTAAGTCT	*ATG8* ChIP-qPCR check
ATG8+50_R	TCAGCAGGAACTAGATATTTACGCTTATCA	*ATG8* ChIP-qPCR check
ATG8+150_F	GGAGAGGATTGCTGACAGGTTCAAG	*ATG8* ChIP-qPCR check
ATG8+150_R	AAATGAAGATGGCCTTCTCAGGGGG	*ATG8* ChIP-qPCR check

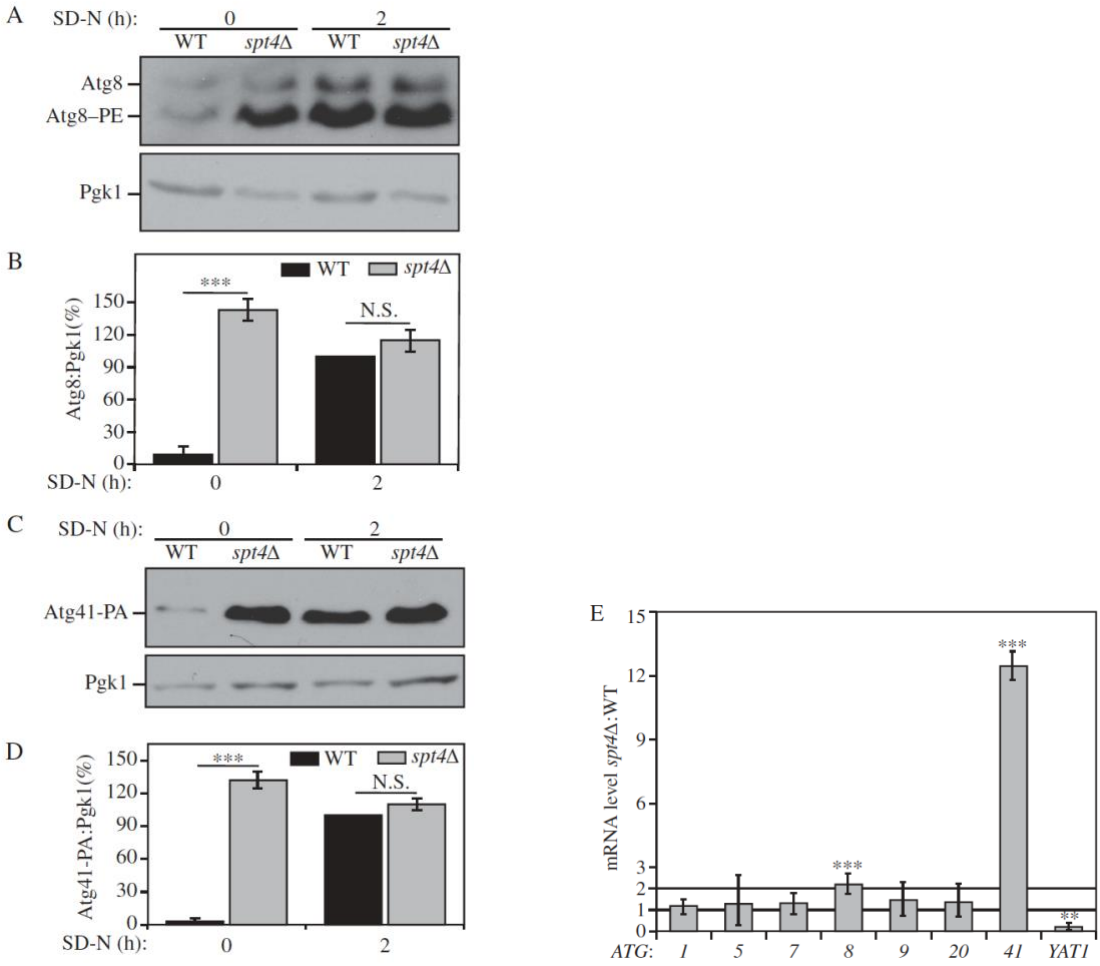

Figure 2.1 Spt4 negatively regulates *ATG8*/Atg8 and *ATG41*/Atg41 expression in growing conditions

(**A-D**) Analysis of Atg8 and Atg41 protein levels. Protein extracts were generated from (**A**) wild-type (TVY1, *pep4*Δ) and *spt4*Δ (WXY100, *pep4*Δ) cells, or (**C**) wild-type (ZYY108) and *spt4*Δ (WXY114) cells expressing Atg41-PA, after growth in YPD to mid-log phase (growing conditions) and shifted to SD-N medium for 2 h (nitrogen starvation). Western blots were probed with anti-Atg8, anti-PA and anti-Pgk1 (loading control) antisera or antibodies. (**B and D**) Quantitative analysis of Atg8 and Atg41 protein levels, respectively. The protein level of either Atg8 or Atg41-PA after 2 h of starvation was set as 1 and other values were normalized; the error bar represents the SEM of at least 3 independent experiments. N.S., not significant, ***, $p < 0.005$. (**E**) Wild-type (WLY176) and *spt4*Δ (WXY105) cells were cultured until mid-log phase and collected in growing conditions. mRNA levels were quantified by RT-qPCR. The mRNA level of different *ATG* genes and *YAT1* (negative control) in *spt4*Δ cells were normalized to that of the corresponding genes in wild-type cells, which was set as 1. Error bars represent the SEM of at least 3 independent experiments; two-tailed t test was used for statistical significance. p values are reported for the comparison between WT and *spt4*Δ strains in growing conditions. **, $p < 0.01$; ***, $p < 0.005$.

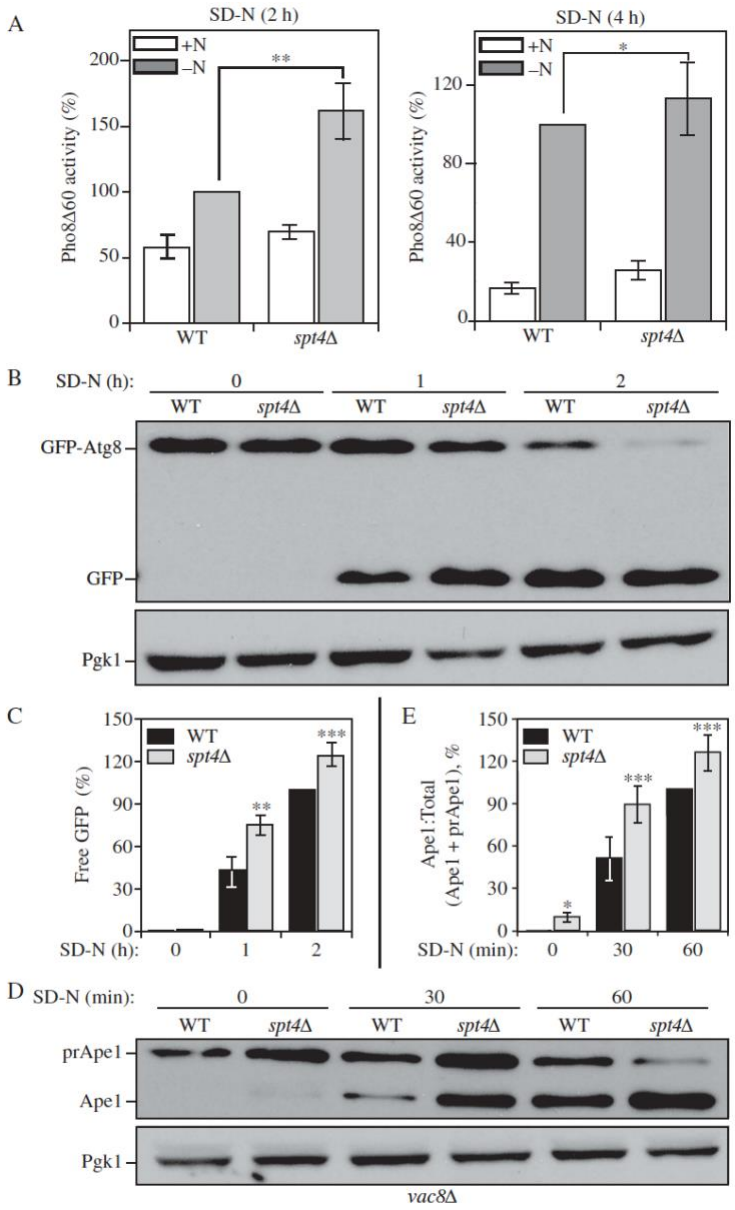

Figure 2.2 Spt4 negatively regulates autophagy activity

(**A**) Autophagy activity was measured with the quantitative Pho8Δ60 assay in WT (JMY347) and *spt4*Δ (WXY131) cells under growing conditions (+N) and after 2 or 4 h of nitrogen starvation (-N). Error bars represent the SEM of at least 3 independent experiments. *, $p < 0.05$; **, $p < 0.01$. (**B**-**C**) Autophagy activity was measured using the GFP-Atg8 processing assay. Wild-type (WXY112) and *spt4*Δ cells (WXY113) with *CUP1* promoter-driven *GFP-ATG8* were grown to mid-log phase in YPD and then starved (SD-N) for the indicated times. Samples from growing (YPD, 0 h) and starvation (SD-N, t = 1–2 h) conditions were collected. Proteins were analyzed by western blot with anti-YFP antibody and anti-Pgk1 (loading control) antiserum. The quantitative analysis of processed GFP is shown in (**C**), and the error bar represents the SEM of 3 independent experiments. The processed GFP after 2 h of starvation was set as 1, and other values were normalized. *, $p < 0.05$; **, $p < 0.01$. (**D**-**E**) Wild-type (WXY121) and *spt4*Δ (WXY122) cells with a deletion of *VAC8* were collected in both growing (YPD) and starvation (SD-N, t = 30–60

min) conditions. The precursor (pr) and mature forms of Ape1 were separated by SDS-PAGE and detected with anti-Ape1 antiserum by western blot. Pgk1 was used as a loading control. The ratio of processed Ape1 was quantified in (**E**), and the error bar represents the SEM of 3 independent experiments. The maturation of prApe1 after 60 min of starvation has been set as 1, and other values were normalized. *, $p < 0.05$; ***, $p < 0.005$.

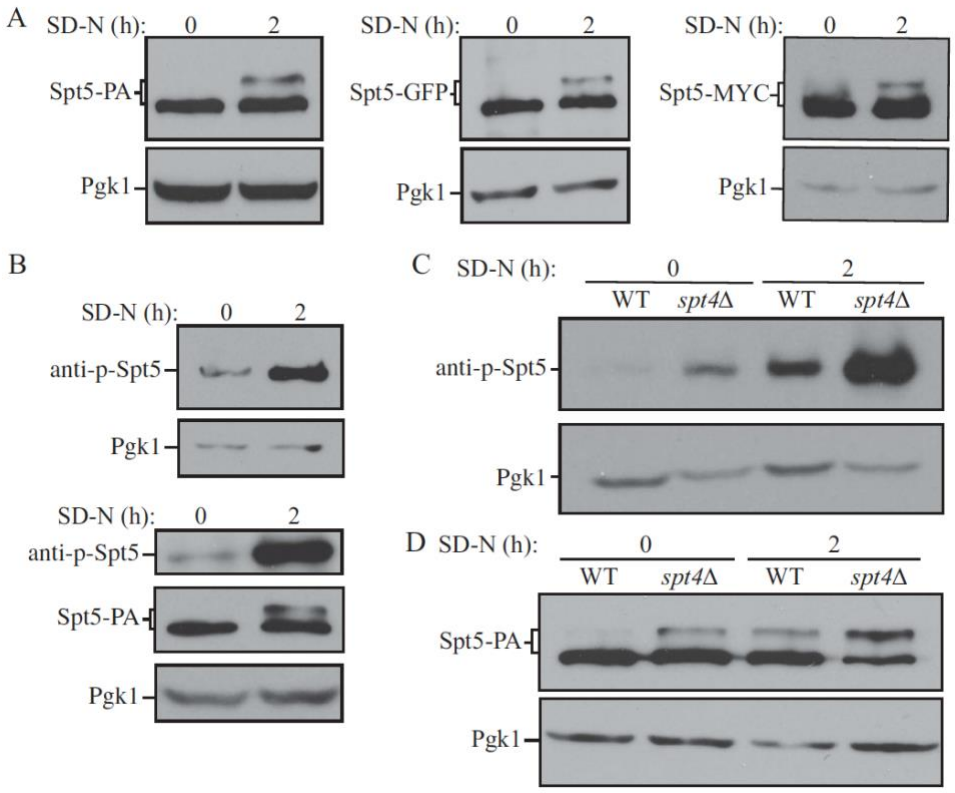

Figure 2.3 Spt5 phosphorylation is enhanced after starvation or in the absence of Spt4
(**A**) The protein A (PA)-, GFP- and MYC-tagged Spt5 strains (WXY102, WXY107, DGY047) were collected in growing (YPD, mid-log phase) and starvation (SD-N, t = 2 h) conditions. The samples were separated by SDS-PAGE and detected by western blot with anti-PA, anti-YFP or anti-MYC antibodies. Anti-Pgk1 antiserum was used to detect the loading control. (**B**) Wild-type (SEY6210) cells were grown to mid-log phase in growing conditions (YPD) and then starved (SD-N) for 2 h. Samples under these 2 conditions were collected and analyzed by western blot. An antibody specific for the phosphorylated form of Spt5 (anti-p-Spt5) was used to detect the phosphorylated band (upper blot). We also examined phosphorylation in a strain expressing Spt5 tagged with PA (WXY102); the total protein level of Spt5 was detected with anti-PA and the phosphorylation of Spt5 was monitored with the anti-p-Spt5 antibody (lower blot) (**C**) Samples from wild-type (WLY176) and *spt4*Δ (WXY105) strains were collected in both growing (YPD) and starvation (SD-N, t = 2 h) conditions for western blot analysis. Spt5 phosphorylation was monitored with the anti-p-Spt5 antibody. (**D**) The Spt5-PA level of wild-type (WXY102) and *spt4*Δ (WXY103) cells in growing (YPD) and starvation (SD-N) conditions was detected by western blot with anti-PA antibodies.

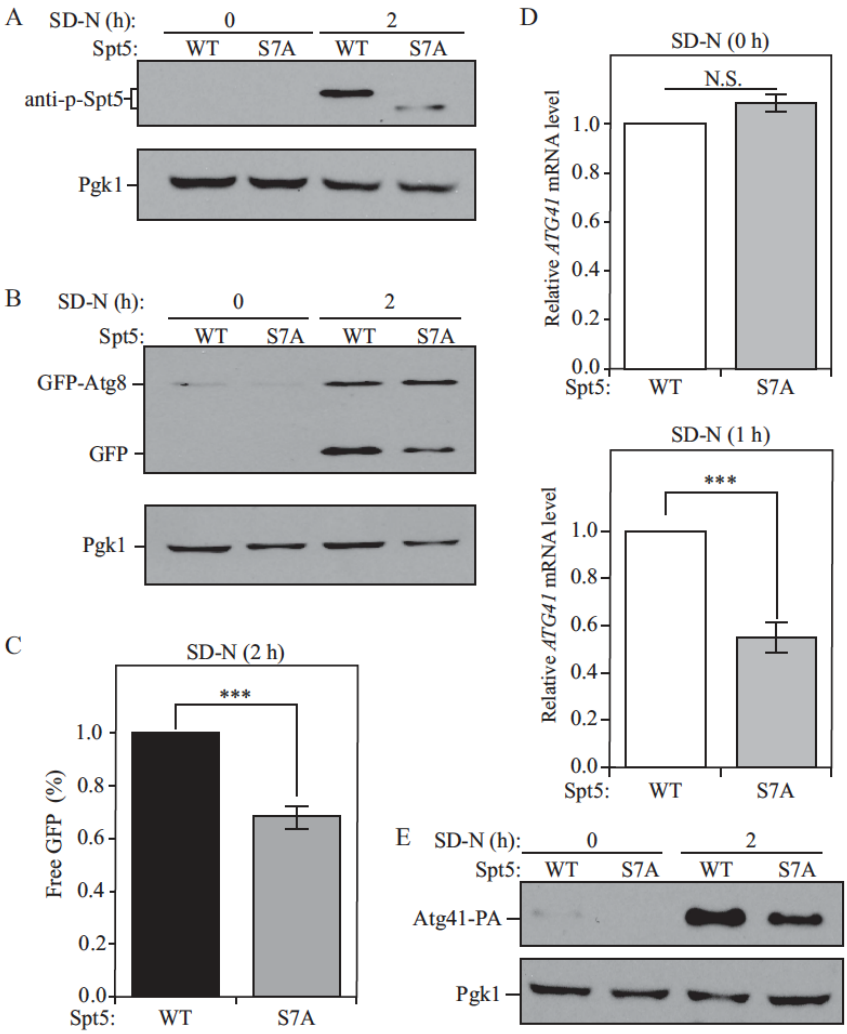

Figure 2.4 Dephosphoryaltion of Spt5 negatively modulates autophagy by downregulating *ATG41* mRNA and protein levels after starvation

(**A**) Samples collected from cells expressing WT (DGY047) and nonphosphorylable Spt5 (DGY048) were analyzed by western blot. The phosphorylation of Spt5 was detected with the specific anti-p-Spt5 antibody. (**B-C**) Autophagy activity was measured by GFP-Atg8 processing in WT (DGY050) and Spt5[S7A] (DGY051) cells harboring endogenous *GFP-ATG8* plasmids under growing conditions and after 2 h of starvation. The quantitative analysis of processed GFP after starvation (there is no processed GFP in the growing condition) is shown in (**C**), and the error bar represents the SEM of 3 independent experiments. The processed GFP of the WT strain after starvation was set as 1, and other values were normalized. ***, $p < 0.005$. (**D**) The mRNA level of *ATG41* in WT (DGY047) and Spt5[S7A] (DGY048) cells was measured by RT-qPCR under growing conditions and starvation (SD-N, 1 h). The error bar represents the SEM of 3 independent experiments, and p values are reported for the comparison between the wild-type and Spt5[S7A] strains during starvation. N.S., not significant, ***, $p < 0.005$. (**E**) The anti-PA antibody was used to detect Atg41-PA in samples (WT, WXY127; Spt5[S7A], WXY128) collected from growing and starvation (SD-N, 2 h) conditions by western blot analysis.

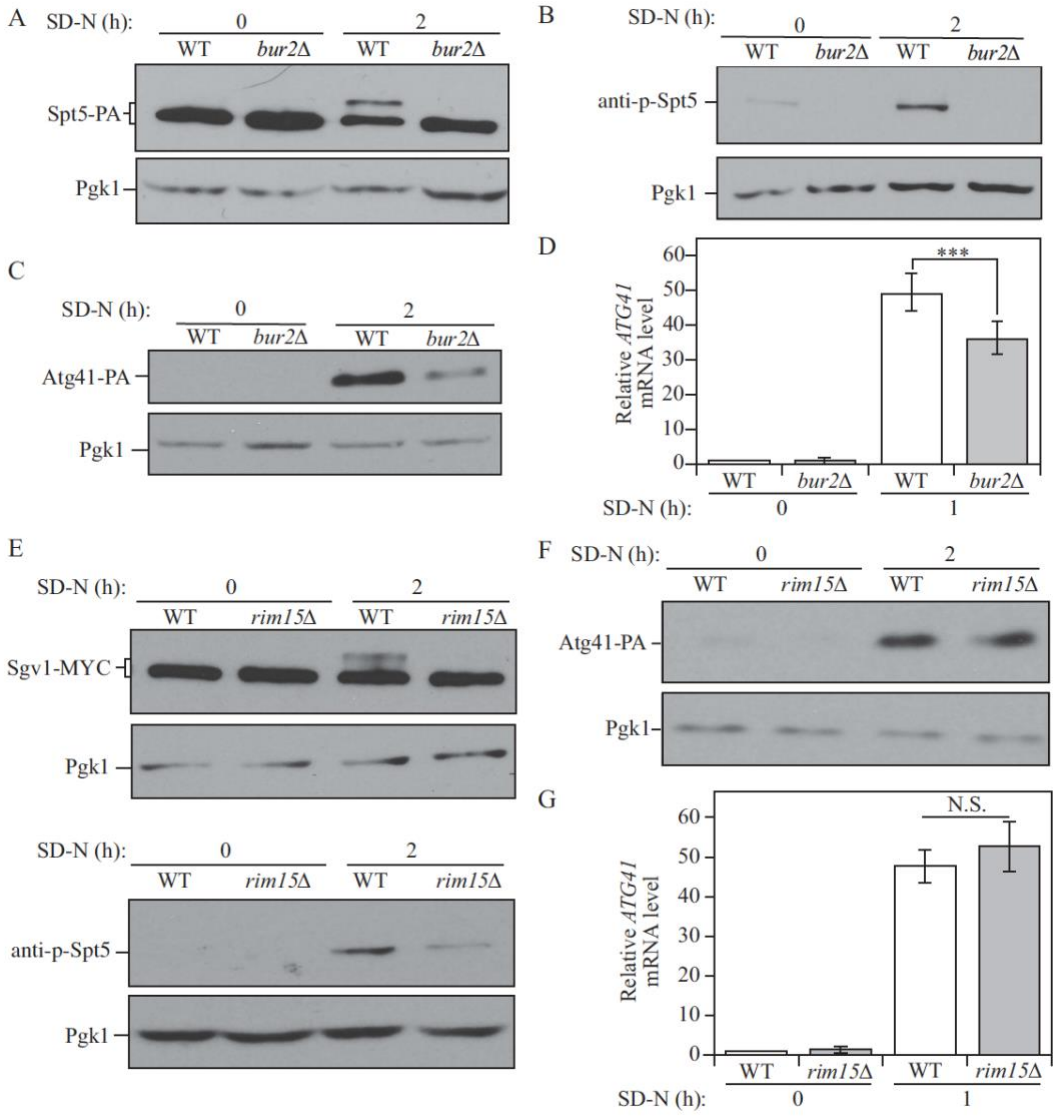

Figure 2.5 The Sgv1-Bur2 complex is responsible for Spt5 phosphorylation after starvation, and Sgv1 is phosphorylated under starvation conditions by the Rim15 kinase

(**A**) Samples from the Spt5-PA wild-type (WXY102) and *bur2*Δ (WXY104) strains were collected in both growing (YPD) and starvation (SD-N) conditions for western blot analysis. Anti-PA antibody and anti-Pgk1 antiserum were used to detect the indicated proteins. (**B**) The Spt5 phosphorylation was detected with anti-p-Spt5 antibody in wild-type (WLY176) and *bur2*Δ (WXY115) samples collected from growing (YPD) and starvation (SD-N, t = 2 h) conditions. (**C**) The Atg41-PA level was probed with anti-PA antibody in wild-type (ZYY108) and *bur2*Δ (WXY116) cells from growing (YPD) and starvation (SD-N, t = 2 h) conditions. (**D**) The wild-type (WLY176) and *bur2*Δ (WXY115) cells were cultured until mid-log phase in growing conditions (YPD) and then shifted to starvation conditions (SD-N) for 1 h. The mRNA level of *ATG41* was measured by RT-qPCR. The error bar represents the SEM of 3 independent experiments, and p values are reported for the comparison between the wild-type and *bur2*Δ strains during starvation. ***, $p < 0.005$. (**E**) The Sgv1-MYC wild-type (WXY117) and *rim15*Δ (WXY120) strains were grown in YPD to mid-log phase and then shifted to starvation conditions

(SD-N) for 2 h. The samples were then collected and analyzed by western blot using antibodies to MYC. The samples from wild-type (WLY176) and *rim15*Δ (WXY123) cells were also collected and Spt5 phosphorylation was detected with the anti-p-Spt5 antibody. Pgk1 was used as the loading control. (**F**) The Atg41-PA wild-type (ZYY108) and *rim15*Δ (WXY124) cells were collected in both growing (YPD) and starvation (SD-N) conditions for western blot analysis. Anti-PA antibody and anti-Pgk1 antiserum were used to detect the indicated proteins. (**G**) RT-qPCR analysis of *ATG41* mRNA level in WT (WLY176) and *rim15*Δ (WXY123) cells under growing and starvation conditions. The error bar represents the SEM of 3 independent experiments.

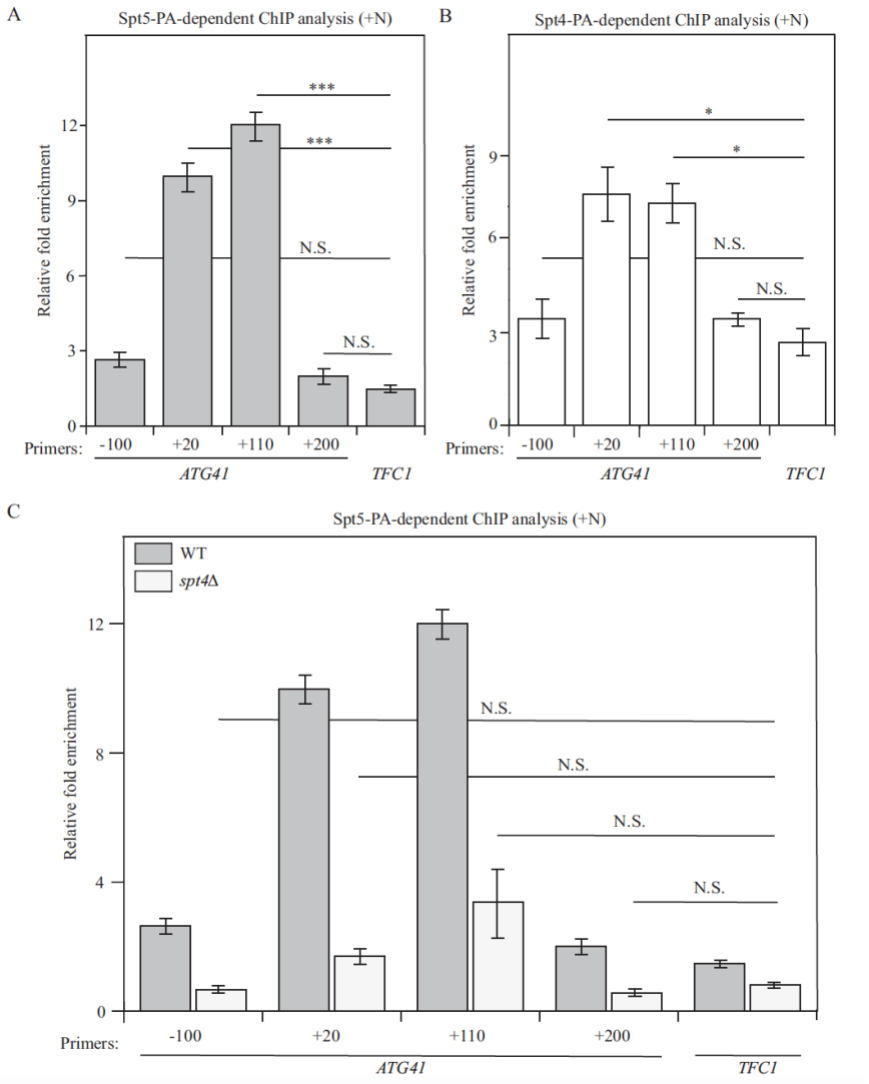

Figure 2.6 Spt5 binds to *ATG41* DNA in an Spt4-dependent manner

(**A-C**) Chromatin immunoprecipitation (ChIP) was done in Spt5-PA (WXY102), Spt4-PA (WXY106) and *spt4*Δ Spt5-PA (WXY103) strains. The ChIP samples were collected in the growing condition (mid-log phase). RT-qPCR was used for quantitative analysis. The primers for ChIP cover different DNA regions from the promoters through the ORF in *ATG41*. "-" indicates upstream of the *ATG* start codon, and "+" indicates downstream of the *ATG* start codon. (**A**) RT-qPCR analysis of ChIP samples of the Spt5-PA (WXY102) strain. The values were normalized to the input. The error bars show the SEM of at least 3 independent experiments. p values in each region are reported for the comparison with the negative control, *TFC1*. ***, $p < 0.005$; N.S., not significant. (**B**) RT-qPCR analysis of ChIP samples of the Spt4-PA (WXY106) strain. The error bars show the SEM of at least 3 independent experiments: *, $p < 0.05$; N.S., not significant. (**C**) RT-qPCR analysis of ChIP samples of Spt5-PA (WXY102) and *spt4Δ* Spt5-PA (WXY103) cells. The values were normalized to the input DNA. *TFC1* was used as a negative control and the error bars represent the SEM of at least 3 independent experiments. The significance analysis for *spt4Δ* strains was noted: N.S., not significant.

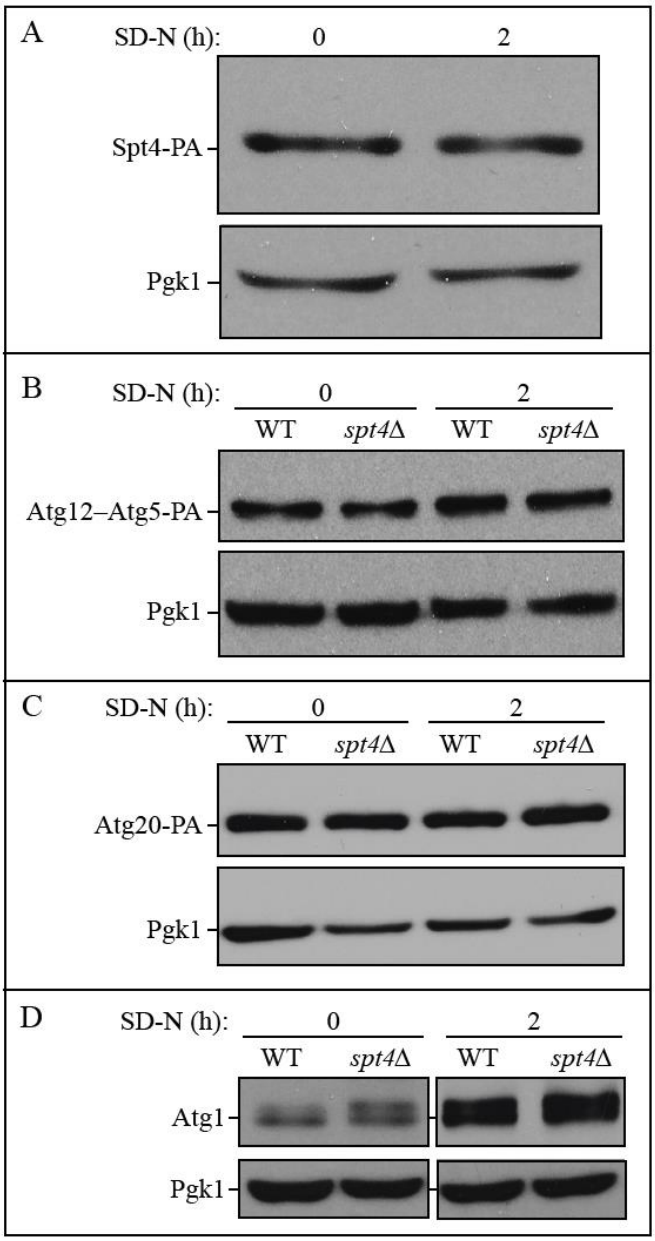

Figure 2.S1 Spt4 protein level does not change after starvation, and protein levels of Atg5, Atg20 and Atg1 remain similar in *spt4*Δ cells.

(**A**) Samples were collected from a strain expressing PA-tagged Spt4 (WXY106) under both growing and starvation conditions, and protein extracts were analyzed by western blot using antibodies to PA; Pgk1 was used as the loading control. (**B-C**) The anti-PA antibody was used to detect Atg5 (as the Atg12–Atg5 conjugate) and Atg20 protein levels,by probing for the PA tag in wild-type (WXY108, WXY110) and *spt4*Δ (WXY109, WXY111) cells in growing (YPD) and starvation (SD-N, t=2 h) conditions. Pgk1 was used as a loading control. (**D**) Samples from the wild-type (WLY176) and *spt4*Δ (WXY105) strains were collected in growing (YPD) and starvation (SD-N, t=2 h) conditions. The samples were analyzed by western blot with anti-Atg1 antibodies; Pgk1 was used as a loading control.

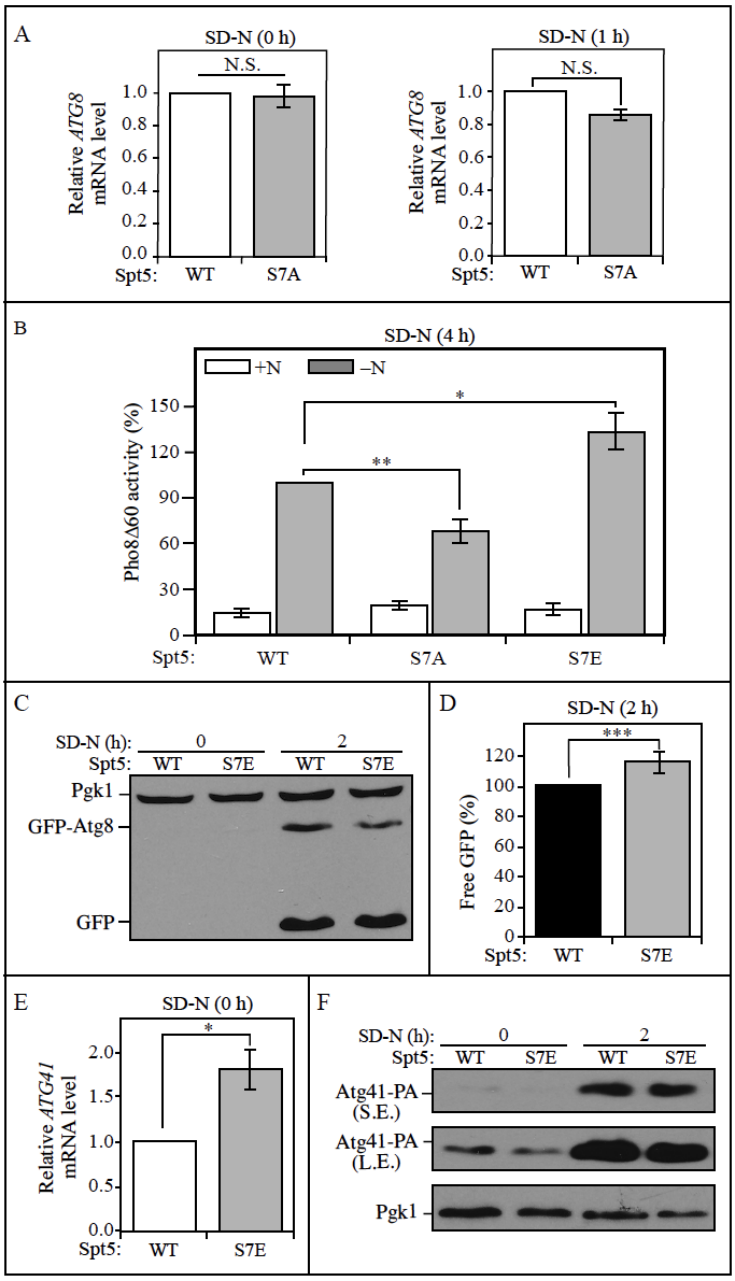

Figure 2.S2 Autophagy activity and *ATG41*/Atg41 expression are upregulated in cells expressing phosphomimetic Spt5[S7E].

(**A**) The RT-qPCR analysis of the *ATG8* mRNA level in WT(DGY047) and Spt5[S7A] (DGY048) cells in growing and starvation conditions. Error bars represent the SEM of at least 3 independent experiments, and WT was set as 1 in both conditions; other values were normalized. N.S., not significant. (**B**) Autophagy was measured with the quantitative Pho8Δ60 assay in WT (DGY047), Spt5[S7A] (DGY048) and Spt5[S7E] (DGY049) cells under growing conditions (+N) and after 4 h of nitrogen starvation (-N). Error bars representthe SEM of at least 3 independent experiments. *, $p<0.05$; **, $p<0.01$. (**C-D**) Autophagy activity was measured with the GFP-Atg8 processing assay in WT (DGY050) and Spt5[S7E] (DGY052)

cells. Proteins were analyzed by western blot with anti-YFP antibody and anti-Pgk1 (loading control) antiserum. The quantitative analysis of processed GFP after starvation is shown in (D), and the error bar represents the SEM of 3 independent experiments. The processed GFP ratio afterstarvation has been set as 1, and other values were normalized. ***, $p<0.005$. (**E**) The mRNA level of *ATG41* was measured by RT-qPCR in WT (DGY047) and Spt5[S7E] (DGY049) cells in growing conditions. Error bars represent the SEM of at least 3 independent experiments, and WTwas set as 1; other values were normalized. *, $p<0.05$. (**F**) The Atg41-PA protein level was tested by western blot and analyzed using anti-PA antibody in WT (WXY127) and Spt5[S7E] (WXY132)cells.

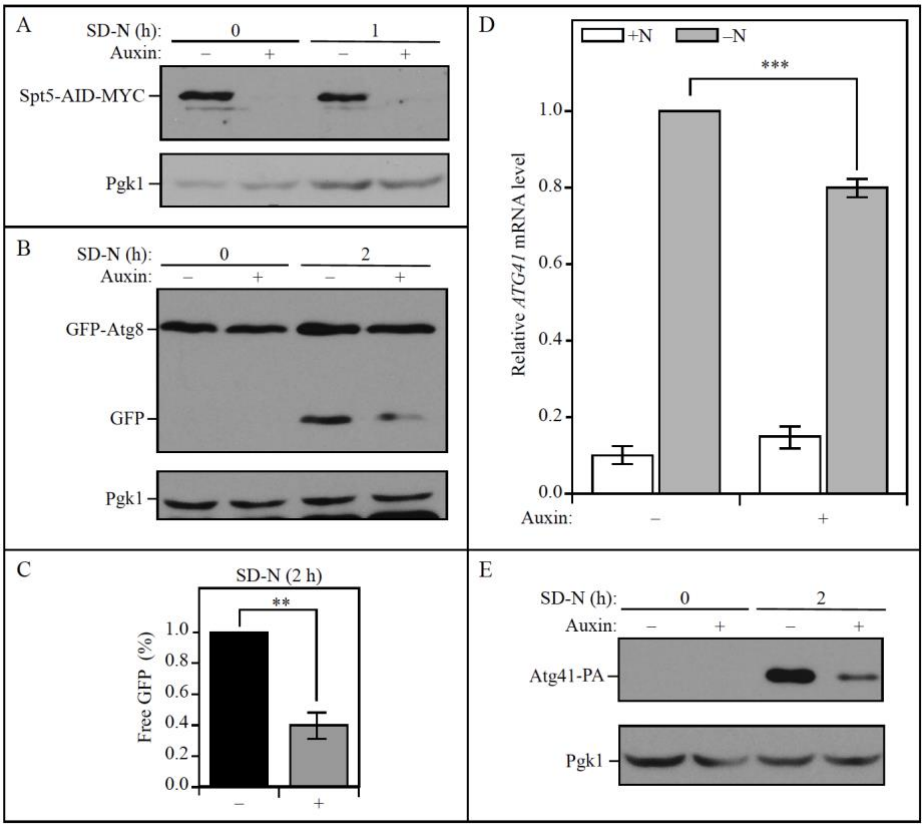

Figure 2.S3 The temporal depletion of Spt5 using an Spt5-inducible degradation strain leads to decreased autophagy activity.

(**A**) Spt5 levels were measured by western blot in an Spt5 auxin-inducible degron (AID) strain (WXY125) in both nutrient-rich and starvation conditions in the presence of DMSO (vehicle) or 300 μM auxin; the loss of Spt5-AID-MYC was detected with anti-MYC antibody after auxin treatment. (**B-C**) Autophagy activity was measured by the GFP-Atg8 processing assay. The Spt5-AID-MYC strain (WXY133) was incubated with DMSO or auxin in both growing (YPD, mid-log phase) and starvation (SD-N, t=2 h) conditions. Anti-YFP antibody and anti-Pgk1 (loading control) antiserum were used to detect the corresponding proteins. The quantitative analysis of processed GFP is shown in (**C**), and the error bar represents the SEM of 3 independent experiments. The processed GFP after 2 h of starvation was set as 1, and other values were normalized. (**D**) The mRNA level of *ATG41* was quantified by RT-qPCR in both growing (+N) and starvation (-N) conditions. The value of the strain treated with DMSO in -N was set as 1, and other values were normalized. The error bars indicate the SEM of at least 3 independent experiments. ***, $p<0.005$. (**E**) Anti-PA antibody was used to detect the protein level of Atg41-PA in the Spt5-AID-MYC strain (WXY134) when the strain was incubated with DMSO or auxin in either growing (SD-N, t=0 h) or starvation (SD-N, t=2 h) conditions.

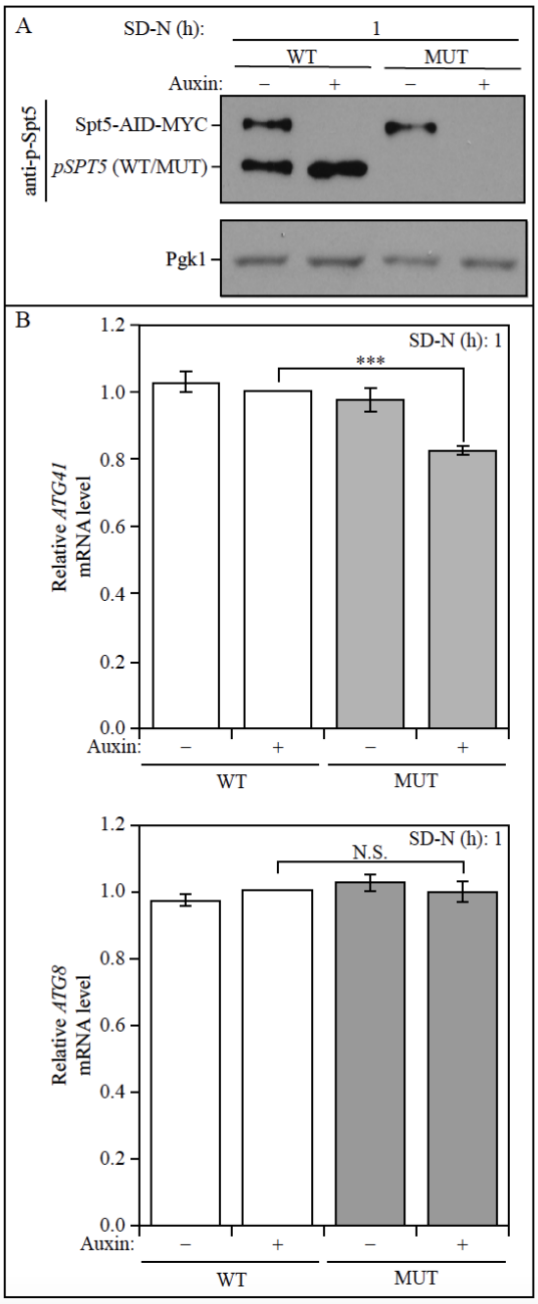

Figure 2.S4 The nonphosphorylable mutant of Spt5 in the Spt5-inducible degradation strain displays a decreased *ATG41* mRNA level.

(**A**) The centromeric HIS3-marked Spt5 WT (WT) and Spt5[S15A] (MUT) plasmids were transformed into the Spt5-inducible degradation strain (WXY125). The anti-p-Spt5 antibody was used to detect Spt5 phosphorylation after starvation. (**B**) The mRNA level of *ATG41* and *ATG8* were quantified by RT-qPCR in Spt5-AID-MYC strains with WT and MUT plasmids incubated with DMSO and auxin in the nutrient-depleted condition. The value of WT with auxin was set as 1, and other values were normalized. The error bars indicate the SEM of at least 3 independent experiments. N.S., not significant; ***, $p<0.005$.

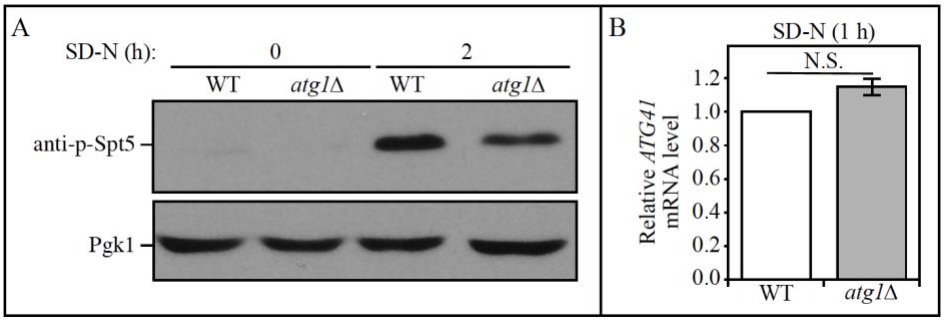

Figure 2.S5. The deletion of *ATG1* results in a partial block of Spt5 phosphorylation but has no effect on *ATG41*

(A) The phosphorylation of Spt5 was detected with anti-p-Spt5 antibody in western blot samples of WT (SEY6210) and *atg1*Δ (WXY126) cells collected from growing and starvation (SD-N=2 h) conditions. (**B**) The RT-qPCR analysis of *ATG41* mRNA level in WT and *atg1*Δ cells after starvation. Error bars represent the SEM of at least 3 independent experiments, and WT was set as 1; the other value was normalized. N.S, not significant.

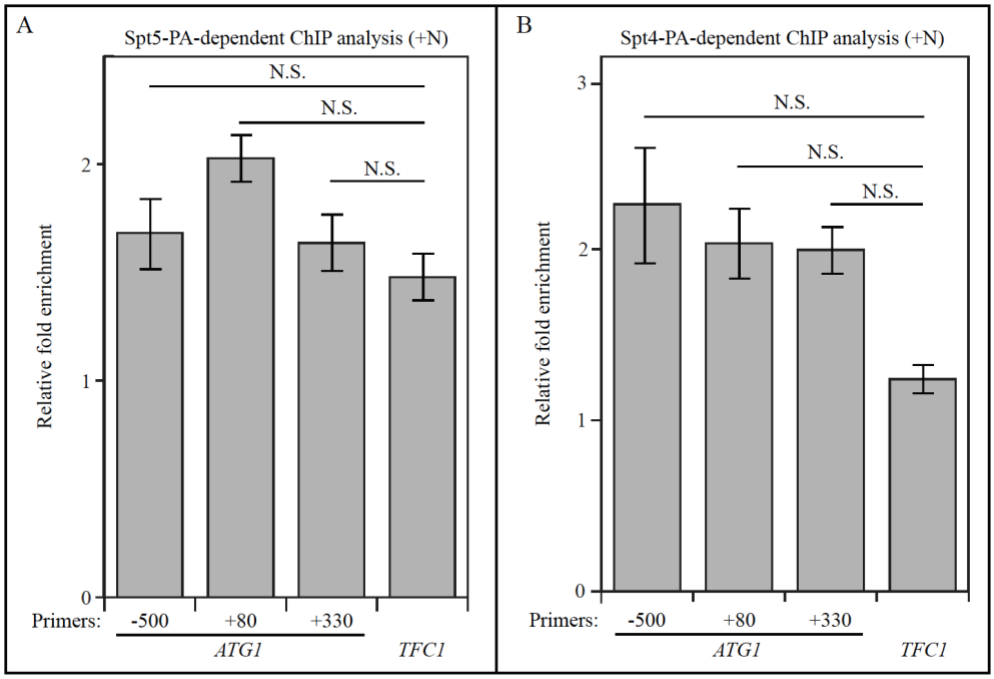

Figure 2.S6 ChIP analysis shows that Spt5 and Spt4 may not bind to *ATG1* DNA
(**A-B**) ChIP analysis was conducted using the protein A-tagged (**A**) Spt5 (WXY102) and (**B**) Spt4 (WXY106)strains on 3 regions of DNA at the *ATG1* locus: -500 base pairs (bps), +80 bps, and +330 bps. The ChIP results were normalized to the input DNA, and *TFC1* was used as a negative control for both strains. N.S., not significant.

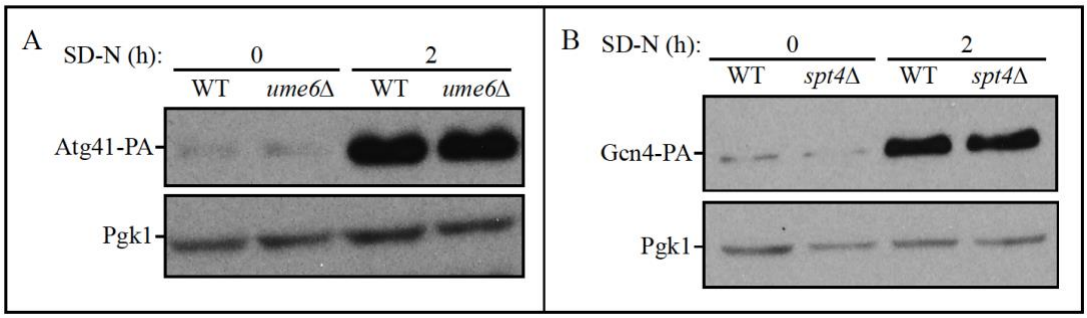

Figure 2.S7 The transcription factors Ume6 and Gcn4 are not involved in Spt4-Spt5 complex regulation on autophagy

(**A**) The Atg41-PA protein level was detected with anti-PA antibody in WT (ZYY108) and *ume6*Δ (WXY129) cells in growing (SD-N, t=0 h) and starvation (SD-N, t=2 h) conditions. Anti-Pgk1 antiserum was used to detect the loading control. (**B**) The Gcn4-PA protein level was analyzed by western blot with the anti-PA antibody in WT (ZYY124) and *spt4*Δ (WXY130) strains.

CHAPTER III Two New Findings of Molecular Mechanisms of Autophagy in *Saccharomyces cerevisiae*[3]

3.1 Abstract

In *Saccharomyces cerevisiae*, autophagosome formation occurs at the phagophore assembly site (PAS), a specific perivacuolar location that works as an organizing center for the recruitment of different autophagy-related (Atg) proteins. However, the PAS is a poorly defined structure, and one unanswered question is what determines the localization of the PAS. The project 3.2 showed that the vacuolar membrane protein Vac8 is required for correct vacuolar localization of the PAS. *VAC8* deletion or mislocalization would result in the block of nonselective autophagy. We also provided evidence that Vac8 anchors the PAS to the vacuolar membrane by recruiting the Atg1-Atg13 initiation complex.

The project 3.3 further examined another aspect of the dynamic role of intracellular membranes and autophagy machinery, in this case focusing on a type of selective autophagy, pexophagy, which can degrade surplus or damaged peroxisomes in yeast. We revealed that endoplasmic reticulum (ER)-mitochondria contact sites are necessary for efficient pexophagy, and disruption of the ER-mitochondria encounter structure (ERMES) results in a severe defect in pexophagy. The mutant on R349 and R350 of Mdm34 (a component of the ERMES) which impairs ERMES formation and diminishes its association with the peroxisomal membrane protein Pex11, also leads to defects in pexophagy.

[3] This chapter is reprinted and modified from two publications: Damián Gatica, Xin Wen, Heesun Cheong, Daniel Klionsky (2020) *Autophagy* (doi: 10.1080/15548627.2020.1776474) and Xu Liu, Xin Wen, Daniel Klionsky (2019) *Contact (Thousand Oaks)* (doi: 10.1177/2515256418821584).

3.2 Vac8 determines phagophore assembly site vacuolar localization during nitrogen starvation-induced autophagy

3.2.1 Introduction

Macroautophagy/autophagy is a key catabolic process in which different cellular components, such as proteins, lipids or even entire organelles, are sequestered, broken down and recycled in order to promote cell survival. Once autophagy is activated, cargo intended for degradation is enveloped by the phagophore, a cup-shaped transient compartment that expands into a double-membrane vesicle called an autophagosome. Once fully matured, autophagosomes fuse with the vacuole, releasing their cargo for degradation by different vacuolar hydrolases. The molecules obtained from cargo degradation are then transported back into the cytosol to be recycled by the cell [121, 125].

Autophagy has been described as both a selective and nonselective process, depending on the type of cargo that is targeted for degradation. On one hand, it is thought that during nonselective autophagy, random parts of the cytoplasm are taken up into phagophores to later be delivered to the vacuole for degradation. On the other hand, during selective autophagy specific cargo such as protein aggregates and damaged or superfluous organelles are recognized by specialized autophagy receptors, that tether the specific cargo to the phagophore membrane to facilitate vacuolar delivery and degradation. The cytoplasm-to-vacuole targeting (Cvt) pathway constitutes a specific type of selective biosynthetic autophagy in yeast, which is used for delivering resident vacuolar enzymes from their site of synthesis in the cytosol to their final destination [161].

In yeast, autophagosome formation occurs at the phagophore assembly site (PAS), a specific perivacuolar location that works as an organizing center for the recruitment of different autophagy-related (Atg) proteins, donor membranes and cytoplasmic cargo required for the

autophagic process [121, 125]. Atg protein recruitment at the PAS occurs in sequential steps [162], starting with the assembly of the Atg1 initiation complex, composed of the protein kinase Atg1, the regulatory protein Atg13, and the Atg17-Atg31-Atg29 subcomplex, which works as a scaffold [163]. In addition to its role in regulating Atg1, Atg13 also functions as an assembly hub for all other members of the initiation complex [54, 164-167]. Even though the essential role of the Atg1 initiation complex in phosphorylating downstream targets, as well as its structural role as a backbone for PAS assembly have been well established, the nature behind its recruitment to the vacuole periphery remains unclear.

Vac8 is a peripheral vacuolar membrane protein that has been implicated in vacuolar inheritance, the Cvt pathway [168] and the formation of nucleus-vacuole junctions [169]. Whereas Vac8 binding to the nuclear membrane protein Nvj1 promotes the formation of nucleus-vacuole junctions and piecemeal microautophagy of the nucleus/micronucleophagy [169-171], Vac8 binding to Atg13 is proposed to be required for the Cvt pathway [142]. Thus, Vac8 has mainly been associated with selective types of autophagy. Nevertheless, previous results from our lab suggest Vac8 could play a role in nonselective autophagy [142, 172], although the exact role of this protein has not been determined.

Here we show that Vac8 is required for efficient and robust nonselective autophagy, and we also determined that Vac8 vacuolar localization is necessary for the recruitment of the Atg1 initiation complex and PAS assembly to the vacuolar periphery.

3.2.2 Results

3.2.2.1 Vac8 is required for efficient autophagy induction

The initial studies of the *vac8*Δ mutant resulted in the characterization of the protein as being required for the selective Cvt pathway. The primary reason for this conclusion was based on the

following observation: the primary cargo of the Cvt pathway, precursor aminopeptidase I (prApe1), accumulates in the *vac8*Δ strain in growing condition but is efficiently delivered to the vacuole when autophagy is induced by nitrogen starvation [142]. Nonetheless, the mutant strain displays a significant defect in autophagy based on maturation of the Pho8Δ60 protein as determined through a radioactive pulse-chase experiment. Pho8Δ60 is an engineered phosphatase that requires nonselective autophagy to reach the vacuole and initiate its enzymatic activity; upon vacuolar delivery a propeptide is removed, resulting in a molecular mass shift that can be monitored through SDS-PAGE. To extend our analysis of the role of Vac8 in autophagy we generated new strains lacking the *VAC8* gene and measured nonselective autophagy using a Pho8Δ60 biochemical assay to follow enzyme activation [173]. Thus, by measuring phosphatase activity we can quantitatively monitor nonselective autophagy. In agreement with our previous findings [142, 172], *VAC8* deletion led to a significant decrease in autophagy activity measured by the Pho8Δ60 assay when compared to wild-type (WT) cells after 3 h of nitrogen starvation (Figure 3.1A). However, *VAC8* deletion failed to produce a complete block in autophagy; *vac8*Δ cells still showed a small but significant amount of autophagy activity compared with a strain where the essential autophagy gene *ATG13* was deleted.

Next, we used a second method to further examine the effect on autophagy of deleting *VAC8*. The GFP-Atg8 processing assay measures autophagy by determining the amount of free GFP that is generated once the chimera is delivered to the vacuole through autophagy and cleaved [141]. During autophagy initiation, Atg8 is lipidated and attached to both the inner and outer membranes of the growing phagophore. Once autophagosomes are completed, the Atg8 bound to the concave surface is trapped inside the autophagosome and is delivered to the vacuole where it is degraded. Tagging GFP at the N terminus of Atg8 makes it possible to measure autophagy

because GFP is relatively resistant to vacuolar hydrolases and can be separated from full-length GFP-Atg8 by western blot. Confirming the Pho8Δ60 assay results, *vac8*Δ cells showed a significant decrease in autophagy activity based on GFP-Atg8 processing when compared to wild-type cells after 2 h of nitrogen starvation (Figure 3.1B,C).

3.2.2.2 Vac8 vacuolar localization is required for efficient autophagy

Vac8 is anchored to the vacuolar membrane via the post-translational modification of its N terminal domain. Thus, Vac8 localization depends on the myristoylation of residue Gly2 and the palmitoylation of residues Cys4, Cys5 and Cys7; mutation of these residues renders Vac8 a cytosolic protein, no longer confined to the vacuolar membrane [168]. One compelling line of data suggesting that Vac8 has a unique function in the Cvt pathway was the observation that a double acylation mutant is completely defective in vacuole inheritance and homotypic vacuole fusion, but is normal for the Cvt pathway [168]. Therefore, it seemed likely that the inheritance and fusion roles of Vac8 depended on its membrane association, whereas a separate soluble pool could fulfill its function in autophagy-related pathways. Mutants of Vac8 that are defective in acylation were previously identified [168]. To test whether acylation of Vac8 has an important role for the Cvt pathway, we generated new strains expressing similar mutations: a myristoylation mutant (G2A), a palmitoylation mutant (C4A C5A C7A) and a myristoylation and palmitoylation double mutant (G2A C4A C5A C7A).

We monitored the Cvt pathway by analyzing the processing of prApe1. When wild-type Vac8 was expressed in the *vac8*Δ mutant, a portion of the prApe1 population was efficiently processed into mature Ape1, whereas the *vac8*Δ mutant containing an empty vector showed only prApe1 in vegetative conditions (Figure 3.2A), suggesting that Vac8 is critical for the Cvt pathway, in agreement with previous results. Next, we examined prApe1 processing in the *vac8*Δ strain

expressing the various established acylation mutants. In apparent contrast to the previous report [168], the myristoylation mutant (G2A), the palmitoylation mutant (C4A C5A C7A) and the myristoylation and palmitoylation double mutant (G2A C4A C5A C7A) failed to completely restore the defect in the Cvt pathway, resulting in a substantial decrease in prApe1 processing; we think this discrepancy between the two sets of data likely represents small differences in culture conditions, because cells that are not in mid-log phase will start to induce autophagy, resulting in prApe1 maturation. These data indicate that Vac8 membrane association is required for an efficient Cvt pathway.

We extended our analysis to examine the requirement of Vac8 acylation for nonselective autophagy, using the Pho8Δ60 assay. The myristoylation (G2A) and the palmitoylation (C4A C5A C7A) Vac8 mutants showed a significant decrease in autophagy when compared to a wild-type strain after 3 h of nitrogen starvation (Figure 3.2B). The *vac8*Δ cells showed no significant difference compared to the mislocalized Vac8 mutants, suggesting Vac8 vacuolar localization is essential for its role in autophagy. Taken together, our data indicate Vac8 acylation and vacuolar localization are necessary for efficiently inducing both Cvt and autophagy pathways.

Moreover, we generated Vac8-inducible degradation strains which co-expressed a second copy of either wild-type Vac8 (Vac8-GFP WT); a $Vac8^{G2,C4,C5,C7A}$-GFP mutant rendering Vac8 cytosolic (Vac8-GFP Cyt); or an ER-localized Vac8 (Vac8-GFP ER) made by replacing the first 7 N-terminal amino acid residues of Vac8 with the transmembrane domain of the ER membrane protein Sec66, as previously described [174]. By inducing the rapid degradation of wild-type Vac8 through the AID system and leaving a GFP-tagged copy of Vac8 in place, these strains allowed us to determine the vacuolar association of different Atg proteins without disrupting vacuolar morphology. With this Vac8-inducible degradation Vac8-GFP mislocalization system, we further

conducted fluorescence microscopy experiments to confirm that Vac8 vacuolar localization is required for correct PAS perivacuolar localization during nitrogen starvation-induced autophagy (data not shown).

3.2.2.3 Vac8 recruits the Atg1 initiation complex to the vacuole

If the correct perivacuolar localization of the PAS is determined by Vac8, we hypothesized that Vac8 localization must also affect Atg13 and Atg1 recruitment to the vacuole. To test this hypothesis, we tagged Atg13 with RFP and took advantage of our Vac8-inducible degradation Vac8-GFP mislocalization system. As described above, Vac8 degradation was induced by adding IAA to the growth medium 30 min before nitrogen starvation. Similar to our RFP-Ape1 results, after 1 h of nitrogen starvation Atg13-RFP association with the vacuole showed no significant difference between DMSO- and IAA-treated cells when the wild-type Vac8-GFP chimera was expressed (Figure 3.3). Cells expressing either Vac8-GFP Cyt or Vac8-GFP ER in the absence of IAA (i.e., also expressing a wild-type copy of Vac8) displayed a reduced level of Atg13-RFP localization to the vacuole, presumably due to competition between the wild-type and mutant forms of Vac8 (Figure 3.3). In contrast to the result with cells expressing wild-type Vac8-GFP, those expressing cytosolic Vac8-GFP or ER-localized Vac8-GFP treated with IAA showed a significant decrease in Atg13-RFP vacuolar localization when compared to the corresponding DMSO-treated controls (Figure 3.3). Besides, similar results were obtained when these experiments were repeated by tagging Atg1 with RFP (Figure 3.4).

3.2.3 Discussion

Autophagy is a critical recycling pathway that requires delicate spatiotemporal organization of multiple cytoplasmic components, such as proteins and membranes from diverse sources, in order to restore cellular homeostasis during nutrient-starvation conditions. Recruitment of the Atg1-

Atg13, Atg17-Atg31-Atg29 initiation complex and the formation of the PAS at the vacuolar membrane periphery constitutes one of these key events. Our results show that the vacuolar membrane protein Vac8 is necessary for the recruitment and proper perivacuolar localization of the initiation complex and the PAS. We further determined that the effect of Vac8 on autophagy is depends on its vacuolar localization. Indeed, Vac8 acylation mutants, which fail to anchor to the vacuolar membrane, showed decreased autophagy activity comparable to the decrease observed in *vac8*Δ cells. Our results underline the role of Vac8 as the main driver behind the initiation complex and PAS perivacuolar localization during autophagy induction in yeast.

While this manuscript was in preparation, a recent publication by *Hollenstein et al.* showed some overlapping results and reached similar conclusions [175]. The authors determined that Vac8 fulfills an important role in autophagy by anchoring the early PAS to the vacuole, coordinating the site of autophagosome formation and later vacuolar fusion. Interestingly, an experiment meant to bypass the need for Vac8 by tethering the middle domain of Atg13, 269–520, directly to the vacuole, failed to restore autophagy activity. Whereas this result could be explained by the failure to include the Atg13 N-terminal HORMA domain [176], another explanation could rely on the failure to include recently described Atg13 lipid-binding motifs. Atg13 lipid-binding motifs overlap with its Vac8-binding domain and are required for efficient autophagy. This possibility indicates the need for flexibility in Atg13 binding between Vac8 and lipid membranes [165]. Thus, constant Atg13 tethering to the vacuolar membrane would probably result in decreased flexibility and would be deleterious for autophagy induction.

3.2.4 Materials and Methods

3.2.4.1 Yeast strains, media and culture growth

A list of selective strains that are used in this project is shown in Table 3.1. *S. cerevisiae* strains with genomic point mutations Vac8G2A, Vac8C4,5,7A, and Vac8G2,C4,C5,C7A were generated as previously described [177]. Yeast cultures were grown in nutrient-rich YPD medium (1% [w:v] yeast extract, 2% [w:v] peptone, 2% [w:v] glucose) to mid-log phase and then samples were collected. Strains grown in YPD were shifted to minus nitrogen medium (0.17% yeast nitrogen base without ammonium sulfate or amino acids, and 2% [w:v] glucose) for the indicated time points and then collected.

3.4.2.2 Fluorescence microscopy

Yeast cultures were grown to OD_{600} ~ 0.5 in YPD, washed and shifted to minus-nitrogen medium for 1 h for autophagy induction. For blue lumenal vacuolar staining, cells were incubated in YPD with 10 μM CellTracker Blue CMAC (Molecular Probes/ThermoFisher Scientific, C2110) for 30 min and then washed to remove excess dye. For red membrane vacuolar staining, cells were incubated in YPD with 30 μM FM 4–64 (Molecular Probes/ThermoFisher Scientific, T3166) for 30 min and then washed to remove excess dye. Images were collected on a DeltaVision Elite deconvolution microscope (GE Healthcare/Applied Precision) with a 100x objective and a CCD camera (CoolSnap HQ; Photometrics). For the quantification of fluorescent puncta associated with the vacuole, stacks of 15 image planes were collected with a spacing of 0.2 μm to cover the entire yeast cell. Analysis was performed on an average projection of the imaging planes on ImageJ software.

3.4.2.3 Statistics and reproducibility

Microscopy data analysis and image processing were carried out using softWoRx software (GE Healthcare). Sample sizing for cellular imaging was chosen to be the minimum number of independent experiments required for statistically significant results. Western blot images were

quantified using ImageJ software. Statistical analyses were performed using GraphPad Prism 6. Statistical significance was determined in all cases from at least 3 independent experiments using either Student's t-test or ANOVA. Differences with a P value <0.05 or lower were considered significant. *p < 0.05, **p < 0.01, ***p < 0.001. The number of independent experiments (n), statistical test utilized, distribution of measurements and significance are described in the figure legends.

3.3 ER-mitochondria contacts are required for pexophagy in *S. cerevisiae*

3.3.1 Introduction

Peroxisomes are single-membrane organelles found in eukaryotes, and they are involved in several important aspects of cellular metabolism, including β-oxidation of fatty acids, a process providing a critical source of metabolic energy [178-180]. In mammals, long-chain fatty acids are converted to medium-chain fatty acids in peroxisomes before they are transported to mitochondria and broken down into carbon dioxide and water. In yeasts and plants, this process is carried out exclusively in peroxisomes [179]. In addition, a byproduct of the process, reactive oxygen species, may be detrimental to cells under certain circumstances. Therefore, to maintain cellular homeostasis, the quantity and quality of peroxisomes must be finely regulated, and autophagy plays an indispensable role in this process.

Defects in peroxisome function can have serious medical consequences, as seen with Zellweger syndrome, Refsum's disease and rhizomelic chondrodysplasia punctata, which can result in severe developmental problems or even be lethal [181]. The accumulation of peroxisomal substrates, or the absence of products that are normally generated through peroxisomal metabolic reactions can result in serious physiological challenges. Thus, it is critical to maintain functional peroxisomes. Conversely, the risks associated with defective organelles that generate reactive

oxygen species, and the energetic requirements of maintaining organelles that function properly means that it is generally beneficial to eliminate them when they become superfluous. The selective autophagy process that recognizes and degrades surplus or damaged peroxisomes is termed pexophagy [94, 182, 183]. Therefore, a more complete knowledge of the molecular mechanisms of pexophagy and how pexophagy is regulated is critical to gain a more complete understanding of peroxisome related diseases and potential therapeutic avenues.

ER-mitochondria contacts are characterized as being critical for cellular physiology, especially mitochondrial biology, such as phospholipid and calcium exchange between mitochondria and the ER [184-186]. The formation of the contacts is mediated by the ER-mitochondria encounter structure (ERMES), mainly consisting of Mmm1, Mdm10, Mdm12, and Mdm34 [187]. Mmm1 is an integral ER membrane protein, whereas Mdm10 and Mdm34 are mitochondrial outer membrane proteins; Mdm12 is cytosolic. These components form the ERMES, connecting the ER and mitochondria. In mammalian cells ER-mitochondria contacts have been suggested to be the sites where autophagosomes form, providing important membrane resources for autophagosome biogenesis [188]. In yeast cells, these contacts are crucial for mitophagy, the process that selectively targets mitochondria for autophagic degradation [189]. In contrast, disruption of ERMES does not affect starvation induced non-selective autophagy.

Here we found that ERMES components are required for efficient pexophagy. Especially, an R349, 350A mutation of Mdm34 leads to diminished ERMES formation and impaired interaction between Mdm34 and Pex11, resulting in significant defects in pexophagy.

3.3.2 Result

3.3.2.1 ER-mitochondria contacts contribute to pexophagy

As mentioned above, in yeast cells ER-mitochondria contacts are required for mitophagy [189]. Recent studies observed that some peroxisomes are adjacent to ER-mitochondria contacts [190, 191]. Accordingly, we asked whether ER-mitochondria contacts play a role in pexophagy. To answer the question, we first examined the localization of peroxisomes relative to ER-mitochondria contacts before and after pexophagy is induced. *PEX14*, which encodes a peroxisomal membrane protein, was chromosomally tagged with mCherry to visualize peroxisomes. Mdm34-GFP, a mitochondrial component of the ERMES, was used to mark ER-mitochondria contacts; both Mdm34 and Mdm10 are mitochondrial, and in the present study we used Mdm34 as the representative mitochondrial ERMES component. To induce pexophagy in *S. cerevisiae*, the cells were first grown in nutrient-rich medium containing glucose (YPD) to mid-log phase, then in medium with glycerol and a minimal level of glucose (SGd), before they were shifted to medium with oleic acid as the sole carbon source (YTO) to promote proliferation of peroxisomes; this specific growth regimen resulted in a large number of peroxisomes, which are otherwise of very low abundance in this organism [192]. The cells were then shifted to conditions of nitrogen starvation in the presence of glucose (SD-N). Under this condition the elevated population of peroxisomes is no longer necessary and pexophagy is activated to degrade the surplus organelles.

When cells were grown in YPD, we observed a small number of peroxisomes with approximately 20% of the cells showing colocalization between Pex14-mCherry and Mdm34-GFP (Figure 3.5A,B). In YTO medium, there was a substantial increase in the total number of peroxisomes detected with Pex14-mCherry. In contrast, the number of Mdm34-GFP puncta per cell decreased and a smaller percentage of cells showed colocalization of this marker with Pex14-mCherry compared to the cells growing in YPD (Figure 3.5A,B). Upon pexophagy induction

following a 1 h shift to nitrogen starvation conditions, more than 50% of the cells showed peroxisomes adjacent to ERMES (Figure 3.5A,B). These observations suggest that ER-mitochondria contact sites very likely play a role in pexophagy.

Next, we wanted to disrupt the ER-mitochondria contacts and then determine whether pexophagy was affected. The contacts between ER and mitochondria are mediated by the four ERMES protein components: Mmm1, Mdm10, Mdm12 and Mdm34 [187]. Mmm1 is an ER membrane protein; Mdm12 is a cytosolic component; and Mdm10 and Mdm34 are localized to the mitochondrial outer membrane. Deletion of individual genes encoding ERMES components leads to failure of establishment of ER-mitochondria contacts. To quantitatively monitor pexophagy activity in these mutant cells, we took advantage of the Pex14-GFP processing assay [193]. When pexophagy is induced, peroxisomes containing Pex14-GFP are transported into the vacuole for degradation. Pex14 is proteolytically degraded, whereas the GFP moiety is relatively resistant to vacuolar degradation and accumulates in the lumen. Analysis of the amount of free GFP by western blot can therefore be used as an indicator of pexophagy activity. In agreement with a proposed role for the ERMES in pexophagy, we observed a severe reduction in the generation of free GFP from the Pex14-GFP processing assay in the *mmml*Δ, *mdm12*Δ, and *mdm34*Δ cells, compared to that seen in the wild type (Figure 3.5C). Previous study has indicated that deletion of either *MMM1*, *MDM12*, or *MDM34* does not affect nonselective autophagy [189]. Taken together, these results show that ER-mitochondria contacts are indispensable for efficient pexophagy.

3.3.2.2 Pexophagy is defective in the *pex11*Δ mutant

Pex11, an integral peroxisomal membrane protein, associates with Mdm34, based on both a bimolecular fluorescence complementation (BiFC) assay and the membrane yeast two-hybrid assay [191]. This interaction contributes to the contacts between peroxisomes and ER-

mitochondria. Decreased colocalization between peroxisomes and ERMES is observed in *pex11*Δ cells compared to that in wild-type cells when cultured in glucose medium [191].

Therefore, we asked whether localization of peroxisomes in proximity to ERMES is also affected under pexophagy-inducing conditions in the *pex11*Δ cells. Indeed, we observed a significantly lower percentage of cells showing colocalization of Pex14-mCherry and Mdm34-GFP in the *pex11*Δ cells after the shift from oleic acid-containing medium to nitrogen starvation conditions (Figure 3.6A,B). Pex11 also regulates peroxisome fission [194]; we observed some large clusters of peroxisomes in the *pex11*Δ cells, but not in the wild type cells, suggesting defects in peroxisome segregation (Figure 3.6A). Furthermore, based on the Pex14-GFP processing assay, the *pex11*Δ mutant displayed significant pexophagy defects (Figure 3.6C).

3.3.2.3 An R349A R350A double mutant of Mdm34 leads to defects in pexophagy

Our further analysis showed that the interaction between Pex11 and several truncation mutants of Mdm34 indicated that residues 343–359 in Mdm34 were necessary for the interaction, and a potentially diminished Pex11 association with $Mdm34^{R349,350A}$ has been further validated by the BiFC assay (data not shown). Therefore, we focused on the $Mdm34^{R349,350A}$ mutant.

The absence of any of the individual ERMES proteins affects assembly of the entire complex [187]. Thus, GFP-tagged Mdm34 stains the mitochondria in ERMES mutant strains, instead of being in puncta form in the wild type [187]. When we compared the localization of $Mdm34^{WT}$-GFP with the $Mdm34^{R347A}$-GFP and the $Mdm34^{R349,350A}$-GFP mutants, we observed a smaller percentage of cells with GFP puncta in the $Mdm34^{R349,350A}$ mutant, but not in the $Mdm34^{R347A}$ mutant where ERMES complex and Pex11-Mdm34 interaction were not significantly affected (Figure 3.7A). This result suggests that the formation of ERMES is partially defective in cells expressing the R349A R350A double mutant form of Mdm34. Based on the Pex14-GFP

processing assay, pexophagy activity was significantly decreased in the cells expressing the Mdm34^{R349,350A} mutant (Figure 3.7B). In contrast, in the Mdm34^{R347A} mutant, pexophagy activity was comparable to that in the wild type cells. Thus, a functional ERMES complex is required for efficient pexophagy.

3.3.3 Discussion

Recent studies have revealed many membrane contact sites between organelles, and they appear to play important roles in cellular physiology [195, 196]. Along these lines, both ER-mitochondrial contacts and ER-plasma membrane contacts play critical roles in autophagosome biogenesis [188, 197]. It was reported that in mammalian cells STX17-dependent localization of ATG14 onto ER-mitochondria contacts is required for autophagosome formation at the contact sites [188]. In yeast cells, ER- mitochondrial contacts are specifically required for mitophagosome formation and mitophagy, but not starvation-induced nonselective autophagy [189]. Here, we found that a substantial number of peroxisomes translocate to ER-mitochondrial contacts upon pexophagy induction, and disruption of the contacts severely diminishes pexophagy activity. These findings suggest that ER-mitochondrial contacts are indispensable platforms for the efficient biogenesis of phagophores that target distinct cargoes under different contexts.

Pex11, a peroxisome integral membrane protein, is suggested to associate with Mdm34, a component of the ERMES mediating ER-mitochondria contacts, contributing to the localization of peroxisomes adjacent to these sites [191]. Deletion of the *PEX11* gene, however, does not result in a block of peroxisomes locating to ER-mitochondria contacts, suggesting that some other unidentified protein(s) may also be involved in establishing the contacts between peroxisomes and the ERMES. Interestingly, Pex11 was also recently suggested to be involved in mediating the

mitochondria-peroxisome contacts [198]. Thus, the pexophagy defects in the *pex11*Δ mutant may also partly be due to decreased contacts between these organelles.

Further characterization of the interaction between Pex11 and Mdm34 indicates that the residue 343–359 in Mdm34 are required for the Pex11-Mdm34 interaction. The Mdm34^{R349,350A} mutant showed impaired ERMES formation and weaker Pex11-Mdm34 interaction. Nonetheless, the observation of significant defects in pexophagy activity in the Mdm34R^{349,350A} mutant suggests that establishment of ERMES and the localization of peroxisomes near ER-mitochondria contacts are required for efficient pexophagy. The deletion of *MMM1* disrupts the ERMES, but not peroxisome-mitochondria contacts [191]. Therefore, the pexophagy defects observed in the *mmm1*Δ mutant suggest that the ER itself plays an important role in this process. Furthermore, the *mdm12*Δ and *mdm34*Δ mutants display stronger defects in pexophagy relative to *mmm1*Δ. Accordingly, we propose that ER-mitochondria contact sites are more critical than peroxisome-mitochondria contacts regarding pexophagy.

Our previous study demonstrated that Atg11 and Atg36 recruit the peroxisomal fission complex to the peroxisomes targeted for degradation, to facilitate the sequestration of the organelles [199]. It was further revealed that the fission machinery is recruited to the peroxisomes close to ER-mitochondria contacts (data now shown). Overall, our results suggest a model where ER-mitochondria contacts are the major sites for recruitment of pexophagy machinery and for the formation of pexophagy-specific autophagosomes.

3.3.4 Materials and Methods

3.3.4.1 Yeast strains, media and growth conditions

Yeast strains used in this study are listed in Table 3.2. For nutrient-rich conditions, yeast cells were either grown in YPD medium (1% yeast extract, 2% peptone, 2% glucose), or synthetic minimal

(SMD; 0.67% yeast nitrogen base, 2% glucose, and auxotrophic amino acids and vitamins as needed) medium. To induce peroxisomal proliferation, cells were first grown in YPD or SMD-Ura to approximately 0.5 OD_{600} before they were shifted to glycerol medium (SGd; 0.67% yeast nitrogen base, 0.1% glucose, and 3% glycerol) for 16 h. Then, yeast extract and peptone were added into the cultures in SGd medium, and the cells were incubated for 4 h. The cells were then shifted to oleic acid medium (YTO; 0.67% yeast nitrogen base, 0.1% oleic acid, 0.1% Tween 40 and auxotrophic amino acids as needed) for 20 h. Pexophagy was induced by shifting the cells to nitrogen starvation medium containing glucose (SD-N; 0.17% yeast nitrogen base without ammonium sulfate or amino acids, and 2% glucose).

3.3.4.2 Fluorescence microscopy

For fluorescence microscopy, yeast cells were grown as described above to induce pexophagy. Samples were collected and then examined by microscopy (Delta Vision, Applied Precision) using a 100× objective, and pictures were captured with a CCD camera (CoolSnap HQ; Photometrics). Mitochondria were stained with MitoTracker Red CMXRos (Molecular Probes/Invitrogen, M7512).

3.3.4.3 Western blot

The western blot was performed as described previously (45). Antibody to YFP (Clontech, 632381) was used to detect GFP-tagged proteins.

Table 3.1 Selective strains used in Project 3.2

Name	Genotype	Reference
DGY056	WLY176 *vac8Δ::HIS3*	This study
DGY057	WLY176 *atg13Δ::HIS3*	This study
DGY058	WLY176 *GFP-ATG8::URA3*	This study
DGY059	DGY058 *vac8Δ::HIS3*	This study
DGY060	SEY6210 *pho8::pho8Δ60* pNHK53::*URA3 VAC8-AID-MYC:: HIS3*	This study
DGY062	WLY176 *VAC8-GFP::HIS3*	This study
DGY063	WLY176 *VAC8^{G2A}-GFP::HIS3*	This study
DGY064	WLY176 *VAC8^{C4,5,7A}-GFP::HIS3*	This study
DGY065	SEY6210 pNHK53::*URA3 VAC8-AID-MYC::HIS3 VAC8-GFP:: LEU2*	This study
DGY066	SEY6210 pNHK53::*URA3 VAC8-AID-MYC::HIS3 VAC8$^{G2A, C4A,C5A,C7A}$-GFP::LEU2*	This study
DGY067	SEY6210 pNHK53::*URA3 VAC8-AID-MYC::HIS3 SEC66-VAC8-GFP::LEU2*	
DGY071	DGY056 *VAC8-GFP::LEU2*	This study
DGY072	DGY056 *VAC8^{G2A,C4A,C5A,C7A}-GFP::LEU2*	This study
DGY074	DGY065 *ATG13-RFP::TRP1*	This study
DGY075	DGY066 *ATG13-RFP::TRP1*	This study
DGY076	DGY067 *ATG13-RFP::TRP1*	This study
DGY077	DGY065 *ATG1-RFP::TRP1*	This study
DGY078	DGY066 *ATG1-RFP::TRP1*	This study
DGY079	DGY067 *ATG1-RFP::TRP1*	This study
WLY176	SEY6210 *pho13Δ pho8::pho8Δ60*	[173]
YTS178	SEY6210 *vac8Δ::HIS5 S.p.*	[172]

Table 3.2 Selective strains used in Project 3.3

Name	Genotype	Reference
TKMY67	SEY6210 *PEX14-GFP::KANMX6*	[199]
TKMY72	SEY6210 *PEX14-GFP::KANMX6 atg1Δ::HIS3*	[199]
XLY401	SEY6210 *RPL7Bp-VN-ATG11::TRP1 PEX14-mCherry::KAN MDM34-GFP::HIS3*	This study
XLY402	SEY6210 *RPL7Bp-VN-ATG11::TRP1 PEX14-mCherry::KAN MDM34-GFP::HIS3 pex11Δ::URA3*	This study
XLY403	SEY6210 *PEX14-GFP::KANMX6 mmm1Δ::HIS3*	This study
XLY404	SEY6210 *PEX14-GFP::KANMX6 mdm12Δ::HIS3*	This study
XLY405	SEY6210 *PEX14-GFP::KANMX6 mdm34Δ::URA3*	This study
XLY420	SEY6210 *MDM34-GFP::HIS3*	This study
XLY421	SEY6210 *MDM34-GFP(K347A)::HIS3*	This study
XLY422	SEY6210 *MDM34-GFP(R349A,R350A)::HIS3*	This study
XLY428	SEY6210 *PEX14-GFP::KANMX6 MDM34-VN::TRP1*	This study
XLY429	SEY6210 *PEX14-GFP::KANMX6 MDM34-VN(K347A)::TRP1*	This study
XLY430	SEY6210 *PEX14-GFP::KANMX6 MDM34-VN(R349A,R350A)::TRP1*	This study

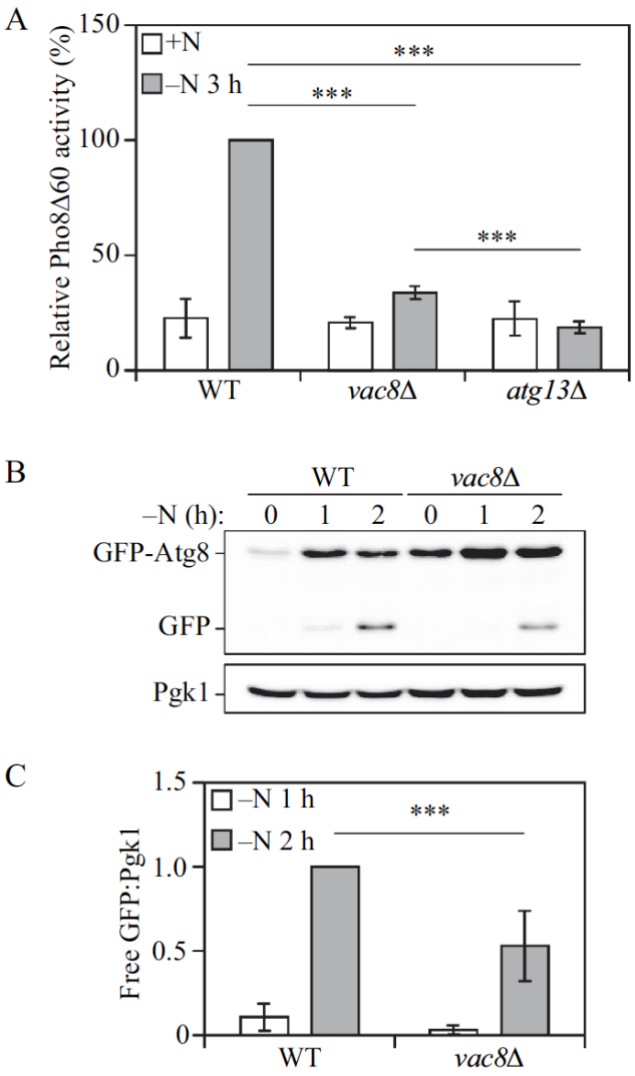

Figure 3.1 Vac8 is required for robust autophagy activity

(**A**) Autophagy activity was measured using the Pho8Δ60 assay in WT, *atg13*Δ and *vac8*Δ strains under nutrient-rich conditions (+N) and after 3 h of nitrogen starvation (-N 3 h). Error bars indicate the standard deviation of 3 independent experiments. ANOVA, ***P < 0.001. (**B**) Autophagy activity was measured with the GFP-Atg8 processing assay in WT and *vac8*Δ strains after 0, 1 and 2 h of nitrogen starvation (-N). A representative image based on detection with anti-YFP is shown. Pgk1 was used as a loading control. (**C**) Quantification of panel (**B**). The ratio of free GFP to Pgk1 after 1 and 2 h of nitrogen starvation (-N) is presented. Error bars indicate the standard deviation of 3 independent experiments. Student's t-test, ***P < 0.001.

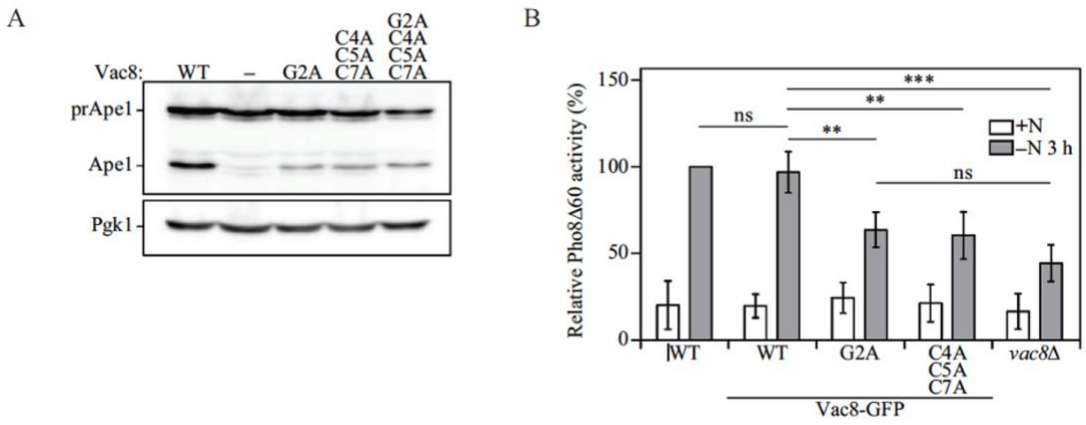

Figure 3.2 Vac8 vacuolar membrane localization is required for correct PAS localization and robust autophagy activity

(**A**) The *vac8Δ* strain (YTS178) was transformed with plasmids expressing wild-type *VAC8*, empty vector, the myristoylation defective *vac8* mutant (*vac8-2*) the palmitoylation defective vac8 mutant (*vac8-3*) or the myristoylation and palmitoylation double mutant (*vac8-4*). The strains were grown in SMD and collected at mid-log phase (OD_{600} = 0.5) and protein extracts were analyzed by western blot using antiserum against Ape1 as described in Materials and Methods. (**B**) Autophagy activity was measured with the Pho8Δ60 assay in wild-type (WT), Vac8-GFP, $Vac8^{G2A}$-GFP, $Vac8^{C4,5,7A}$-GFP and *vac8*Δ strains under nutrient-rich conditions (+N) and after 3 h of nitrogen starvation (-N 3 h). Error bars indicate the standard deviation of 3 independent experiments. ANOVA, **P < 0.01; ***P < 0.001. ns, no significance.

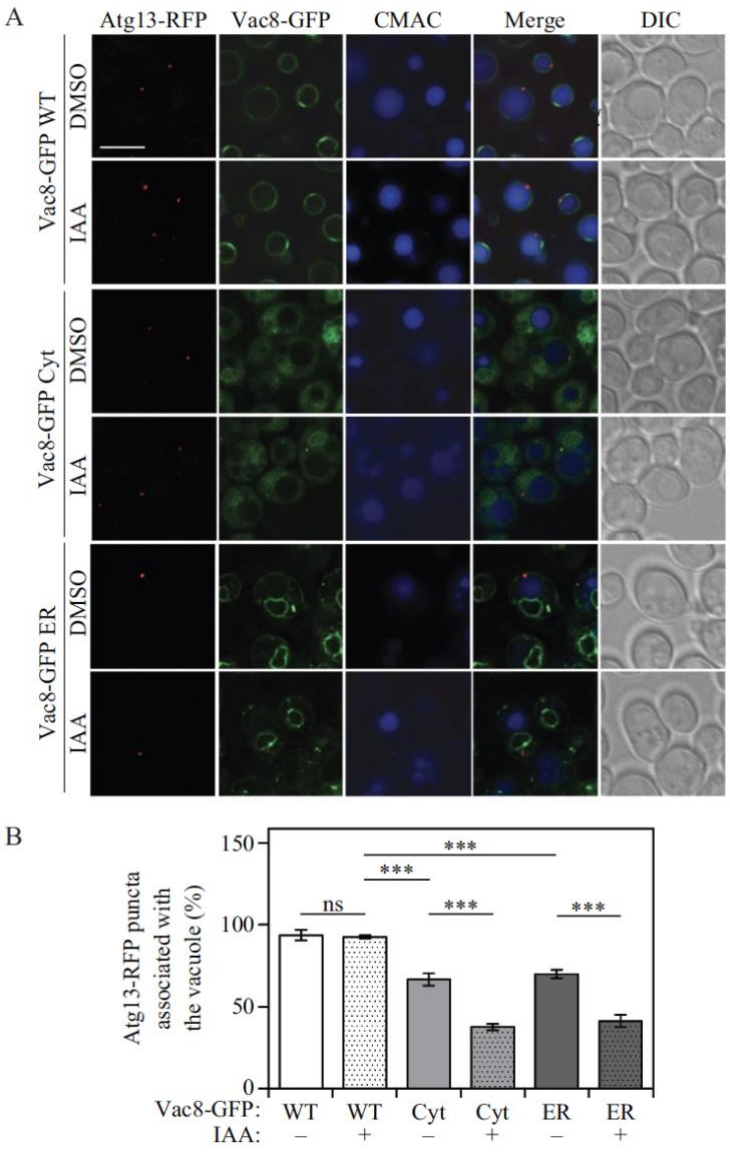

Figure 3.3 Vac8 vacuolar membrane localization is required for correct Atg13 localization (**A**) Atg13-RFP association with the vacuole was determined by fluorescence microscopy after 1 h of nitrogen starvation in strains expressing Vac8-AID-MYC and either Vac8-GFP WT, Vac8-GFP Cyt or Vac8-GFP ER. Strains were treated for 30 min with either IAA to induce Vac8-AID-MYC degradation, or control vehicle DMSO. The vacuolar lumen was stained using CMAC. (**B**) Quantification of panel (**A**). The percentage of cells in which Atg13-RFP puncta associated with the vacuole is presented. ANOVA, ***P < 0.001. ns, no significance.

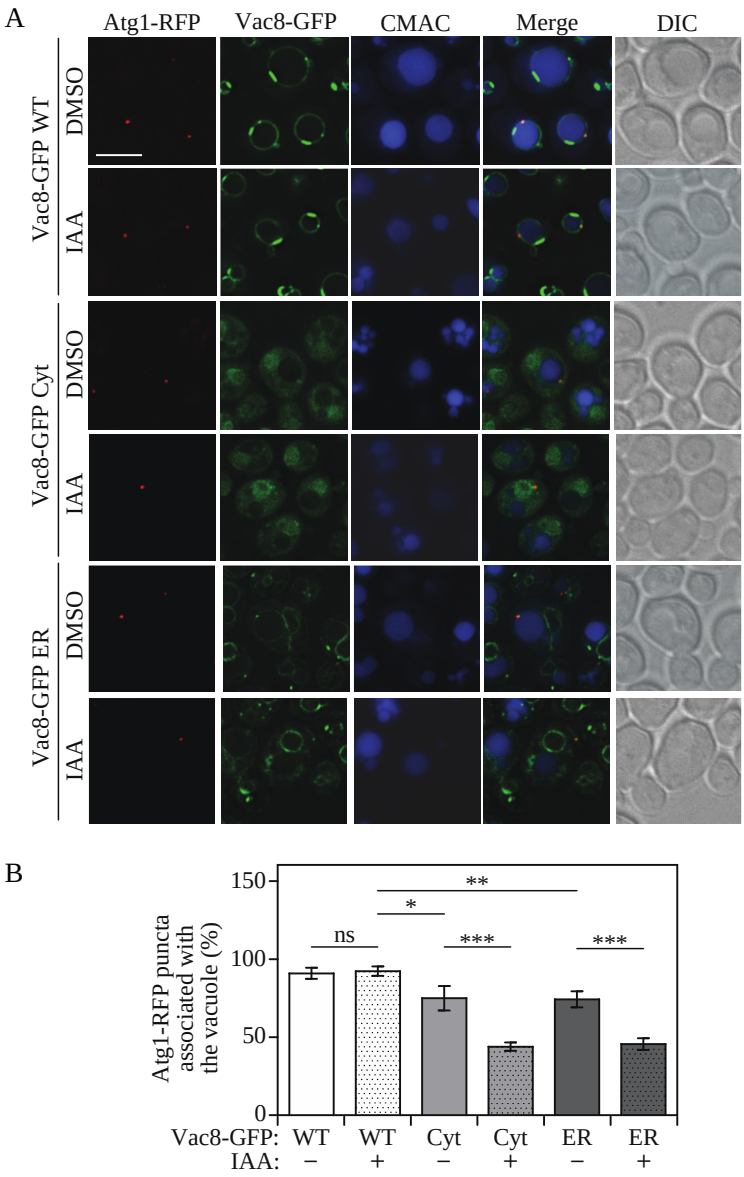

Figure 3.4 Vac8 vacuolar membrane localization is required for correct Atg1 localization
(**A**) Atg1-RFP association with the vacuole was determined by fluorescence microscopy after 1 h of nitrogen starvation in strains expressing Vac8-AID-MYC and either Vac8-GFP WT, Vac8-GFP Cyt or Vac8-GFP ER. Strains were treated for 30 min with either IAA to induce Vac8-AID-MYC degradation, or control vehicle DMSO. The vacuolar lumen was stained using CellTracker Blue CMAC. (**B**) Quantification of panel (**A**). The percentage of cells in which Atg1-RFP puncta associates with the vacuole is presented. ANOVA, ***P<0.001. ns, no significance.

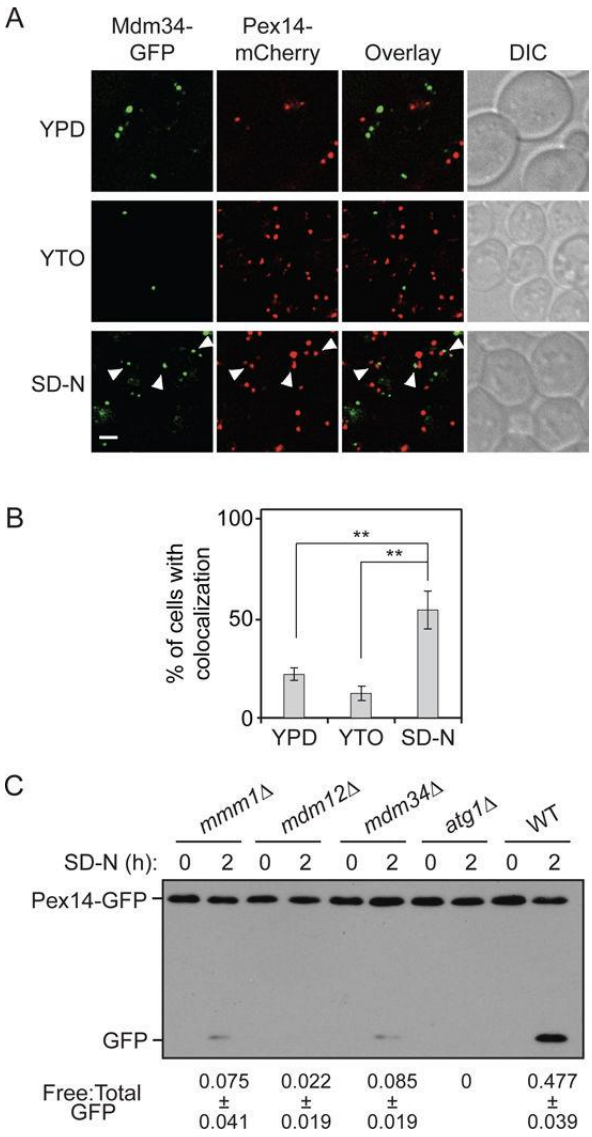

Figure 3.5 ER-mitochondria contacts contribute to pexophagy

(**A**) Pex14-mCherry Mdm34-GFP (XLY401) cells were cultured as described in the Experimental Procedures to induce pexophagy. The cells collected from the cultures in YPD, or YTO and the cells starved in SD-N for 1 h were imaged by fluorescence microscopy. Single Z-sections of representative images are shown. DIC, differential interference contrast. Scale bar: 2.5 μm. The arrowheads mark colocalizing GFP and mCherry puncta. (**B**) Quantification of the percentage of cells showing colocalization of mCherry and GFP puncta in (**A**). Error bars represent the standard deviation (SD) of three independent experiments. Two-tailed student's t-test was performed. **, $p<0.01$. (**C**) Pex14-GFP (TKMY67, WT), Pex14-GFP *mmm1*Δ (XLY403), Pex14-GFP *mdm12*Δ (XLY404), Pex14-GFP *mdm34*Δ (XLY405), and Pex14-GFP *atg1*Δ (TKMY72) cells were cultured as described in the Experimental Procedures to induce pexophagy. The samples collected from cultures in YTO (SD-N 0 h) and 2 h after nitrogen starvation (SD-N 2 h) were TCA precipitated, lysed, subjected to SDS-PAGE and analyzed by western blot. The ratio of free GFP to total GFP (free GFP+Pex14-GFP) was calculated for the samples. Average values ± s.d. of n = 3 independent experiments are shown as indicated.

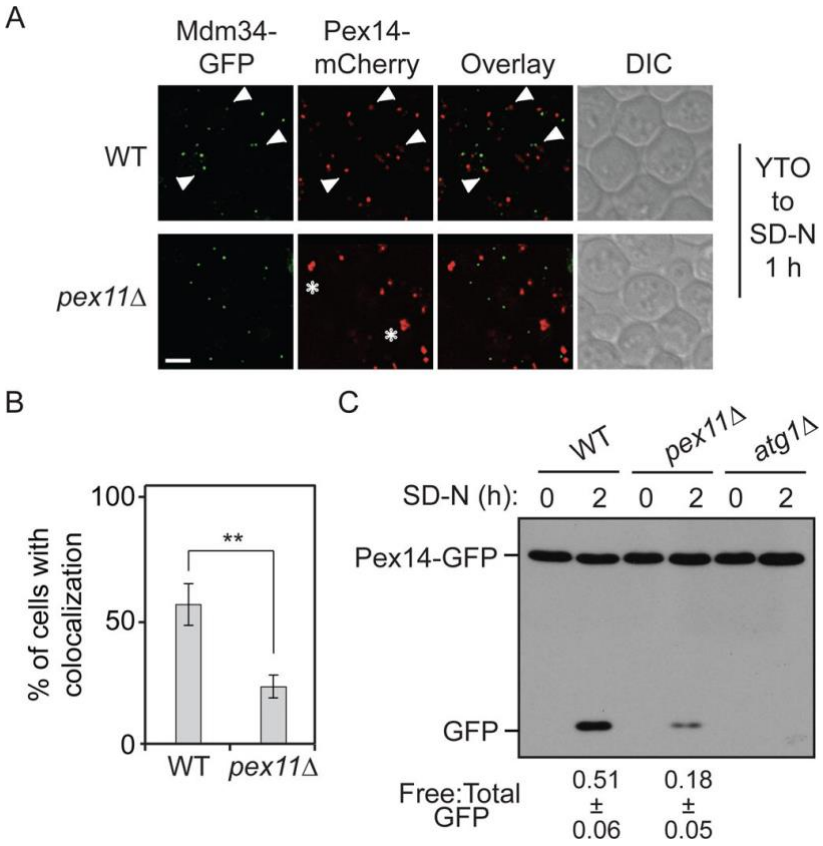

Figure 3.6 Pexophagy is defective in the *pex11*Δ mutant

(**A**) Pex14-mCherry Mdm34-GFP (XLY401, WT), and Pex14-mCherry Mdm34-GFP *pex11*Δ (XLY402) cells were cultured as described in the Experimental Procedures to induce pexophagy. After nitrogen starvation for 1 h, the cells were collected and imaged by fluorescence microscopy. Single Z-sections of representative images are shown. Scale bar: 2.5 μm. The arrowheads mark colocalizing GFP and mCherry puncta. The asterisks mark clusters of peroxisomes. (**B**) Quantification of the percentage of cells showing colocalization of mCherry and GFP puncta in (**A**). Error bars represent the standard deviation (SD) of three independent experiments. Two-tailed student's t-test was performed. **, $p<0.01$. (**C**) Pex14- GFP (TKMY67, WT), Pex14-GFP *pex11*Δ (XLY406), and Pex14-GFP *atg1*Δ (TKMY72) cells were cultured as described in the Experimental Procedures to induce pexophagy. The samples collected from cultures in YTO (SD-N 0 h) and 2 h after nitrogen starvation (SD-N 2 h) were TCA precipitated, lysed, subjected to SDS-PAGE and analyzed by western blot. The ratio of free GFP to total GFP (free GFP+Pex14-GFP) was calculated for the samples. Average values ± s.d. of n = 3 independent experiments are shown as indicated.

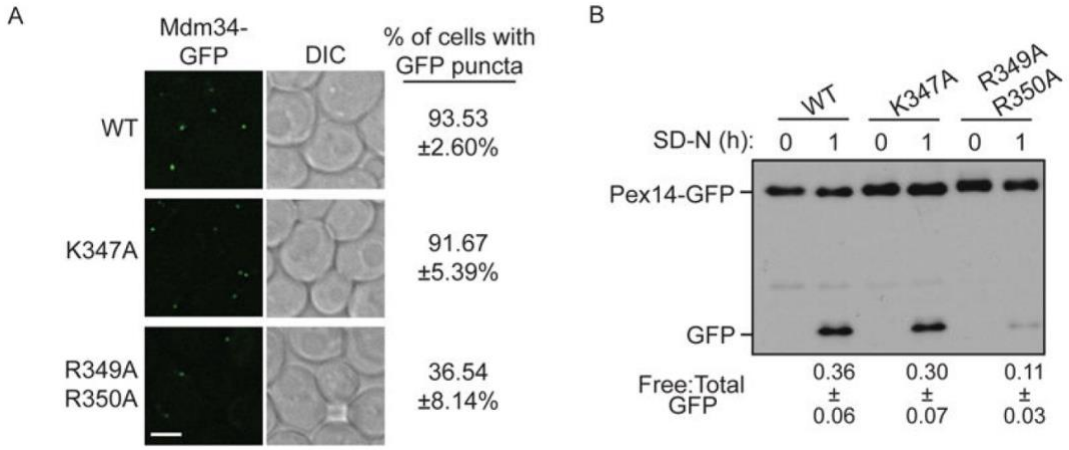

Figure 3.7 An R349A R350A double mutant of Mdm34 leads to defects in pexophagy
(**A**) Mdm34-GFP (XLY420, WT), Mdm34^{K347A}-GFP (XLY421) and Mdm34^{R349,350A}-GFP (XLY422). The percentage of cells showing GFP puncta was quantified. Average values ± s.d. of n = 3 independent experiments are shown as indicated. (**B**) Pex14-GFP Mdm34-VN (XLY428, WT), Pex14-GFP Mdm34^{K347A}-VN (XLY429), and Pex14-GFP Mdm34^{R349,350A}-VN (XLY430) cells were cultured as described in the Materials and Methods to induce pexophagy. The samples collected from cultures in YTO (SD-N 0 h) and 1 h after nitrogen starvation (SD-N 1 h) were TCA precipitated, lysed, subjected to SDS-PAGE and analyzed by western blot. The ratio of free GFP to total GFP (free GFP+Pex14-GFP) was calculated. Average values ± s.d. of n = 3 independent experiments are shown as indicated.

CHAPTER IV Summary[4]

Autophagy, a highly conserved lysosomal degradation pathway, plays an important role in cell physiology. The malfunction of autophagy is linked to various diseases, including cancer, neurodegeneration, metabolic disorders, heart disease and various rare diseases. Over the past several decades, research on autophagy has been advanced especially in the field of its regulation and molecular mechanism. By using *Saccharomyces cerevisiae* as a model system, my thesis has further expanded our understanding in the regulation and molecular mechanism of autophagy by investigating 1) the transcriptional regulation of the Spt4-Spt5 complex in autophagy; 2) the importance of Vac8 in phagophore assembly site (PAS) vacuolar localization and 3) the role of ER-mitochondria contact sites in pexophagy.

4.1 The transcription factor Spt4-Spt5 complex regulates the expression of *ATG8* and *ATG41*

The tight regulation of autophagy is important to maintain it at a proper magnitude, although little is known about the complicated regulatory networks that control autophagy at the transcriptional level. In mammalian cells, promoter-proximal pausing has been identified to control the output of transcripts with the help of the DSIF complex (comprised of homologs of Spt4 and Spt5), whereas there is no clear evidence showing that budding yeast shares a similar mechanism. In this project, for the first time, we revealed a negative role of Spt4 within the Spt4-Spt5 complex in regulating transcription in budding yeast. Furthermore, Spt4 and Spt5 carry out different functions regarding

[4] This chapter is reprinted partly from Xin Wen, Damián Gatica, Zhangyuan Yin, Zehan Hu, Jörn Dengjel, and Daniel J. Klionsky (2020) *Autophagy* (doi: https://doi.org/10.1080/15548627.2019.1659573), Damián Gatica, Xin Wen, Heesun Cheong, Daniel Klionsky (2020) *Autophagy* (doi: 10.1080/15548627.2020.1776474) and Xu Liu, Xin Wen, Daniel Klionsky (2019) *Contact (Thousand Oaks)* (doi: 10.1177/2515256418821584), with minor modifications

this regulation, in which Spt4 has a negative function in growing conditions whereas Spt5 is always required for efficient transcription of *ATG41*. Because autophagy plays a crucial physiological role, and its dysfunction is associated with many diseases, our results can also advance an understanding of the transcriptional control of autophagy, which may provide new directions for future therapeutics (Figure 4.1).

However, there are still many remaining questions that await further analysis. For example, the deletion of *BUR2* leads to a decreased level of *ATG8*/Atg8 (data not shown), while the nonphosphorylable Spt5 strain (Spt5[S7A]) causes no significant changes in the level of *ATG8*. Therefore, there appears to be another unknown mechanism behind the Sgv1-Bur2 kinase complex to directly regulate *ATG8*. Another question that remains to be answered is how the Sgv1 kinase complex senses the starvation signal and further enhances the phosphorylation of Spt5. Finally, our initial exploration of the negative function of Spt4 with regard to particular *ATG* genes was based on a raw large-scale PRO-seq analysis (data not shown), but it will also be important to determine what other genes that may affect autophagy, if any, are negatively regulated by Spt4.

4.2 Vac8 determines phagophore assembly site vacuolar localization

Previous studies had suggested that *VAC8* deletion leads to a decrease in nonselective autophagy activity, but the mechanism by which Vac8 regulates autophagy remained poorly understood. Dr. Damián Gatica and I worked together to show that the vacuolar membrane protein Vac8 is necessary for the recruitment and proper perivacuolar localization of the Atg1-Atg13 initiation complex and the PAS. We further determined that the effect of Vac8 on autophagy is unrelated to its function in preserving vacuolar morphology, but rather depends on its vacuolar localization. We also found that Vac8 acylation mutants, which fail to anchor to the vacuolar membrane, show decreased autophagy activity comparable to the decrease observed in *vac8*Δ cells. Furthermore,

mislocalization experiments targeting Vac8 to the cytosol, ER or peroxisomes resulted in autophagy activity defects similar to the ones observe in *VAC8* deletion strains. Targeting Vac8 to other cellular components also revealed that correct Vac8 vacuolar localization is necessary for proper recruitment of the Atg1-Atg13 initiation complex, PAS localization and Atg9 anterograde trafficking to the vacuolar periphery (data not shown here). The importance of Vac8 in the proper vacuolar assembly of all of these components can be best explained by its ability to bind Atg13 [165, 170, 200]. Truncating Atg13 and deleting its Vac8-binding domain decrease autophagy activity to similar levels as seen with deletion of *VAC8* and truncated Atg13 *vac8*Δ double-mutant strains, suggesting that the effect of *VAC8* deletion in autophagy can be explained by Atg13 failure to properly localize to the vacuole.

In mammals, autophagy initiation and phagophore expansion have been mostly attributed to specific PtdIns3P-rich ER subdomains [6]. Once fully matured, autophagosomes must be transported to fuse with lysosomes to degrade their cargo, a process that heavily relies on the cytoskeletal network [122]. In contrast, due to the perivacuolar nature of the PAS, Atg protein recruitment and phagophore expansion, nonselective autophagy in yeast does not depend on the cytoskeleton [193]. Our results underline the role of Vac8 as the main driver behind the initiation complex and PAS perivacuolar localization during autophagy induction in yeast. Vac8 interaction with Atg13 fulfills a double role: Whereas Vac8 function restricts the initiation complex and PAS assembly to the vacuolar periphery, Atg13 acts as a molecular hub for the recruitment of Atg1 and the Atg17-Atg31-Atg29 complex, and later downstream targets [54, 164-167]. Although Vac8-mediated spatiotemporal organization of the initiation complex is not essential for autophagy, its involvement in coordinating the formation of autophagosomes in close proximity with their final

vacuolar destination highlights its importance in improving the efficiency and strength of the autophagic process.

4.3 ER-mitochondria contacts are required for pexophagy in *S. cerevisiae*

Peroxisomes play important toles in lipid metabolism. Surplus or damaged peroxisomes can be selectively targeted for autophagic degradation, a process termed pexophagy. Maintaining a proper level of pexophagy is critical for cellular homeostasis. Recently, studies have implicated the role of membrane contact sites in nonselective autophagy, but no papers had been published on the topic of pexophagy. The result of this project suggests a model where ER-mitochondria contacts are the major sites for recruitment of pexophagy machinery and for the formation of pexophagy-specific autophagosomes (Figure 4.2).

Though the model seems intriguing, there are some aspects that we can further explore: 1) Although the Mdm34^{R349,350A} mutant shows impaired ERMES formation and weaker Pex11-Mdm34 interaction, we cannot tell whether this mutation directly diminishes the Pex11-Mdm34 interaction, or if the decreased ERMES formation in the mutant indirectly affects the interaction between the two proteins. 2) Decreased ERMES formation may cause partial defects in lipid transfer between the ER and mitochondria, which may affect mitochondrial protein function. Thus, we cannot fully exclude the possibility that defective pexophagy activity in the Mdm34^{R349,350A} mutant may be due to general mitochondrial defects.

Aside from the ERMES complex, the ER membrane protein complex (EMC) proteins also contribute to the contacts between ER and mitochondria to facilitate lipid transfer between the organelles [201]. It is likely that the EMC proteins also play roles in mitophagy and pexophagy. It was also demonstrated that a pool of autophagosomes form at ER-plasma membrane contact sites in mammalian cells [197]. ESYT (extended synaptotagmin) proteins, which are involved in

tethering between the ER and plasma membrane, recruit VMP1 and the class III phosphatidylinositol 3-kinase complex to promote local phosphatidylinositol-3-phosphate synthesis and autophagosome biogenesis [197]. In yeast cells, the tethering machinery between cortical ER and plasma membrane has been characterized [202, 203]. It will be of interest to test whether ER-plasma membrane contacts also contribute to nonselective and/or selective autophagy pathways in yeast cells.

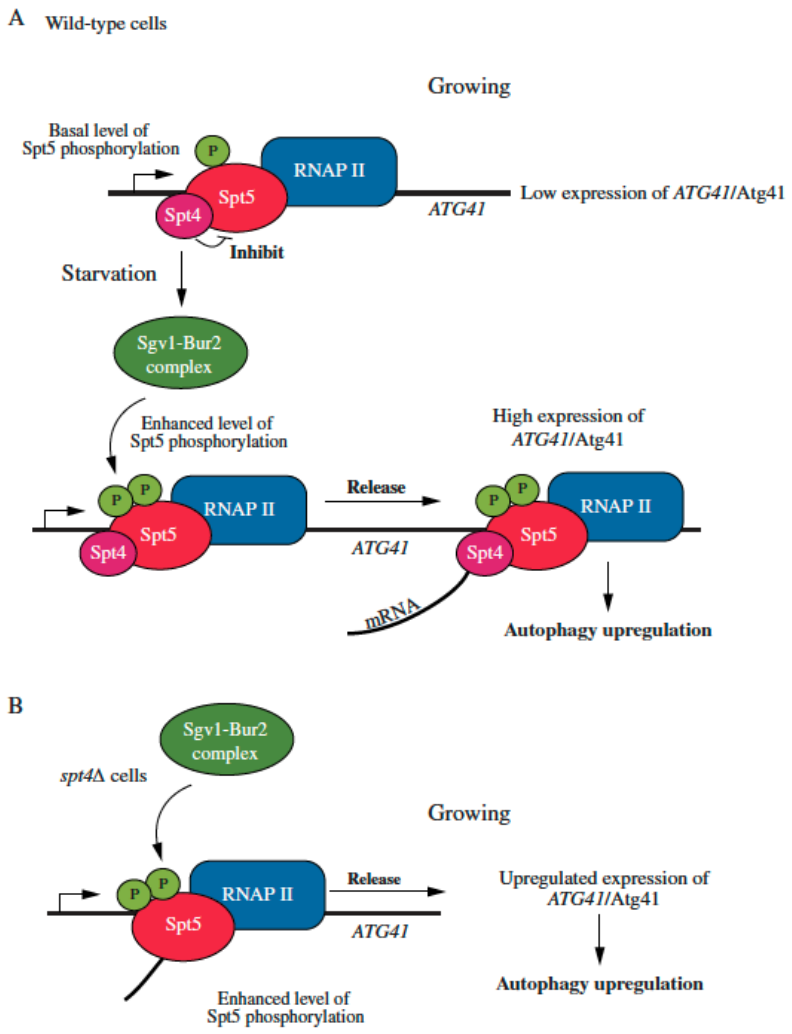

Figure 4.1 A model for Spt4-Spt5-dependent regulation of *ATG41*
(**A**) In wild-type cells under growing conditions, the Spt4-Spt5 complex may inhibit transcription of *ATG41* through an Spt4-dependent interference with Spt5 phosphorylation, causing the complex to accumulate near the transcription start site (TSS). After starvation, phosphorylation of Spt5 by the Sgv1-Bur2 kinase complex releases the inhibitory effect of Spt4 on *ATG41* transcription, and the Spt4-Spt5 complex participates in transcription elongation. (**B**) In *spt4Δ* cells, Spt5 does not accumulate near the TSS of *ATG41*, and transcription actively proceeds. Spt5 can also be more efficiently phosphorylated upon the deletion of *SPT4*.

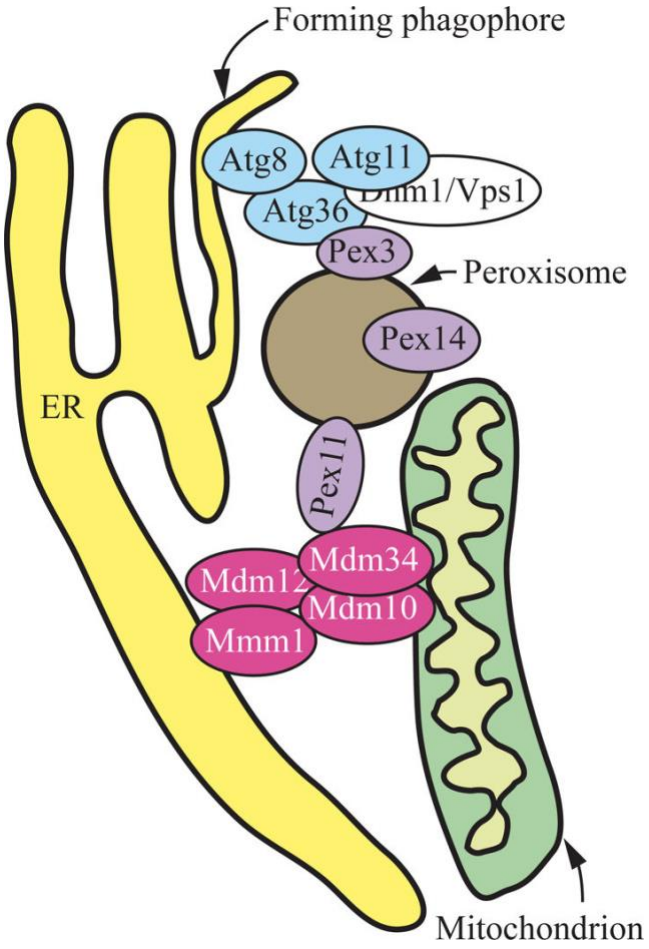

Figure 4.2 A model for the role of ER-mitochondria contact sites in pexophagy
The ERMES is composed of Mmm1 (ER), Mdm12 (cytosolic), Mdm10 and Mdm34 (mitochondria). Pex11 interaction with Mdm34 facilitates peroxisomal localization to the ER-mitochondria contact sites. Pex3 binds Atg36, the pexophagy receptor, which binds the scaffold protein Atg11. The latter two proteins recruit the components Dnm1 and Vps1 to facilitate peroxisome fission. Atg11 promotes binding of Atg36 to Atg8-PE, which is present on the forming phagophore membrane. The interaction between Atg36 and Atg8, which has been shown previously (Motley et al., 2012), allows selective peroxisome sequestration.

Bibliography

1. Yang, Z. and D.J. Klionsky, *Eaten alive: a history of macroautophagy.* Nat Cell Biol, 2010. **12**(9): p. 814-22.
2. Klionsky, D.J., et al., *A unified nomenclature for yeast autophagy-related genes.* Dev Cell, 2003. **5**(4): p. 539-45.
3. Klionsky, D.J., et al., *Guidelines for the use and interpretation of assays for monitoring autophagy (3rd edition).* Autophagy, 2016. **12**(1): p. 1-222.
4. Yang, Z. and D.J. Klionsky, *Mammalian autophagy: core molecular machinery and signaling regulation.* Curr Opin Cell Biol, 2010. **22**(2): p. 124-31.
5. Yorimitsu, T. and D.J. Klionsky, *Autophagy: molecular machinery for self-eating.* Cell Death Differ, 2005. **12 Suppl 2**: p. 1542-52.
6. Abada, A. and Z. Elazar, *Getting ready for building: signaling and autophagosome biogenesis.* EMBO Rep, 2014. **15**(8): p. 839-52.
7. Suzuki, K., et al., *The pre-autophagosomal structure organized by concerted functions of APG genes is essential for autophagosome formation.* EMBO J, 2001. **20**(21): p. 5971-81.
8. Mizushima, N., *The role of the Atg1/ULK1 complex in autophagy regulation.* Curr Opin Cell Biol, 2010. **22**(2): p. 132-9.
9. Burman, C. and N.T. Ktistakis, *Regulation of autophagy by phosphatidylinositol 3-phosphate.* FEBS Lett, 2010. **584**(7): p. 1302-12.
10. Chen, Y. and D.J. Klionsky, *The regulation of autophagy - unanswered questions.* J Cell Sci, 2011. **124**(Pt 2): p. 161-70.
11. Mizushima, N., et al., *A protein conjugation system essential for autophagy.* Nature, 1998. **395**(6700): p. 395-8.
12. Geng, J. and D.J. Klionsky, *The Atg8 and Atg12 ubiquitin-like conjugation systems in macroautophagy. 'Protein modifications: beyond the usual suspects' review series.* EMBO Rep, 2008. **9**(9): p. 859-64.
13. Shpilka, T., N. Mizushima, and Z. Elazar, *Ubiquitin-like proteins and autophagy at a glance.* J Cell Sci, 2012. **125**(Pt 10): p. 2343-8.
14. Reggiori, F., et al., *The Atg1-Atg13 complex regulates Atg9 and Atg23 retrieval transport from the pre-autophagosomal structure.* Dev Cell, 2004. **6**(1): p. 79-90.
15. Knorr, R.L., R. Lipowsky, and R. Dimova, *Autophagosome closure requires membrane scission.* Autophagy, 2015. **11**(11): p. 2134-2137.
16. Hurley, J.H., *The ESCRT complexes.* Crit Rev Biochem Mol Biol, 2010. **45**(6): p. 463-87.
17. Hurley, J.H. and P.I. Hanson, *Membrane budding and scission by the ESCRT machinery: it's all in the neck.* Nat Rev Mol Cell Biol, 2010. **11**(8): p. 556-66.

18. Hurley, J.H., *ESCRTs are everywhere.* EMBO J, 2015. **34**(19): p. 2398-407.
19. Devenish, R.J. and D.J. Klionsky, *Autophagy: mechanism and physiological relevance 'brewed' from yeast studies.* Front Biosci (Schol Ed), 2012. **4**: p. 1354-63.
20. Epple, U.D., et al., *Aut5/Cvt17p, a putative lipase essential for disintegration of autophagic bodies inside the vacuole.* J Bacteriol, 2001. **183**(20): p. 5942-55.
21. Wirawan, E., et al., *Autophagy: for better or for worse.* Cell Res, 2012. **22**(1): p. 43-61.
22. Dou, Y., et al., *Physical association and coordinate function of the H3 K4 methyltransferase MLL1 and the H4 K16 acetyltransferase MOF.* Cell, 2005. **121**(6): p. 873-85.
23. Eisenberg, T., et al., *Induction of autophagy by spermidine promotes longevity.* Nat Cell Biol, 2009. **11**(11): p. 1305-14.
24. Chen, H., et al., *The histone H3 lysine 56 acetylation pathway is regulated by target of rapamycin (TOR) signaling and functions directly in ribosomal RNA biogenesis.* Nucleic Acids Res, 2012. **40**(14): p. 6534-46.
25. Fullgrabe, J., et al., *The histone H4 lysine 16 acetyltransferase hMOF regulates the outcome of autophagy.* Nature, 2013. **500**(7463): p. 468-71.
26. Nakatogawa, H., Y. Ichimura, and Y. Ohsumi, *Atg8, a ubiquitin-like protein required for autophagosome formation, mediates membrane tethering and hemifusion.* Cell, 2007. **130**(1): p. 165-78.
27. Abeliovich, H., et al., *Dissection of autophagosome biogenesis into distinct nucleation and expansion steps.* J Cell Biol, 2000. **151**(5): p. 1025-34.
28. Kirisako, T., et al., *Formation process of autophagosome is traced with Apg8/Aut7p in yeast.* J Cell Biol, 1999. **147**(2): p. 435-46.
29. Kadosh, D. and K. Struhl, *Repression by Ume6 involves recruitment of a complex containing Sin3 corepressor and Rpd3 histone deacetylase to target promoters.* Cell, 1997. **89**(3): p. 365-71.
30. Laherty, C.D., et al., *Histone deacetylases associated with the mSin3 corepressor mediate mad transcriptional repression.* Cell, 1997. **89**(3): p. 349-56.
31. Taunton, J., C.A. Hassig, and S.L. Schreiber, *A mammalian histone deacetylase related to the yeast transcriptional regulator Rpd3p.* Science, 1996. **272**(5260): p. 408-11.
32. Bartholomew, C.R., et al., *Ume6 transcription factor is part of a signaling cascade that regulates autophagy.* Proc Natl Acad Sci U S A, 2012. **109**(28): p. 11206-10.
33. Pedruzzi, I., et al., *TOR and PKA signaling pathways converge on the protein kinase Rim15 to control entry into G0.* Mol Cell, 2003. **12**(6): p. 1607-13.
34. Wei, M., et al., *Life span extension by calorie restriction depends on Rim15 and transcription factors downstream of Ras/PKA, Tor, and Sch9.* PLoS Genet, 2008. **4**(1): p. e13.
35. Liang, C.Y., L.C. Wang, and W.S. Lo, *Dissociation of the H3K36 demethylase Rph1 from chromatin mediates derepression of environmental stress-response genes under genotoxic stress in Saccharomyces cerevisiae.* Mol Biol Cell, 2013. **24**(20): p. 3251-62.
36. Jang, Y.K., L. Wang, and G.B. Sancar, *RPH1 and GIS1 are damage-responsive repressors of PHR1.* Mol Cell Biol, 1999. **19**(11): p. 7630-8.
37. Bernard, A., et al., *Rph1/KDM4 mediates nutrient-limitation signaling that leads to the transcriptional induction of autophagy.* Curr Biol, 2015. **25**(5): p. 546-55.

38. Loewith, R., et al., *Pho23 is associated with the Rpd3 histone deacetylase and is required for its normal function in regulation of gene expression and silencing in Saccharomyces cerevisiae.* J Biol Chem, 2001. **276**(26): p. 24068-74.
39. Jin, M., et al., *Transcriptional regulation by Pho23 modulates the frequency of autophagosome formation.* Curr Biol, 2014. **24**(12): p. 1314-1322.
40. Bernard, A., et al., *A large-scale analysis of autophagy-related gene expression identifies new regulators of autophagy.* Autophagy, 2015. **11**(11): p. 2114-2122.
41. Hofman-Bang, J., *Nitrogen catabolite repression in Saccharomyces cerevisiae.* Mol Biotechnol, 1999. **12**(1): p. 35-73.
42. Magasanik, B. and C.A. Kaiser, *Nitrogen regulation in Saccharomyces cerevisiae.* Gene, 2002. **290**(1-2): p. 1-18.
43. Feller, A., et al., *Transduction of the nitrogen signal activating Gln3-mediated transcription is independent of Npr1 kinase and Rsp5-Bul1/2 ubiquitin ligase in Saccharomyces cerevisiae.* J Biol Chem, 2006. **281**(39): p. 28546-54.
44. Robertson, L.S. and G.R. Fink, *The three yeast A kinases have specific signaling functions in pseudohyphal growth.* Proc Natl Acad Sci U S A, 1998. **95**(23): p. 13783-7.
45. Nissan, T., et al., *Decapping activators in Saccharomyces cerevisiae act by multiple mechanisms.* Mol Cell, 2010. **39**(5): p. 773-83.
46. Hu, G., et al., *A conserved mechanism of TOR-dependent RCK-mediated mRNA degradation regulates autophagy.* Nat Cell Biol, 2015. **17**(7): p. 930-942.
47. Gatica, D., et al., *The Pat1-Lsm Complex Stabilizes ATG mRNA during Nitrogen Starvation-Induced Autophagy.* Mol Cell, 2019. **73**(2): p. 314-324 e4.
48. Popelka, H. and D.J. Klionsky, *Post-translationally-modified structures in the autophagy machinery: an integrative perspective.* FEBS J, 2015. **282**(18): p. 3474-88.
49. Boya, P., F. Reggiori, and P. Codogno, *Emerging regulation and functions of autophagy.* Nat Cell Biol, 2013. **15**(7): p. 713-20.
50. Wani, W.Y., et al., *Regulation of autophagy by protein post-translational modification.* Lab Invest, 2015. **95**(1): p. 14-25.
51. Xie, Y., et al., *Posttranslational modification of autophagy-related proteins in macroautophagy.* Autophagy, 2015. **11**(1): p. 28-45.
52. Kijanska, M., et al., *Activation of Atg1 kinase in autophagy by regulated phosphorylation.* Autophagy, 2010. **6**(8): p. 1168-78.
53. Yeh, Y.Y., et al., *The identification and analysis of phosphorylation sites on the Atg1 protein kinase.* Autophagy, 2011. **7**(7): p. 716-26.
54. Kamada, Y., et al., *Tor-mediated induction of autophagy via an Apg1 protein kinase complex.* J Cell Biol, 2000. **150**(6): p. 1507-13.
55. Budovskaya, Y.V., et al., *The Ras/cAMP-dependent protein kinase signaling pathway regulates an early step of the autophagy process in Saccharomyces cerevisiae.* J Biol Chem, 2004. **279**(20): p. 20663-71.
56. Stephan, J.S., et al., *The Tor and cAMP-dependent protein kinase signaling pathways coordinately control autophagy in Saccharomyces cerevisiae.* Autophagy, 2010. **6**(2): p. 294-5.
57. Kamada, Y., et al., *Tor directly controls the Atg1 kinase complex to regulate autophagy.* Mol Cell Biol, 2010. **30**(4): p. 1049-58.

58. Stephan, J.S., et al., *The Tor and PKA signaling pathways independently target the Atg1/Atg13 protein kinase complex to control autophagy.* Proc Natl Acad Sci U S A, 2009. **106**(40): p. 17049-54.
59. Budovskaya, Y.V., et al., *An evolutionary proteomics approach identifies substrates of the cAMP-dependent protein kinase.* Proc Natl Acad Sci U S A, 2005. **102**(39): p. 13933-8.
60. Yeh, Y.Y., K. Wrasman, and P.K. Herman, *Autophosphorylation within the Atg1 activation loop is required for both kinase activity and the induction of autophagy in Saccharomyces cerevisiae.* Genetics, 2010. **185**(3): p. 871-82.
61. Delorme-Axford, E. and D.J. Klionsky, *A missing piece of the puzzle: Atg11 functions as a scaffold to activate Atg1 for selective autophagy.* Autophagy, 2015. **11**(12): p. 2139-41.
62. Reggiori, F., et al., *Early stages of the secretory pathway, but not endosomes, are required for Cvt vesicle and autophagosome assembly in Saccharomyces cerevisiae.* Mol Biol Cell, 2004. **15**(5): p. 2189-204.
63. Mao, K., et al., *Atg29 phosphorylation regulates coordination of the Atg17-Atg31-Atg29 complex with the Atg11 scaffold during autophagy initiation.* Proc Natl Acad Sci U S A, 2013. **110**(31): p. E2875-84.
64. Feng, W., et al., *Phosphorylation of Atg31 is required for autophagy.* Protein Cell, 2015. **6**(4): p. 288-96.
65. Papinski, D. and C. Kraft, *Atg1 kinase organizes autophagosome formation by phosphorylating Atg9.* Autophagy, 2014. **10**(7): p. 1338-40.
66. Papinski, D., et al., *Early steps in autophagy depend on direct phosphorylation of Atg9 by the Atg1 kinase.* Mol Cell, 2014. **53**(3): p. 471-83.
67. Aoki, Y., et al., *Phosphorylation of Serine 114 on Atg32 mediates mitophagy.* Mol Biol Cell, 2011. **22**(17): p. 3206-17.
68. Tanaka, C., et al., *Hrr25 triggers selective autophagy-related pathways by phosphorylating receptor proteins.* J Cell Biol, 2014. **207**(1): p. 91-105.
69. Stack, J.H., et al., *A membrane-associated complex containing the Vps15 protein kinase and the Vps34 PI 3-kinase is essential for protein sorting to the yeast lysosome-like vacuole.* EMBO J, 1993. **12**(5): p. 2195-204.
70. Vergne, I. and V. Deretic, *The role of PI3P phosphatases in the regulation of autophagy.* FEBS Lett, 2010. **584**(7): p. 1313-8.
71. Obara, K., et al., *The Atg18-Atg2 complex is recruited to autophagic membranes via phosphatidylinositol 3-phosphate and exerts an essential function.* J Biol Chem, 2008. **283**(35): p. 23972-80.
72. Busse, R.A., et al., *Qualitative and quantitative characterization of protein-phosphoinositide interactions with liposome-based methods.* Autophagy, 2013. **9**(5): p. 770-7.
73. Juris, L., et al., *PI3P binding by Atg21 organises Atg8 lipidation.* EMBO J, 2015. **34**(7): p. 955-73.
74. Cebollero, E., et al., *Phosphatidylinositol-3-phosphate clearance plays a key role in autophagosome completion.* Curr Biol, 2012. **22**(17): p. 1545-53.
75. Yu, X., et al., *Myotubularin family phosphatase ceMTM3 is required for muscle maintenance by preventing excessive autophagy in Caenorhabditis elegans.* BMC Cell Biol, 2012. **13**: p. 28.
76. Vergne, I., et al., *Control of autophagy initiation by phosphoinositide 3-phosphatase Jumpy.* EMBO J, 2009. **28**(15): p. 2244-58.

77. Wang, X., J.S. Pattison, and H. Su, *Posttranslational modification and quality control.* Circ Res, 2013. **112**(2): p. 367-81.
78. Nazio, F., et al., *mTOR inhibits autophagy by controlling ULK1 ubiquitylation, self-association and function through AMBRA1 and TRAF6.* Nat Cell Biol, 2013. **15**(4): p. 406-16.
79. Shi, C.S. and J.H. Kehrl, *Traf6 and A20 differentially regulate TLR4-induced autophagy by affecting the ubiquitination of Beclin 1.* Autophagy, 2010. **6**(7): p. 986-7.
80. Kuang, E., et al., *Regulation of ATG4B stability by RNF5 limits basal levels of autophagy and influences susceptibility to bacterial infection.* PLoS Genet, 2012. **8**(10): p. e1003007.
81. Yi, C., et al., *Function and molecular mechanism of acetylation in autophagy regulation.* Science, 2012. **336**(6080): p. 474-7.
82. Hamai, A. and P. Codogno, *New targets for acetylation in autophagy.* Sci Signal, 2012. **5**(231): p. pe29.
83. Guimaraes, R.S., et al., *Assays for the biochemical and ultrastructural measurement of selective and nonselective types of autophagy in the yeast Saccharomyces cerevisiae.* Methods, 2015. **75**: p. 141-50.
84. Mijaljica, D., et al., *Receptor protein complexes are in control of autophagy.* Autophagy, 2012. **8**(11): p. 1701-5.
85. Scott, S.V., et al., *Cvt19 is a receptor for the cytoplasm-to-vacuole targeting pathway.* Mol Cell, 2001. **7**(6): p. 1131-41.
86. Kraft, C., M. Peter, and K. Hofmann, *Selective autophagy: ubiquitin-mediated recognition and beyond.* Nat Cell Biol, 2010. **12**(9): p. 836-41.
87. Lynch-Day, M.A. and D.J. Klionsky, *The Cvt pathway as a model for selective autophagy.* FEBS Lett, 2010. **584**(7): p. 1359-66.
88. Hutchins, M.U. and D.J. Klionsky, *Vacuolar localization of oligomeric alpha-mannosidase requires the cytoplasm to vacuole targeting and autophagy pathway components in Saccharomyces cerevisiae.* J Biol Chem, 2001. **276**(23): p. 20491-8.
89. Watanabe, Y., et al., *Selective transport of alpha-mannosidase by autophagic pathways: structural basis for cargo recognition by Atg19 and Atg34.* J Biol Chem, 2010. **285**(39): p. 30026-33.
90. Yuga, M., et al., *Aspartyl aminopeptidase is imported from the cytoplasm to the vacuole by selective autophagy in Saccharomyces cerevisiae.* J Biol Chem, 2011. **286**(15): p. 13704-13.
91. Kanki, T., et al., *Atg32 is a mitochondrial protein that confers selectivity during mitophagy.* Dev Cell, 2009. **17**(1): p. 98-109.
92. Okamoto, K., N. Kondo-Okamoto, and Y. Ohsumi, *Mitochondria-anchored receptor Atg32 mediates degradation of mitochondria via selective autophagy.* Dev Cell, 2009. **17**(1): p. 87-97.
93. Kanki, T., et al., *A genomic screen for yeast mutants defective in selective mitochondria autophagy.* Mol Biol Cell, 2009. **20**(22): p. 4730-8.
94. Motley, A.M., J.M. Nuttall, and E.H. Hettema, *Pex3-anchored Atg36 tags peroxisomes for degradation in Saccharomyces cerevisiae.* EMBO J, 2012. **31**(13): p. 2852-68.
95. Kuma, A., M. Komatsu, and N. Mizushima, *Autophagy-monitoring and autophagy-deficient mice.* Autophagy, 2017. **13**(10): p. 1619-1628.
96. Jiang, P. and N. Mizushima, *Autophagy and human diseases.* Cell Res, 2014. **24**(1): p. 69-79.

97. Levine, B. and G. Kroemer, *Biological Functions of Autophagy Genes: A Disease Perspective.* Cell, 2019. **176**(1-2): p. 11-42.
98. Frake, R.A., et al., *Autophagy and neurodegeneration.* J Clin Invest, 2015. **125**(1): p. 65-74.
99. Levine, B. and G. Kroemer, *Autophagy in the pathogenesis of disease.* Cell, 2008. **132**(1): p. 27-42.
100. Mizushima, N., et al., *Autophagy fights disease through cellular self-digestion.* Nature, 2008. **451**(7182): p. 1069-75.
101. White, E., *The role for autophagy in cancer.* J Clin Invest, 2015. **125**(1): p. 42-6.
102. Galluzzi, L., et al., *Metabolic control of autophagy.* Cell, 2014. **159**(6): p. 1263-76.
103. Zhang, Y., J.R. Sowers, and J. Ren, *Targeting autophagy in obesity: from pathophysiology to management.* Nat Rev Endocrinol, 2018. **14**(6): p. 356-376.
104. Ueno, T. and M. Komatsu, *Autophagy in the liver: functions in health and disease.* Nat Rev Gastroenterol Hepatol, 2017. **14**(3): p. 170-184.
105. Rubinstein, Y.R., et al., *The case for open science: rare diseases.* JAMIA Open, 2020. **3**(3): p. 472-486.
106. Lieberman, A.P., et al., *Autophagy in lysosomal storage disorders.* Autophagy, 2012. **8**(5): p. 719-30.
107. Meske, V., et al., *The autophagic defect in Niemann-Pick disease type C neurons differs from somatic cells and reduces neuronal viability.* Neurobiol Dis, 2014. **64**: p. 88-97.
108. Vanier, M.T. and G. Millat, *Structure and function of the NPC2 protein.* Biochim Biophys Acta, 2004. **1685**(1-3): p. 14-21.
109. Li, X., et al., *Structure of human Niemann-Pick C1 protein.* Proc Natl Acad Sci U S A, 2016. **113**(29): p. 8212-7.
110. Liao, G., et al., *Cholesterol accumulation is associated with lysosomal dysfunction and autophagic stress in Npc1 -/- mouse brain.* Am J Pathol, 2007. **171**(3): p. 962-75.
111. Maetzel, D., et al., *Genetic and chemical correction of cholesterol accumulation and impaired autophagy in hepatic and neural cells derived from Niemann-Pick Type C patient-specific iPS cells.* Stem Cell Reports, 2014. **2**(6): p. 866-80.
112. Lee, H., et al., *Pathological roles of the VEGF/SphK pathway in Niemann-Pick type C neurons.* Nat Commun, 2014. **5**: p. 5514.
113. Sarkar, S., et al., *Impaired autophagy in the lipid-storage disorder Niemann-Pick type C1 disease.* Cell Rep, 2013. **5**(5): p. 1302-15.
114. Hruska, K.S., et al., *Gaucher disease: mutation and polymorphism spectrum in the glucocerebrosidase gene (GBA).* Hum Mutat, 2008. **29**(5): p. 567-83.
115. Mistry, P.K., et al., *Gaucher disease: Progress and ongoing challenges.* Mol Genet Metab, 2017. **120**(1-2): p. 8-21.
116. Awad, O., et al., *Altered TFEB-mediated lysosomal biogenesis in Gaucher disease iPSC-derived neuronal cells.* Hum Mol Genet, 2015. **24**(20): p. 5775-88.
117. Farfel-Becker, T., et al., *Neuronal accumulation of glucosylceramide in a mouse model of neuronopathic Gaucher disease leads to neurodegeneration.* Hum Mol Genet, 2014. **23**(4): p. 843-54.
118. Osellame, L.D., et al., *Mitochondria and quality control defects in a mouse model of Gaucher disease--links to Parkinson's disease.* Cell Metab, 2013. **17**(6): p. 941-953.
119. Sun, Y., et al., *Neuronopathic Gaucher disease in the mouse: viable combined selective saposin C deficiency and mutant glucocerebrosidase (V394L) mice with*

glucosylsphingosine and glucosylceramide accumulation and progressive neurological deficits. Hum Mol Genet, 2010. **19**(6): p. 1088-97.
120. Xu, Y.H., et al., *Multiple pathogenic proteins implicated in neuronopathic Gaucher disease mice.* Hum Mol Genet, 2014. **23**(15): p. 3943-57.
121. Feng, Y., et al., *The machinery of macroautophagy.* Cell Res, 2014. **24**(1): p. 24-41.
122. Baba, M., et al., *Ultrastructural analysis of the autophagic process in yeast: detection of autophagosomes and their characterization.* J Cell Biol, 1994. **124**(6): p. 903-13.
123. Yang, Z. and D.J. Klionsky, *An overview of the molecular mechanism of autophagy.* Curr Top Microbiol Immunol, 2009. **335**: p. 1-32.
124. He, C. and D.J. Klionsky, *Regulation mechanisms and signaling pathways of autophagy.* Annu Rev Genet, 2009. **43**: p. 67-93.
125. Wen, X. and D.J. Klionsky, *An overview of macroautophagy in yeast.* J Mol Biol, 2016. **428**(9 Pt A): p. 1681-99.
126. Reggiori, F. and D.J. Klionsky, *Autophagic processes in yeast: mechanism, machinery and regulation.* Genetics, 2013. **194**(2): p. 341-61.
127. Shintani, T. and D.J. Klionsky, *Autophagy in health and disease: a double-edged sword.* Science, 2004. **306**(5698): p. 990-5.
128. Yao, Z., et al., *Atg41/Icy2 regulates autophagosome formation.* Autophagy, 2015. **11**(12): p. 2288-99.
129. Xie, Z., U. Nair, and D.J. Klionsky, *Atg8 controls phagophore expansion during autophagosome formation.* Mol Biol Cell, 2008. **19**(8): p. 3290-8.
130. Hartzog, G.A. and J. Fu, *The Spt4-Spt5 complex: a multi-faceted regulator of transcription elongation.* Biochim Biophys Acta, 2013. **1829**(1): p. 105-15.
131. Wada, T., et al., *DSIF, a novel transcription elongation factor that regulates RNA polymerase II processivity, is composed of human Spt4 and Spt5 homologs.* Genes Dev, 1998. **12**(3): p. 343-56.
132. Yamaguchi, Y., et al., *NELF, a multisubunit complex containing RD, cooperates with DSIF to repress RNA polymerase II elongation.* Cell, 1999. **97**(1): p. 41-51.
133. Ni, Z., et al., *P-TEFb is critical for the maturation of RNA polymerase II into productive elongation in vivo.* Mol Cell Biol, 2008. **28**(3): p. 1161-70.
134. Yamada, T., et al., *P-TEFb-mediated phosphorylation of hSpt5 C-terminal repeats is critical for processive transcription elongation.* Mol Cell, 2006. **21**(2): p. 227-37.
135. Chen, Y., et al., *DSIF, the Paf1 complex, and Tat-SF1 have nonredundant, cooperative roles in RNA polymerase II elongation.* Genes Dev, 2009. **23**(23): p. 2765-77.
136. Booth, G.T., et al., *Divergence of a conserved elongation factor and transcription regulation in budding and fission yeast.* Genome Res, 2016. **26**(6): p. 799-811.
137. Ammerer, G., et al., *PEP4 gene of Saccharomyces cerevisiae encodes proteinase A, a vacuolar enzyme required for processing of vacuolar precursors.* Mol Cell Biol, 1986. **6**(7): p. 2490-9.
138. Rondon, A.G., et al., *Molecular evidence for a positive role of Spt4 in transcription elongation.* EMBO J, 2003. **22**(3): p. 612-20.
139. Klionsky, D.J. and S.D. Emr, *Membrane protein sorting: biosynthesis, transport and processing of yeast vacuolar alkaline phosphatase.* EMBO J, 1989. **8**(8): p. 2241-50.
140. Klionsky, D.J., *Monitoring autophagy in yeast: the Pho8Delta60 assay.* Methods Mol Biol, 2007. **390**: p. 363-71.

141. Shintani, T. and D.J. Klionsky, *Cargo proteins facilitate the formation of transport vesicles in the cytoplasm to vacuole targeting pathway.* J Biol Chem, 2004. **279**(29): p. 29889-94.
142. Scott, S.V., et al., *Apg13p and Vac8p are part of a complex of phosphoproteins that are required for cytoplasm to vacuole targeting.* J Biol Chem, 2000. **275**(33): p. 25840-9.
143. Liu, Y., et al., *Phosphorylation of the transcription elongation factor Spt5 by yeast Bur1 kinase stimulates recruitment of the PAF complex.* Mol Cell Biol, 2009. **29**(17): p. 4852-63.
144. Swaney, D.L., et al., *Global analysis of phosphorylation and ubiquitylation cross-talk in protein degradation.* Nat Methods, 2013. **10**(7): p. 676-82.
145. Holt, L.J., et al., *Global analysis of Cdk1 substrate phosphorylation sites provides insights into evolution.* Science, 2009. **325**(5948): p. 1682-6.
146. Morawska, M. and H.D. Ulrich, *An expanded tool kit for the auxin-inducible degron system in budding yeast.* Yeast, 2013. **30**(9): p. 341-51.
147. Wood, A. and A. Shilatifard, *Bur1/Bur2 and the Ctk complex in yeast: the split personality of mammalian P-TEFb.* Cell Cycle, 2006. **5**(10): p. 1066-8.
148. Yorimitsu, T., et al., *Protein kinase A and Sch9 cooperatively regulate induction of autophagy in Saccharomyces cerevisiae.* Mol Biol Cell, 2007. **18**(10): p. 4180-9.
149. Tardiff, D.F., K.C. Abruzzi, and M. Rosbash, *Protein characterization of Saccharomyces cerevisiae RNA polymerase II after in vivo cross-linking.* Proc Natl Acad Sci U S A, 2007. **104**(50): p. 19948-53.
150. Scheidegger, A. and S. Nechaev, *RNA polymerase II pausing as a context-dependent reader of the genome.* Biochem Cell Biol, 2016. **94**(1): p. 82-92.
151. Hu, G., et al., *The role of transcriptional 'futile cycles' in autophagy and microbial pathogenesis.* Microb Cell, 2015. **2**(8): p. 302-304.
152. Longtine, M.S., et al., *Additional modules for versatile and economical PCR-based gene deletion and modification in Saccharomyces cerevisiae.* Yeast, 1998. **14**(10): p. 953-61.
153. Gueldener, U., et al., *A second set of loxP marker cassettes for Cre-mediated multiple gene knockouts in budding yeast.* Nucleic Acids Res, 2002. **30**(6): p. e23.
154. Abeliovich, H., et al., *Chemical genetic analysis of Apg1 reveals a non-kinase role in the induction of autophagy.* Mol Biol Cell, 2003. **14**(2): p. 477-90.
155. Klionsky, D.J., R. Cueva, and D.S. Yaver, *Aminopeptidase I of Saccharomyces cerevisiae is localized to the vacuole independent of the secretory pathway.* J Cell Biol, 1992. **119**(2): p. 287-99.
156. Huang, W.P., et al., *The itinerary of a vesicle component, Aut7p/Cvt5p, terminates in the yeast vacuole via the autophagy/Cvt pathways.* J Biol Chem, 2000. **275**(8): p. 5845-51.
157. Geng, J., et al., *Post-Golgi Sec proteins are required for autophagy in Saccharomyces cerevisiae.* Mol Biol Cell, 2010. **21**(13): p. 2257-69.
158. Aparicio, O., et al., *Chromatin immunoprecipitation for determining the association of proteins with specific genomic sequences in vivo.* Curr Protoc Mol Biol, 2005. **Chapter 21**: p. Unit 21 3.
159. Winston, F., C. Dollard, and S.L. Ricupero-Hovasse, *Construction of a set of convenient Saccharomyces cerevisiae strains that are isogenic to S288C.* Yeast, 1995. **11**(1): p. 53-5.
160. Gerhardt, B., et al., *The vesicle transport protein Vps33p is an ATP-binding protein that localizes to the cytosol in an energy-dependent manner.* J Biol Chem, 1998. **273**(25): p. 15818-29.

161. Gatica, D., V. Lahiri, and D.J. Klionsky, *Cargo recognition and degradation by selective autophagy.* Nat Cell Biol, 2018. **20**(3): p. 233-242.
162. Suzuki, K., et al., *Hierarchy of Atg proteins in pre-autophagosomal structure organization.* Genes Cells, 2007. **12**(2): p. 209-18.
163. Cao, Y., et al., *In vivo reconstitution of autophagy in Saccharomyces cerevisiae.* J Cell Biol, 2008. **182**(4): p. 703-13.
164. Fujioka, Y., et al., *Structural basis of starvation-induced assembly of the autophagy initiation complex.* Nat Struct Mol Biol, 2014. **21**(6): p. 513-21.
165. Gatica, D., et al., *The carboxy terminus of yeast Atg13 binds phospholipid membrane via motifs that overlap with the Vac8-interacting domain.* Autophagy, 2020. **16**(6): p. 1007-1020.
166. Jao, C.C., et al., *A HORMA domain in Atg13 mediates PI 3-kinase recruitment in autophagy.* Proc Natl Acad Sci U S A, 2013. **110**(14): p. 5486-91.
167. Yamamoto, H., et al., *The Intrinsically Disordered Protein Atg13 Mediates Supramolecular Assembly of Autophagy Initiation Complexes.* Dev Cell, 2016. **38**(1): p. 86-99.
168. Wang, Y.X., N.L. Catlett, and L.S. Weisman, *Vac8p, a vacuolar protein with armadillo repeats, functions in both vacuole inheritance and protein targeting from the cytoplasm to vacuole.* J Cell Biol, 1998. **140**(5): p. 1063-74.
169. Pan, X., et al., *Nucleus-vacuole junctions in Saccharomyces cerevisiae are formed through the direct interaction of Vac8p with Nvj1p.* Mol Biol Cell, 2000. **11**(7): p. 2445-57.
170. Jeong, H., et al., *Mechanistic insight into the nucleus-vacuole junction based on the Vac8p-Nvj1p crystal structure.* Proc Natl Acad Sci U S A, 2017. **114**(23): p. E4539-E4548.
171. Kvam, E. and D.S. Goldfarb, *Nucleus-vacuole junctions and piecemeal microautophagy of the nucleus in S. cerevisiae.* Autophagy, 2007. **3**(2): p. 85-92.
172. Cheong, H., et al., *Atg17 regulates the magnitude of the autophagic response.* Mol Biol Cell, 2005. **16**(7): p. 3438-53.
173. Noda, T. and D.J. Klionsky, *The quantitative Pho8Delta60 assay of nonspecific autophagy.* Methods Enzymol, 2008. **451**: p. 33-42.
174. Fakieh, M.H., et al., *Intra-ER sorting of the peroxisomal membrane protein Pex3 relies on its luminal domain.* Biol Open, 2013. **2**(8): p. 829-37.
175. Hollenstein, D.M., et al., *Vac8 spatially confines autophagosome formation at the vacuole in S. cerevisiae.* J Cell Sci, 2019. **132**(22).
176. Suzuki, S.W., et al., *Atg13 HORMA domain recruits Atg9 vesicles during autophagosome formation.* Proc Natl Acad Sci U S A, 2015. **112**(11): p. 3350-5.
177. Toulmay, A. and R. Schneiter, *A two-step method for the introduction of single or multiple defined point mutations into the genome of Saccharomyces cerevisiae.* Yeast, 2006. **23**(11): p. 825-31.
178. Lodhi, I.J. and C.F. Semenkovich, *Peroxisomes: a nexus for lipid metabolism and cellular signaling.* Cell Metab, 2014. **19**(3): p. 380-92.
179. Sibirny, A.A., *Yeast peroxisomes: structure, functions and biotechnological opportunities.* FEMS Yeast Res, 2016. **16**(4).
180. Smith, J.J. and J.D. Aitchison, *Peroxisomes take shape.* Nat Rev Mol Cell Biol, 2013. **14**(12): p. 803-17.

181. Wanders, R.J., et al., *Genetic relation between the Zellweger syndrome, infantile Refsum's disease, and rhizomelic chondrodysplasia punctata.* N Engl J Med, 1986. **314**(12): p. 787-8.
182. Farre, J.C., et al., *PpAtg30 tags peroxisomes for turnover by selective autophagy.* Dev Cell, 2008. **14**(3): p. 365-76.
183. Till, A., et al., *Pexophagy: the selective degradation of peroxisomes.* Int J Cell Biol, 2012. **2012**: p. 512721.
184. Kornmann, B. and P. Walter, *ERMES-mediated ER-mitochondria contacts: molecular hubs for the regulation of mitochondrial biology.* J Cell Sci, 2010. **123**(Pt 9): p. 1389-93.
185. Prudent, J. and H.M. McBride, *The mitochondria-endoplasmic reticulum contact sites: a signalling platform for cell death.* Curr Opin Cell Biol, 2017. **47**: p. 52-63.
186. Rowland, A.A. and G.K. Voeltz, *Endoplasmic reticulum-mitochondria contacts: function of the junction.* Nat Rev Mol Cell Biol, 2012. **13**(10): p. 607-25.
187. Kornmann, B., et al., *An ER-mitochondria tethering complex revealed by a synthetic biology screen.* Science, 2009. **325**(5939): p. 477-81.
188. Hamasaki, M., et al., *Autophagosomes form at ER-mitochondria contact sites.* Nature, 2013. **495**(7441): p. 389-93.
189. Bockler, S. and B. Westermann, *Mitochondrial ER contacts are crucial for mitophagy in yeast.* Dev Cell, 2014. **28**(4): p. 450-8.
190. Cohen, Y., et al., *Peroxisomes are juxtaposed to strategic sites on mitochondria.* Mol Biosyst, 2014. **10**(7): p. 1742-8.
191. Mattiazzi Usaj, M., et al., *Genome-Wide Localization Study of Yeast Pex11 Identifies Peroxisome-Mitochondria Interactions through the ERMES Complex.* J Mol Biol, 2015. **427**(11): p. 2072-87.
192. Hutchins, M.U., M. Veenhuis, and D.J. Klionsky, *Peroxisome degradation in Saccharomyces cerevisiae is dependent on machinery of macroautophagy and the Cvt pathway.* J Cell Sci, 1999. **112 (Pt 22)**: p. 4079-87.
193. Reggiori, F., et al., *The actin cytoskeleton is required for selective types of autophagy, but not nonspecific autophagy, in the yeast Saccharomyces cerevisiae.* Mol Biol Cell, 2005. **16**(12): p. 5843-56.
194. Thoms, S. and R. Erdmann, *Dynamin-related proteins and Pex11 proteins in peroxisome division and proliferation.* FEBS J, 2005. **272**(20): p. 5169-81.
195. Helle, S.C., et al., *Organization and function of membrane contact sites.* Biochim Biophys Acta, 2013. **1833**(11): p. 2526-41.
196. Phillips, M.J. and G.K. Voeltz, *Structure and function of ER membrane contact sites with other organelles.* Nat Rev Mol Cell Biol, 2016. **17**(2): p. 69-82.
197. Nascimbeni, A.C., et al., *ER-plasma membrane contact sites contribute to autophagosome biogenesis by regulation of local PI3P synthesis.* EMBO J, 2017. **36**(14): p. 2018-2033.
198. Shai, N., et al., *Systematic mapping of contact sites reveals tethers and a function for the peroxisome-mitochondria contact.* Nat Commun, 2018. **9**(1): p. 1761.
199. Mao, K., et al., *The progression of peroxisomal degradation through autophagy requires peroxisomal division.* Autophagy, 2014. **10**(4): p. 652-61.
200. Park, J., et al., *Quaternary structures of Vac8 differentially regulate the Cvt and PMN pathways.* Autophagy, 2020. **16**(6): p. 991-1006.

201. Lahiri, S., et al., *A conserved endoplasmic reticulum membrane protein complex (EMC) facilitates phospholipid transfer from the ER to mitochondria.* PLoS Biol, 2014. **12**(10): p. e1001969.
202. Manford, A.G., et al., *ER-to-plasma membrane tethering proteins regulate cell signaling and ER morphology.* Dev Cell, 2012. **23**(6): p. 1129-40.
203. Quon, E., et al., *Endoplasmic reticulum-plasma membrane contact sites integrate sterol and phospholipid regulation.* PLoS Biol, 2018. **16**(5): p. e2003864.